NMDA Receptors Control Arf6 Activity via BRAG1 and BRAG2 in Spines of Neuronal Dendrites

Dissertation to obtain the academic degree
Doctor rerum naturalium (Dr. rer. nat.)
submitted to the Department of Biology, Chemistry and Pharmacy
of Freie Universität Berlin

authored by
Mohammad Nael Elagabani
from Vienna, Austria

2016

supervised by Dr. Hans-Christian Kornau

reviewed by Prof. Dr. Stephan Sigrist

Mein Dank gilt Doktor Hans-Christian Kornau mir als Promovend zu ermöglichen bei seiner Arbeitsgruppe teilzunehmen, sowie für die zur Verfügung gestellten Expressionsplasmide, die Laborleitung und Kommentare zu dieser Arbeit. Ich möchte mich auch bei Professor Stephan Sigrist für die Gutachtung meiner Doktorarbeit bedanken. An der Anfertigung dieser Dissertation waren Frau Dusica Briševac mit der Kultivierung der Neuronen und Herstellung der Viren, sowie Frau Alexandra Epp und Frau Katrin Büttner mit Ihrer technischen Unterstützung, und Frau Magda Krejczy mit Ihrer Hilfe bei der Mikroskopie an lebenden Zellen, essentiell beteiligt. Ich teile meine hiesigen sowie letzten Erfolge mit Kate. Darüber hinaus bin ich für die Anteilnahme meiner Familie dankbar, aber auch für die Gesellschaft meiner Freunde.

Ihnen möchte ich ans Herz legen,

‚Ein schlauer Mann kann mehr aus einer einfältigen Frage lernen, als ein einfältiger Mann von einer schlauen Antwort.'

- Samy Sorge, ungef. Wortlaut

Project realization:

supervised by Dr. Hans-Christian Kornau

April 2012 – March 2016

1st Reviewer:

Dr. Hans-Christian Kornau
Neuroscience Research Center, Institute of Biochemistry,
Charité University Medicine Berlin, Berlin, Germany

2nd Reviewer:

Prof. Dr. Stephan Sigrist
Department of Neurogenetics, Institute of Biology,
Free University Berlin, Berlin, Germany
Cluster of Excellence NeuroCure, Charité University
Medicine Berlin, Berlin, Germany

Disputation:

Friday, 07th October 2016

Abbreviations

NMDA	N-methyl D-aspartate
AMPA	α-amino 3-hydroxy-5-methyl-4-isoxazolepropionic acid
Arf	ADP-ribosylation factor
BRAG	Brefeldin A-resistant Arf-GEF
PSD	postsynaptic density
AP5	D-2-amino-5-phosphonopentanoate
mGlu receptors	metabotropic glutamate receptors

Berlin, Juni 2016

NMDA-Rezeptoren regulieren die Aktivität von Arf6 über BRAG1 und BRAG2 in Spines neuronaler Dendriten

GLUTAMAT-REZEPTOREN vermitteln die grundlegende Signalübertragung erregender Nervenzellen zentraler Nervensysteme. Die neuronalen Verknüpfungen zu pyramidalen Projektionsneuronen werden hauptsächlich über glutamaterge Synapsen an dornenförmigen Fortsätzen, den Spines, ihrer Dendriten gebildet (BOYER ET AL., 1998).

NMDA-Rezeptoren sind spannungsabhängige Glutamat-Rezeptoren. Die Vielfalt der regulatorischen NMDA-Rezeptor Untereinheiten der Familie GluN2 führte in Wirbeltierhirnen zur Entstehung von unterschiedlichen Rezeptor-assoziierten Signalproteinkomplexen (KENNEDY, 2000; RYAN ET AL., 2013). Die am häufigsten vorkommenden regulatorischen NMDA-Rezeptor Untereinheiten im Vorderhirn sind GluN2A und GluN2B (PAOLETTI ET AL., 2013).

Durch die Einbindung der kleinen GTPase Arf6 werden zelluläre Abläufe an Membranen, am Zytoskelett und im vesikulären Transportsystem auf einander abgestimmt (DONALDSON, 2003; MYERS AND CASANOVA, 2008). Während der neuronalen Entwicklung trägt Arf6 zur Bildung von dendritischen Spines bei (MIYAZAKI ET AL., 2005; RAEMAEKERS ET AL., 2012). Zu den stark angereicherten Proteinen glutamaterger Synapsen unter den Arf6-Regulatoren gehören EFA6A, BRAG1 und BRAG2 (CHOI, 2006; LOWENTHAL ET AL., 2015). BRAG1 und BRAG2 sind im Stande die Stärken von evozierten Membranströmen an Synapsen adulter Neuronen des Hippocampus zu beeinflussen (SCHOLZ ET AL., 2010; MYERS ET AL., 2012). Die vorgelegte Studie untersuchte Wechselwirkungen zwischen NMDA-Rezeptoren und BRAG1 oder BRAG2, um Mechanismen zur Aktivierung von Arf6 an neuronalen Synapsen zu erforschen.

Die Expression von BRAG1, BRAG2 und GluN2A steigerte sich im Laufe der neuronalen Entwicklung. In Neuronenkulturen steigerten durch Liganden-Bindung zwei getrennte Signalwege den GDP/GTP-Austausch von Arf6, der GluN2B-BRAG1 Signalweg in jungen Neuronen und der GluN2A-BRAG2 Signalweg in reifen Neuronen. Die Änderungen des Arf6 Aktivitätsniveaus verlangten einen Kalziumeinstrom durch den Ionenkanal des NMDA-Rezeptors.

Beim Fehlen von BRAG1 in jungen Kulturen konnten NMDA-Rezeptoren keine Arf6 Aktivierung verursachen. Das Fehlen der BRAG2 Expression beeinflusste Neuronen hingegen nur im reifen Stadium. Ohne BRAG2 Expression blieb in reifen Neuronenkulturen der Einfluss von GluN2A-haltigen Rezeptoren auf die Arf6 Aktivierung aus, und die Konzentration von Arf6-GTP erhöhte sich durch eine Rückkehr zum GluN2B-BRAG1 Signalweg. In diesem Zustand war das Arf6 Aktivitätsniveau mit dem in jungen Neuronen vergleichbar. Das Fehlen von BRAG2 in Knockout-Mäusen hatte außerdem Auswirkungen auf die morphologischen Maße von Spines auf pyramidalen Neuronen der Zellschicht 5 im parietalen Kortex.

Die Untersuchungen der Proteinbindungen legten nahe, dass BRAG1 und BRAG2 funktionelle Bestandteile des NMDA-Rezeptor Komplexes sind. Die Wechselwirkung zwischen BRAG Proteinen und GluN2-Untereinheiten erfolgte über mittig in den zytosolischen Rezeptorsegmenten liegende Regionen. Aminoterminal zur katalytische Domäne liegende Bereiche in BRAG1 und BRAG2 vermittelten die spezifische Bindung an die GluN2-Untereinheiten. Die GluN2-BRAG Bindung wurde durch die eingestellte Kalziumkonzentration beeinflusst, sodass die Regulierung der BRAG GEF-Funktion mit Calmodulin in Verbindung stehen könnte.

Wesentliche Resultate dieser Arbeit sind Bestandteil einer kürzlich erschienenen Publikation, die auch weitere Funktionen der beschriebenen Arf6 Aktivierung näher veranschaulicht (ELAGABANI ET AL., 2016). Über NMDA-Rezeptoren könnte der BRAG GEF-Mechanismus den Bedarf an aktivem Arf6 den neuronalen Erregungs- und Entwicklungsstadien anpassen und ein enger Zusammenhang zur Plastizität der Stärken von Synapsen bestehen. Die hier beschriebenen Signalwege zur Regulation von Arf6 könnten Einfluss nehmen auf (1) die Zusammensetzung der Spine-Membran, (2) die Umstrukturierung des dort befindlichen Zytoskeletts und (3) die Umverteilung synaptischer Proteine wie AMPA- und NMDA-Rezeptoren.

SYNOPSIS

NMDA Receptors Control Arf6 Activity via BRAG1 and BRAG2 in Spines of Neuronal Dendrites

Glutamate receptors are the fundamental mediators of electrical excitatory signals between the principal neurons of all known central nervous systems. Most glutamatergic synapses onto principal neurons of the brain form specifically on small protrusions, called spines, from long dendritic extensions of neuron cell bodies (BOYER ET AL., 1998).

The NMDA receptor is the only voltage-gated glutamate receptor of the central nervous system. In vertebrates the variety of the regulatory subunits of the GluN2 family has led to a diversity of enzymes in the synaptic signalling machine that became tightly linked to cytosolic NMDA receptor domains (KENNEDY, 2000; RYAN ET AL., 2013). The most common GluN2 subunit paralogs in the forebrain are GluN2A and GluN2B (PAOLETTI ET AL., 2013).

Activity of the small GTPase Arf6 is frequently implicated in cellular processes, when membranes, the cytoskeleton, and vesicular trafficking need to be modified in concert (DONALDSON, 2003; MYERS AND CASANOVA, 2008). During neuron development, Arf6 plays also a role in spine formation (MIYAZAKI ET AL., 2005; RAEMAEKERS ET AL., 2012). Amongst Arf6 regulators, EFA6A, BRAG1 and BRAG2 were shown to be abundant in glutamatergic synapses (CHOI, 2006; LOWENTHAL ET AL., 2015). BRAG1 and BRAG2 also affect the size of glutamate receptor membrane currents from mature neurons of the hippocampus after electrical stimulation (SCHOLZ ET AL., 2010; MYERS ET AL., 2012). In this study interactions between NMDA receptors and BRAG1 or BRAG2 will be investigated for a possible role in synaptic activation of Arf6 in dendritic spines on principal neurons of the neocortex.

Protein levels of GluN2A, BRAG1 and BRAG2 increased during neuronal maturation. After NMDA receptor ligand binding, GluN2B-BRAG1 signalling was identified as the predominant route of elevating Arf6 GDP/GTP-exchange in young neurons, while GluN2A-BRAG2 signalling could be assigned to mature neurons. Calcium influx through the ion channels of NMDA receptors was necessary for the changes in active Arf6 levels.

Depleting BRAG1 abolished NMDA receptor-triggered Arf6 activation in young neurons. The absence of BRAG2 only affected mature neurons. BRAG2 depleted neurons lacked the control of GluN2A-containing receptors over Arf6 and bore a high-level Arf6 activation tone via a return to the GluN2B-BRAG1 signalling route, comparable to young neurons in culture. The absence of BRAG2 affected the morphology of dendritic spine populations of principal layer 5 neurons in the parietal neocortex of conditional BRAG2 knockout mice.

Protein interaction assays suggested that BRAG1 and BRAG2 are constituents of the NMDA receptor complex. Physical binding to BRAG proteins was mediated by interactions at central regions of the cytosolic receptor segments. Segments of the BRAG proteins between the amino-terminus and the catalytic domain mediated the subtype-selective binding to GluN2 subunits. GluN2 subunit-BRAG protein interactions were sensitive to ambient calcium concentrations, and functional regulation of BRAGs was tied to interaction with calmodulin, as proposed elsewhere (MYERS ET AL., 2012).

The essential results of this dissertation contributed to a study, in which further functional aspects of neuronal BRAG-mediated Arf6 activation were elaborated (ELAGABANI ET AL., 2016). NMDA receptor-triggered BRAG GEF-activity might modulate active Arf6 levels according to neuronal excitability and maturational stages, and connect Arf6 functions with synaptic plasticity. The described signalling pathways regulating Arf6 activation might be involved in (1) the modification of spine membrane composition, (2) cytoskeletal remodelling, and (3) amongst other synaptic proteins, AMPA and NMDA receptor trafficking.

RESULT FIGURE INDEX

Figures I, NMDA receptors recruit BRAG family members during the maturation of cortical neurons

Figures II, BRAG1 and BRAG2 play different roles in the regulation of Arf6 in neuronal maturation

Figures III, Mechanisms of BRAG-mediated Arf6 activation

INDEX

D,Discussion

APPENDIX

Preperation protocols

A, Introduction

A, 1, Glutamatergic synapses

Neurons in the human brain communicate at specialized sites, termed synapses (Foster et al., 2010), with a number of approximately 10^{15} contacts per individual (Kandel ER, 2012). Via synapses, neurons excite or inhibit each other. Chemical synapses in the brain form where a neuron releases signal molecules, called neurotransmitters, from a protrusion, called axon, directly onto the cell membrane of another neuron. In the cerebral cortex, inhibitory neuron communication is generally local and structured around principal neuron circuits. By contrast, principal neurons can possess myelinated axon arbors that project throughout the central nervous system and release the excitatory neurotransmitter glutamate. All neurons share the characteristic of extending a number of protrusions away from their cell bodies, or somata. These protrusions are referred to as neurites; or dendrites, when they are not attached to the axon initial segment of the cell body where fast neuronal firing is generated. Dendrites serve the purpose of enhancing single neurons in their capacity to form synaptic contacts and networks. They achieve this by increasing their branching with brain size, which supports them in the broad collection of neuronal stimuli (Purves D, 1988).

During evolution the majority of postsynaptic sites (Sarnat and Netsky, 1985), which build the receiving half of excitatory synapses on dendrites of principal neurons, specialized into membrane protrusions with volumes of around 0.1 femtolitre. Through locating their postsynaptic sites into the tips of these protrusions, so-called dendritic spines, synaptic effects become spatially secluded. This modification allows spiny excitatory neurons to increase the level of their input processing (Cash and Yuste, 1999; Grunditz et al., 2008). Since their discovery (Cajal, 1899), it was assumed that spines refine neuronal networks formed by axons and dendrites. Excitatory spines also exist on some types of cortical inhibitory neurons, and appear to have similar functional roles, as their counterparts on principal neurons (Guirado et al., 2014). The postsynaptic parts of synapses onto spines appear in electron microscope pictures as dark thickenings of the plasma membrane called postsynaptic densities (PSDs, Gray, 1959). In PSDs, signalling and scaffolding protein networks embed ion pore-forming glutamate receptors, the fundamental mediators of excitatory synaptic neurotransmission (Monaghan et al., 1989). Together they build the intricate postsynaptic complex of a glutamatergic synapse with a layered architecture (Valtschanoff and Weinberg, 2001) and highly organized arrangement around receptor/pore subunits (Okabe, 2007; Sheng and Hoogenraad, 2007), above all α-amino 3-hydroxy-5-methyl-4-isoxazolepropionic acid (AMPA) and N-methyl D-aspartate (NMDA) receptors (Ascher and Nowak, 1988). After binding their agonist glutamate released from presynaptic endings of excitatory neurons, activated ionotropic glutamate receptors translate the resulting conformational change into forming a cation-selective aqueous pore, and serve as ion channels.

Synaptic activity in spines has multi-layered consequences. One of the consequences is that channeled ions pass by cytosolic extensions of receptor subunits and associated proteins. By that, interaction partners of glutamate receptor complexes in the spine compartment stay exposed to domains of increased ion concentrations until the ions are cleared off by transporters, or buffered (Naraghi and Neher, 1997; Matthews and Dietrich, 2015). Interaction partners of the synaptic spine

compartment include selected kinases, phosphatases, scaffold and small GTPase-related signalling proteins (FAN ET AL., 2014). The thinning attachment of spines, called spine neck, opposes synaptic currents electrically, chemically and physically. In the course of synaptic activity, spine necks at the base of spines retain diffusion of signalling molecules and ion fluxes, i.e. from the ionotropic glutamate receptor complexes in PSDs typically at the tips of spines; working together to turn the spine lumen into an electrobiochemical compartment (YUSTE, 2013). As a consequence of their small volumes, spine compartments provide atypical reaction conditions for the molecules inside them, making it likely that the presence and dynamics of even single molecules in spines are of physiological importance (BITO, 2010).

Glutamatergic neurotransmission that excites spines is occasionally fine-tuned by direct electrical neuroinhibition through γ-amino butyric acid receptors acting as anion channels (HIGLEY, 2014). Voltage-gated calcium and sodium channels respond to changes in membrane polarization and take part in the electrical signalling in spines, as well (ARAYA ET AL., 2007; YUSTE AND DENK, 1995). Primarily, synaptic strength, equal to the size of membrane depolarization through synaptic stimulation, is modulated biochemically, through molecular interactions, signals and processes, which respond to calcium currents and neurotransmitter or neuromodulator receptor activation (KANDEL AND SCHWARTZ, 2013). Structural self-remodeling and functional plasticity of synaptic neurotransmission is a fundamental feature of dendritic spines and enables principal neurons to form and then modify their circuits under precise regulation (LÜSCHER AND MALENKA, 2012). Glutamate receptors are central in connecting synaptic plasticity to synaptic activity. When these receptors are active they depolarize dendritic segments, but also modulate (1) on-going protein trafficking (COLLINGRIDGE ET AL., 2004) and (2) the assembly of actin fibres in spines (MATSUZAKI ET AL., 2004). This ultimately adjusts how many glutamate-binding ion channels are about to be incorporated into the PSD, minutes to hours after synaptic modulation has been triggered (NEWPHER AND EHLERS, 2008). Glutamatergic synapses are therefore able to fine-tune the neurotransmission they are mediating. The underlying processes are object to rigorous research.

A, 2, NMDA receptor complexes

The human genome encodes four families of glutamate receptors divided into current-transmitting, or ionotropic, and G-protein-coupled, or metabotropic glutamate (mGlu) receptors. Ionotropic glutamate receptors are classified in three groups and named after ligands that specifically activate them: kainate, AMPA and NMDA receptors. AMPA receptors are the most fundamental channels regarding synaptic signalling, for mediating fast currents in the few millisecond range and responding linearly to synaptic glutamate release. Their receptor complexes regulate synaptic strength by increasing neuronal excitation towards the NMDA receptor activation threshold. NMDA receptors are minimally active under basal neuron firing and can be fully opened when the postsynaptic neuron is already active and depolarized (NOWAK ET AL., 1984; MARKRAM ET AL., 1997), making the NMDA receptor the only ligand- and voltage-gated glutamate receptor in the central nervous system (Figure, *Major Ionotropic Glutamate Receptors Involved in Long-Term Synaptic Potentiation and Long-Term Synaptic Depression*, p. 3).

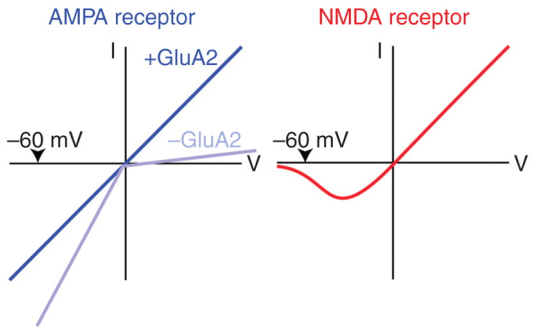

Figure, '*Major Ionotropic Glutamate Receptors Involved in Long-Term Synaptic Potentiation and Long-Term Synaptic Depression*' (Illustration taken from LÜSCHER AND MALENKA, 2012).

The current–voltage (I-V) curves demonstrate the 'linear I-V relationship' in AMPA receptors, while in NMDA receptors the I-V relationship is 'complex', due to the voltage-dependent block at negative potentials.

The major way of NMDA receptors to regulate synaptic strength is by mediating calcium influx and calcium-dependent processes (amongst many, also see EHLERS, 2000). The most prominent proteins that are under the control of NMDA receptors are Ca^{2+}/calmodulin-dependent protein kinase 2 (CaMK2), protein phosphatase 3 or calcineurin, protein phosphatase 1, Synaptic Ras-GAP, Ras nucleotide-releasing factors, kalirin, and calpain. They respond to ambient calcium concentrations either by binding the ions directly, e.g. via an EF domain, or by interacting with calcium-binding proteins.

As AMPA receptors increasingly reach synaptic sites, after neuronal stimulation and increased NMDA receptor activity (ANDRÁSFALVY AND MAGEE, 2004; HAYASHI ET AL., 2000; ZHANG ET AL., 2015), depolarization events intensify and basal neurotransmission is stabilized (HSIA ET AL., 1998; ABRAHAMSSON ET AL., 2008). The necessary components to stabilize synapses are contained in PSDs and build a sophisticated signalling machinery inside synaptic structures (KENNEDY, 2000). In case depolarization event numbers are reduced in stable synapses, NMDA receptors increasingly return to resting state and AMPA receptors begin to be internalized upon weak synaptic stimulation (LÜSCHER AND MALENKA, 2012; see Figure, *Postsynaptic expression mechanisms of long-term synaptic potentiation and long-term synaptic depression*, p. 4). Especially at the level of one synapse, the NMDA receptor complex mediates processes that contribute fundamentally to bridging this gap between synaptic activity and synaptic plasticity. Another important aspect in the formation of synapses associated to NMDA receptors is the role of mechanisms that actively block strengthening of synaptic sites (ADESNIK ET AL., 2008). In order to develop synapses that respond appropriately to neuronal input, NMDA receptors recruit synapse-stabilizing and synapse-destabilizing factors that equally contribute to the neuronal selection of functional synapses (GRAY ET AL., 2011). Adding to this idea is that upon their formation, many young synapses are devoid of AMPA receptors, express only NMDA receptors and are therefore electrically silent (ISAAC ET AL., 1995). Consequently, in a large number of newly formed synapses, initial stimulation of NMDA receptors and synapse activation may only be physiologically achieved, when back-propagating potentials elicited at neuronal firing or active neighbouring spines depolarize the spinal membrane timely and sufficiently (HÄUSSER ET AL., 2000). In neonates, newly formed synapses may also be activated by γ-amino butyric acid receptor activity, shown to be excitatory at this stage of age (BEN-ARI, 2002).

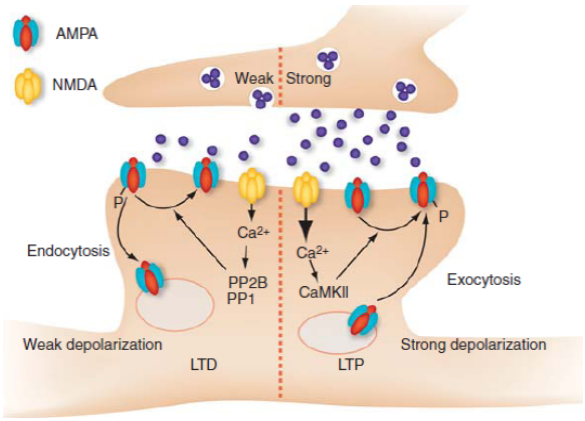

Figure, *Postsynaptic expression mechanisms of long-term synaptic potentiation and long-term synaptic depression* (Illustration taken from LÜSCHER AND MALENKA, 2012).

Changes in synaptic strength are orchestrated by NMDA receptor activity and defined by AMPA receptor dynamics. (left) Weak stimulation leads NMDA receptor signalling to activate phosphatases, which trigger AMPA receptor removal from synapses. (right) Strong synaptic stimuli cause kinase signalling, which induces AMPA receptor exocytosis. Both processes are calcium signal-dependent. (LTD, long-term depression; LTP, long-term potentiation; PP, phosphatase protein; CaMK, calcium/calmodulin kinase; blue circles, glutamate)

The physiological role of NMDA receptors in memory encoding became evident in a memory task study to test their functions in the hippocampus. In a water maze experiment designed to test spatial memory, rats were infused with the competitive NMDA receptor ligand blocker D-2-amino-5-phosphonopentanoate (AP5) and showed memory impairments in comparison to the control group not receiving AP5. These deficits were presented together with a blockade to elicit synaptic strengthening in the AP5-treated hippocampi (STEELE AND MORRIS, 1999). The observed memory-related changes were connected to receptor antagonism during the memory task and the authors concluded that NMDA receptors and hippocampal synaptic plasticity are involved in the 'consolidation of spatial information into long-term memory'.

Cloning studies identified NMDA receptors as assemblies of four from a total of seven different subunits with sizes ranging from ~900 to ~1500 amino acids (HOLLMANN AND HEINEMANN, 1994; PAOLETTI ET AL., 2013). The variation in size comes mainly from differences in the C-terminal domains. The seven genes of the subunits are grouped into three families according to sequence homology: GluN1-3. The functional tetrameric receptor consists always of two GluN1 subunits containing binding sites for the endogenous agonists glycine and D-serine. Once bound, they prime the receptor for activation. There are eight described isoforms of GluN1 with distinct properties and expression patterns (PAOLETTI ET AL., 2013) that affect the properties of NMDA receptor currents (BLIZNYUK ET AL., 2015). Although GluN1 subunits can form homomeric receptors, physiologically significant NMDA receptors are (1) dimers of the same GluN1-containing heterodimers with GluN2 subunits (most frequently GluN1/2A or GluN1/2B), or they are (2) heterotrimeric in combination with GluN2 and/or GluN3 subunits that form a dimer of different GluN1-containing heterodimers (most frequently GluN1/2A/2B receptors) (PAOLETTI ET AL., 2013).

All ionotropic glutamate receptors consist of the same basal structure of four modules (SCHWENK ET AL., 2012; Figure, *Structure of ionotropic glutamate receptors*, *left*, p. 5). (1) The most N-terminal domain is involved in binding allosteric regulators. (2) The receptor segment following the N-terminal domain is completely extracellular, like the first module, but contains the agonist-binding domains. (3) The transmembrane domain possesses three membrane-spanning regions and a re-entering loop that can participate in forming an ion pore. (4) The cytosolic C-terminal domain, which is particularly emphasized in this study, is involved in vesicular trafficking, has no intrinsic structure and is crucial for PSD-anchoring and coupling to a large set of signalling molecules (Figure, *Structure of ionotropic glutamate receptors, right*, p. 5).

Glutamatergic synapses onto neurons of the neocortex show predictable developmental changes in glutamate receptor contents, which are conserved in evolution, at least from amphibians to mammals (MCKAY ET AL., 2012). Amongst NMDA receptors, GluN2B-containing receptors are the most abundant in the early postnatal brain (MONYER ET AL., 1994). In spines, they keep nascent synapses from immaturely incorporating AMPA receptors (HANSE ET AL., 2013), initiate signalling pathways leading to synapse strengthening (LEONARD ET AL., 1999), contribute to spine organelle organization (FERREIRA ET AL., 2015), et cetera. Sudden coordinated exit of GluN2B subunits from synaptic sites can be observed when spines mature and their synapses strengthen (DUPUIS ET AL., 2013). As a consequence, GluN2B subunits may fulfill functions that are unique to early stages in synaptic development (FELDMAN AND KNUDSEN, 1998; KÖHR ET AL., 2003). Findings on the early lifetime of spines have been expanded by observations of spine elimination and synapse silencing, when stable synapses seem to develop backwards in maturation. This infers that once they are strengthened, spines are less mobile, but stay dynamic and can be completely eliminated depending on the synaptic input (HASEGAWA ET AL., 2015). With higher NMDA receptor activity, levels of GluN2A mRNA increase in immature neuronal cultures (HOFFMANN ET AL., 2000). Incorporation of GluN2A into NMDA receptor complexes is a repeatedly documented event in glutamate receptor subunit expression of glutamatergic synapses. GluN2A-containing receptors have been frequently equated to the mature form of NMDA receptor complexes in the forebrain, because their synaptic expression parallels synaptic maturation, circuit refinement and adoption of learned behavior (DUMAS, 2005).

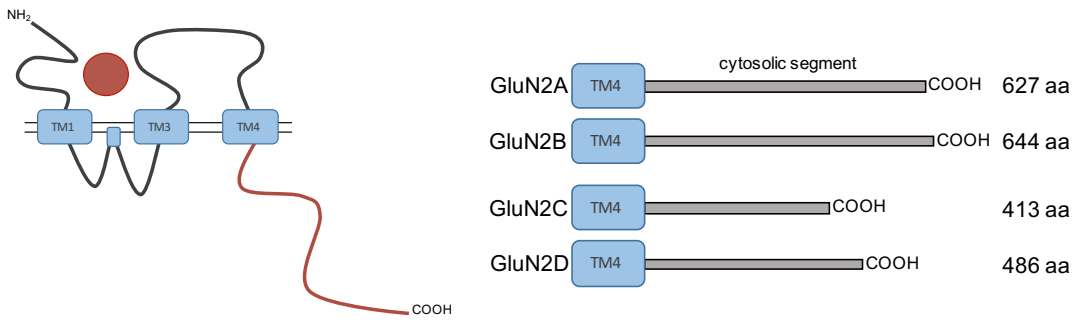

Figure, (left) ***Structure of ionotropic glutamate receptor subunits and (right) schematic mapping of GluN2 C-terminal cytosolic regions.***

The cytosolic tail is important for localization and mobility of the receptors (drawn in red). The approximate binding of the endogenous ligand glutamate (red circle) takes place extracellularly.

The balance in the amounts of GluN2A subunits and GluN2B subunits contained in a synapse, as well, as the amount of AMPA receptors in relation to them, are so far the most reliable biochemical and electrophysiological indicators for the maturation of the excitatory glutamatergic synapses onto principal cortical neurons. A prolonged residence of AMPA receptors in synapses mediates strengthening of synaptic activity at basal membrane potentials. Due to their gating properties, GluN2A-containing NMDA receptors carry more charges during fast, potentiating synaptic stimuli than GluN2B-NMDA receptors (Erreger et al., 2005) and might assist neurons to diversify neuronal firing, when the significance of receptor properties unfolds at the levels of neuronal circuitry and network processing.

The functional implications of glutamate receptor subunit changes have been explored before. (Endele et al., 2010; Foster et al., 2010; Myung et al., 2005). In terms of the molecular basis, the various ways of NMDA receptors to interact with signalling proteins might contribute to complex animal behavior (Grant, 2016). The evolutionary divergence between the cytosolic domains of the four GluN2 subunit paralogs may be the foundation, on which distinct signalling complexes in synaptic structures were able to emerge (Ryan et al., 2013). The multitude of physically stable signalling structures may explain the diversity and robustness of synaptic processes.

Despite the challenges to comprehend the molecular composition of large postsynaptic complexes, many interactions relevant for synaptic plasticity have been described. Efforts were made to learn how signalling cascades act in concert to regulate synaptic functions. The parallel increase in the number of synaptic protein paralogs along their evolution with GluN2 subunits, i.e. the MAGUK family including Dlg1/SAP97, Dlg2/PSD93, Dlg3/SAP102, Dlg4/PSD95 (Nithianantharajah et al., 2013), has been suggested as a premise to test the concept of emerging postsynaptic signalling networks. A compilation of identified protein interactions currently suggests the existence of a central NMDA receptor-PSD95-GKAP-Shank-Homer-mGlu receptor module embedded into a synaptic CaMK2 platform that is primarily involved in the regulation of synaptic strength (reviewed in Feng and Zhang, 2009; Hell, 2014; see also Figure, *Microdomains in dendritic spines and their signalling modules*, p. 7).

Despite of the proximity, AMPA receptor complexes are not part of the stable NMDA receptor complex. AMPA receptor complexes interact with the PSD via adaptor proteins (i.e. transmembrane AMPA receptor proteins, TARPs) and their stability at synapses is regulated by the phosphorylation state of TARPs (Opazo et al., 2010). Some kinases adjusting receptor phosphorylation states can be recruited to the receptor complexes by their individual adaptor proteins. A-kinase adaptor proteins, for instance, relay the synaptic interactions of protein kinase A and other enzymes to the NMDA receptor complex (Skroblin et al., 2010). Extrasynaptic neurotransmitter receptors outside the PSD might receive different cues from synaptic activity than receptors at synaptic sites. Although still under debate, this might lead to the activation of opposing intracellular signalling pathways (Hardingham and Bading, 2010).

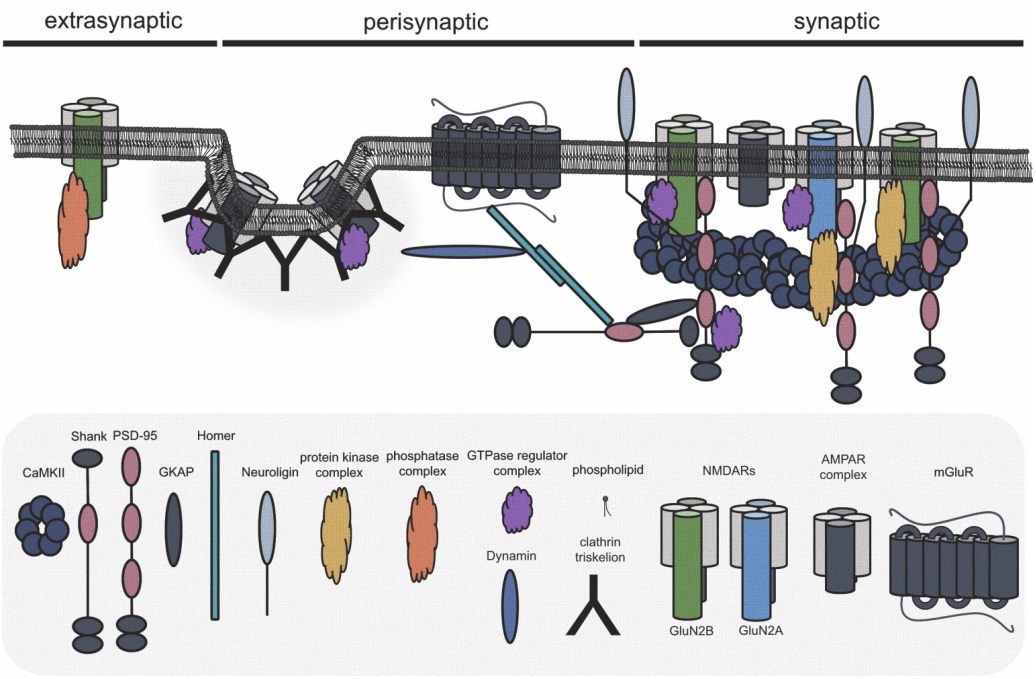

Figure, *Microdomains* (adapted from NEWPHER AND EHLERS, 2009) *and signalling modules in spines* (adapted from GRANT AND O'DELL, 2001, and FENG AND ZHANG, 2009).

In synaptic regions, cell-adhesion and PSD scaffold proteins, glutamate receptors, and signalling proteins assemble after incorporation into the PSD as stable signalling modules with regulatory functions. Scaffold proteins are essential in synapse formation by establishing transsynaptic junctions and postsynaptic receptor-signalling protein complexes (GRANT AND O'DELL, 2001). While diverse families of transsynaptic cell adhesion proteins mediate nascent synapse formation, neuroligin is also involved in recruiting AMPA receptors to synapses (MONDIN ET AL., 2011). Calcium/calmodulin kinase 2 (CaMK2) has been suggested as a bedrock of the glutamatergic synapse (HELL, 2014), and was shown to interact with PSD-95, other CaMK2 molecules, other protein kinases and the GluN2B subunit of NMDA receptors, reflecting its importance in activating and potentiating synapses (SANZ-CLEMENTE ET AL., 2013). The most dominant cohesive force of PSDs are members of the MAGUK family, eg. PSD-95, to which a broad variety of synaptic interactions are coupled. Via guanylate kinase-associated protein (GKAP; KIM ET AL., 1997) and shanks (NAISBITT ET AL., 1999), the PSD is also the anchor for peri- and extrasynaptic structures. PDZ domains are shown in dark red. Other domains involved are guanylate kinase and src homology 3 domains (in grey).
Dynamin-3 was shown to navigate large structures in the perisynaptic region via interaction with homer-mGlu receptor complexes (GRAY ET AL., 2003; LU ET AL., 2007). The perisynaptic region is also where the majority of membrane internalization takes place, i.e. stable structures called endocytic zones regulated by small GTPases and their effectors and regulators. Extrasynaptic regions contain GluN2B-receptors and mediate phosphatase signalling, which is mainly associated to forms of LTD and mechanisms that counteract excitotoxicity (ZHOU ET AL., 2013).

On a larger scale, the scaffold of structural and signalling proteins in PSDs dictates the dynamic distribution of glutamate receptor complexes and assists in their arrangement into microdomains of synaptic sites on dendritic spines (NEWPHER AND EHLERS, 2009). The synaptic site, which is aligned to active release sites of the presynaptic plasma membrane, is dominated by AMPA and GluN2-containing NMDA receptor complexes and includes all signalling events inside the PSD. This site is surrounded by a perisynaptic region, containing also mGlu and GluN3-containing receptors with distinctive sets of associated signalling pathways.

A dynamic extension of perisynaptic sites are (1) areas of active actin cytoskeleton remodeling and (2) endocytic zones, which harbor sorting proteins of the vesicular trafficking and the vesicle coat-recruitment machinery. A coherent force of perisynaptic sites might be motor proteins like dynamin-3 that can link the apparatus of endocytic zones dynamically to the PSD and might therefore have regulatory aspects in membrane trafficking (LU ET AL., 2007).

Small GTPases are central regulators that are prevalent in all synaptic microdomains of spines, and are involved in their associated processes. Careful elaboration of the interactions and signalling between synaptic proteins and regulators of every subfamily of the Ras superfamily (Figure, *Ras-related GTPases*, p. 9) made it clear that small GTPases are implicated in every aspect of the dynamic and coordinated features of a viable synapse.

A, 3, Arf6-mediated trafficking and actin cytoskeleton regulation

From the endoplasmatic reticulum where they are generated, membrane proteins are transferred between membrane compartments via vesicular trafficking. Eventually, they can be inserted into the plasma membrane via the secretory pathway. After internalization from the surface, membrane proteins are taken up by a variety of endosomes, where sorting events retain, return, or shuttle proteins throughout the cell. The transfer of internalized proteins, returning from endosomes, to the plasma membrane is in certain contexts specifically known as protein recycling (RADHAKRISHNA, 1997). During vesicular trafficking small patches of lipid membrane that contain integral proteins bud into spheres, or vesicles, and are actively carried along the cytoskeleton. Loaded vesicles ultimately fuse with their target membrane to release the cargo. Every manipulation of lipid membrane in the course of vesicular trafficking requires the involvement of the cytoskeleton and a tight interplay of proteins that remodel, and anchor to it. These steps are coordinated in part by small GTPases of the Ras superfamily, which use conformations, induced by the interaction with GTP, as a signal to recruit and instruct the large trafficking machinery (SEGEV, 2009). Typically, regulation of individual members of the Ras superfamily depends on a multitude of regulatory factors. This machinery adjusts local lipid composition of membranes (FUNAKOSHI ET AL., 2011), assures accuracy of the vesicle content (BONIFACINO AND LIPPINCOTT-SCHWARTZ, 2003), moulds membrane into the necessary form for vesicle fission (ANTONNY, 2006), and is required for vesicle mobility, the trafficking to the right destination (SEGEV, 2009) and fusion with the right membrane (ZERIAL AND MCBRIDE, 2001).

The requirement to shuttle cell components between different cell compartments makes this trafficking machinery a driver of a large number of cellular functions, including glutamate receptor sorting and distribution during neuronal plasticity, as suggested in PARK ET AL., 2004. In the mentioned study, Rab11 signalling in hippocampal neurons was essential in mobilizing AMPA receptors from the reserve pools in dendrites towards the plasma membrane, after the delivery of stimuli that strengthen synaptic transmission. This reserve pool could only be tapped into through NMDA receptor-mediated signalling, but did not include trafficking NMDA receptors themselves. This AMPA receptor mobilization was unrelated to newly synthesized AMPA receptors but specifically relied on AMPA receptors that had been

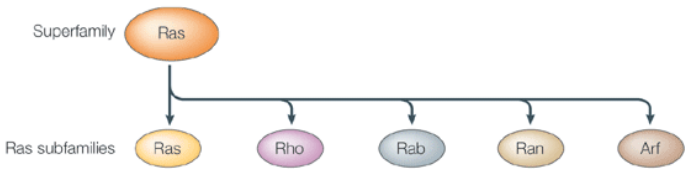

Figure, *Ras-related GTPases.*

'The Ras-related GTPases that make up the Ras superfamily have high sequence identity (40-85%), although the individual proteins have unique functions and preferred targets' (Illustration adapted from KENNEDY ET AL., 2005).

internalized from the surface of the dendritic plasma membrane. Dendrites therefore contain a network of endosomes that gives individual spines a potent tool to fine-tune their AMPA receptor contents and change synaptic strength.

As another example for small GTPase signalling during vesicular trafficking, and focus of this study, activation of Arf6 leads to membrane ruffling, via activating phosphatidlylinositol phosphate kinases (FUNAKOSHI ET AL., 2011). Furthermore, Arf6 is involved in the formation of highly mobile, actin fibre-rich membrane protrusions via phospholipase D (KIM ET AL., 2015), while being implicated in vesicle biogenesis via clathrin and the AP-2 adaptor protein complex (KRAUSS ET AL., 2003). It has been suggested that any type of change at membranes is initiated by membrane ruffling, which consists of a meshwork of newly formed actin fibres beneath a patch of lipid membrane (LORRA AND HUTTNER, 1999). The peculiarity about Arf6 is that it regulates endosomal sorting of internalized membrane proteins, and although centred on the plasma membrane, Arf6 actions shuttle them from endosomes to the cell surface (D'SOUZA-SCHOREY ET AL., 1998; MYERS AND CASANOVA, 2008; MONTAGNAC ET AL., 2011; CHESNEAU ET AL., 2012).

In the active state, Arfs expose an N-terminal myristoylation for tight membrane anchoring (D'SOUZA-SCHOREY AND STAHL, 1995). Arf6 is the only member of its family to locate to the plasma membrane, regardless of its activation cycle phase (MACIA ET AL., 2004). Since membrane anchoring regulates the activity of Ras family proteins, the separation of Arf6 activation and Arf6 plasma membrane recruitment is a peculiarity that might expand the areas of Arf6 function (RANDAZZO ET AL., 2000). This becomes physiologically relevant, as signals from different cell compartments might influence Arf6 activity in different ways. There are six known members in the mammalian ADP-ribosylation factor (Arf) family. An extended family of Arf has been identified, including Arf domain proteins, Arf-like proteins and Arf-related proteins. The reason for the existence of the high number of these factors is unclear; however, it appears necessary for trafficking regulation at the diverse membrane sites of the different endosomes in a cell (RANDAZZO ET AL., 2000).

The mammalian Arfs are grouped into three classes: Arf1 to Arf3 in class 1, Arf4 and Arf5 in class 2 and Arf6 in class 3 (MOSS AND VAUGHAN, 1993). Like all small GTPases, Arf proteins bind free GTP to induce changes in their conformation. They possess intrinsic GTPase activity that hydrolyzes Arf-bound GTP to GDP. There are numerous proteins interacting with proteins of the Ras superfamily to influence whether small GTPases are bound to GDP or GTP. These accessory proteins are either categorized as guanine

nucleotide exchange factors (GEFs) or GTPase-activating proteins (GAPs), depending on whether they promote the GTP- or the GDP-bound state, respectively. GEFs and GAPs work principally in two distinct ways. While GAPs promote the GDP-bound state by accelerating the otherwise slow, intrinsic GTPase activity of small GTPases by their active centre called arginine finger, GEFs use their active centre called glutamate finger to remove guanine from the guanine-binding site of small GTPases. Other than what the name 'exchange factor' is inferring, GEFs promote the GTP-bound state of small GTPases by releasing bound GDP during their GEF activity and allowing free GTP to access the newly unoccupied guanine-binding sites (Donaldson and Jackson, 2011). The sheer over-abundance of free GTP over free GDP in cells makes it more likely that guanine-free small GTPases bind GTP.

GEFs therefore relieve GDP-locked small GTPases to assist them in proceeding in their guanine binding cycle. It has been proposed that Arf is distinct in its functionality from other Ras family proteins, in that Arf-related processes require the entire guanine binding cycle of Arf to perform their tasks (Donaldson, 2003). This idea was derived from the observation that Arf mutants, capable of obtaining only one activation state, do not promote or block one specific mechanism like mutants of other Ras family proteins. Surprisingly, they yield cell states based on processes stalling in a particular step. It was consequently assumed that Arf-related processes are regulated by different sets of accessory proteins, i.e. a mixture of Arf-GEFs and -GAPs, pulling the process along. They coordinate the Arf activation cycle in the moment of action that is correlated to the cell stimulus and function. Arf-driven processes gain physiological meaning only in their activation context. This has moved Arf-GEFs and Arf-GAPs in spines closer to the centre of investigations about Arf-related functions.

A, 4, BRAG-mediated Arf6 activation in the brain

BRAGs are known guanine exchange factors (GEFs) for members of the small GTPase family Arf (Donaldson and Jackson, 2011). BRAG proteins locate to the plasma membrane with the help of their pleckstrin homology (PH) domain. Their PH domain is atypically involved in the GEF mechanism and potentiates the nucleotide exchange rate, in the case of BRAG2 by three orders of magnitude, through spatial coordination with substrates (Aizel et al., 2013). Human BRAGs are encoded in three genes BRAG1/IQSEC2, BRAG2/IQSEC1, and BRAG3/IQSEC3 located in chromosomes X, 3, and 6, respectively. BRAG proteins appear early in animal evolution from a Sec7-domain containing ancestor, but the three modern genes diverted from their ancestral BRAG gene only later in higher mammals (Cox et al., 2004). The Sec7-domain is essential for the catalytic activity of GTPase-GEFs. All BRAGs can be found in the brain and are highly enriched in excitatory and inhibitory synapses. All BRAG family members possess a post-synaptic density protein 95, drosophila disc large tumor suppressor, and zonula occludens-1 protein (PDZ)-ligand domain (PDZL), known to interact with the abundant PDZ-binding domains among PSD proteins (Figure, *Microdomains and signalling modules in spines*, p. 7). In cells, BRAG proteins appear adjacent to membranes, and accumulate in neuronal PSDs to the same extent as NMDA receptors (BRAG1 and BRAG2 around 10% as abundant as PSD-95; Lowenthal et al., 2015).

An interesting aspect of BRAGs is their tight involvement in receptor signalling at the plasma membrane. Physical receptor binding has been reported to modify BRAG GEF-activity, which allows BRAG proteins to help Arf6 integrate cues from the cell periphery (Sakagami et al., 2013; Sanda et al., 2009;

Dunphy et al., 2006; Hiroi et al., 2006; Fukaya et al., 2011; Scholz et al., 2010). GEFs of small GTPases are generically regulated by auto-inhibition by their PH domain. The switch from auto-inhibition to the active form is mediated by membrane binding and large conformational changes. BRAG proteins are an exception to this principle because of their atypical PH domain (Aizel et al., 2013). Instead, binding to calmodulin by its IQ-like domain may have regulatory qualities giving BRAG proteins the ability to respond to fluctuations in calcium concentrations (Myers et al., 2012). Nonetheless, BRAG functions might not be limited to the plasma membrane. Due to their atypical PH domain, BRAG proteins are not restricted by phosphoinositide specificity and might extend their functionality further out than the vesicular trafficking machinery at the plasma membrane (Aizel et al., 2013). BRAG proteins contain coiled-coil domains that in the case of BRAG1 were shown to mediate the formation of BRAG multimers that precipitate at the plasma membrane (Myers et al., 2012).

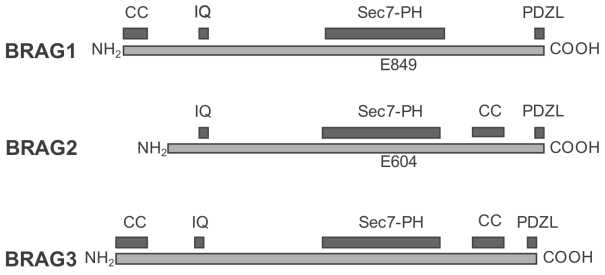

Figure, *Structure of BRAG family members* (adapted from Myers et al., 2012).

(CC, coiled-coil domain; IQ, IQ-like domain; PDZL, PDZ ligand;
E849/604, glutamate inside the BRAG1/2 glutamate finger)

In Myers et al., 2012, the calcium-sensing features of BRAG1's IQ-like motif were investigated. BRAG1 was shown to bind calmodulin only in calcium-free conditions, which also affected the regulation of its GEF-activity. In a calmodulin pulldown assay, this motif was required for human BRAG1 to bind calcium-free calmodulin, which could be released by adding calcium to the reaction solution. Calmodulin's ability to regulate BRAG1 Arf6-GEF activity was demonstrated by a BRAG1 mutant incapable of binding calmodulin. Over-expression of this mutant increased Arf6-GTP levels. However, the mutant did not respond to NMDA stimulation in neuronal cultures as the wild type did. It was concluded that calcium fluxes mediated by NMDA receptors might initiate calmodulin release from BRAG1, likely to cause conformational changes and affect its Arf6-GEF activity. If generalized, this behaviour qualifies BRAG proteins to be calcium-sensing players of synaptic plasticity, and regulators of synaptic Arf6.

Generally, intellectual disability appears, as intelligence quotients drop below 70 and impairs performance before the age of 18. The first polymorphisms associated to hereditary intellectual disability were mapped in 1988. The observed 'seizures, autistic traits, psychiatric problems and delayed early language skills' were not collectively seen as a syndrome, and therefore referred to as non-syndromic. Several of these polymorphisms on the X-chromosome inside the locus of BRAG1 were later linked to pathologic alterations of BRAG1 functions and were located inside the catalytic and calmodulin binding

domain sequences (SHOUBRIDGE ET AL., 2010). BRAG2 and BRAG3 deficiencies have not been investigated so far. BRAG1 is expressed early in murine embryos including the neocortex, the roof of the midbrain, cerebellum, medulla oblongata, spinal cord and dorsal root ganglia (MORLEO ET AL., 2008). In contrast to BRAG2, BRAG1 influences synaptic maturation not only by its GEF-activity, but also through incorporation into the PSD to enhance synaptic transmission by an unknown mechanism (BROWN ET AL., 2016).

BRAG2-stimulated Arf6 activity has been connected to the regulated internalization, sorting and endosomal trafficking of several transmembrane proteins. BRAG2-Arf6 signalling is involved in cell migration, signal protein exocytosis, endosomal sorting of membrane proteins, and neuronal morphogenesis. Arf6 activation through direct interaction between BRAG2 and the GluA2 subunit of AMPA receptors was reported to control internalization of AMPA receptors, and to be necessary for induction of low frequency stimulated LTD (SCHOLZ ET AL., 2010). The form of LTD, which BRAG2 mediated, depended on activation of mGlu receptors that triggers dephosphorylation of GluA2 at Y876 to set their C-termini free for direct interaction with BRAG2. BRAG1-Arf6 signalling is involved in the depression of synaptic transmission mediated by GluA1 subunit-containing AMPA receptors (MYERS ET AL., 2012) through the activation of c-Jun N-terminal kinase. The two studies had in common that AMPA receptor internalization was dependent on the studied BRAG-signalling mechanisms, and NMDA receptor activation was crucial in the induction of the observed BRAG-dependent processes.

Protein recycling represents the process in which endocytosed membrane proteins are exocytosed after endosomal sorting, to fine-tune their distribution. AMPA receptors are not exempt from this, and endocytosis and vesicular trafficking were observed inside spines by electron microscopy (RÁCZ ET AL., 2004). Importantly, Arf6-containing endosomes were suggested to be involved in the redistribution of AMPA receptors (ZHENG ET AL., 2015).

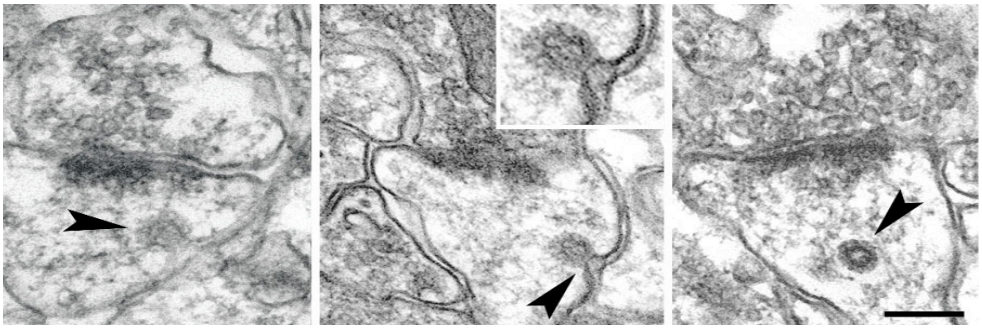

Figure, '*Endocytosis in spines.*

Arrowheads point to coated pit assembly (left), vesicle scission (middle) and internal trafficking (right). Bars, 200 nm.' (electron microscopic pictures taken from RÁCZ ET AL., 2004)

Neuronal dendrites and their spine protrusions contain networks of membranous structures cluttered with signalling and effector proteins occupied with regulating a dynamic trafficking of membrane proteins. In the case of glutamate receptors, trafficking and recycling affect synaptic strength, and it is under debate how regulators of vesicular trafficking influence neurotransmission. It has been pointed out that

controlled recycling of AMPA receptors is the decisive process in the regulation of synaptic plasticity (LÜSCHER ET AL., 1999). While delivery of receptors to the plasma membrane is necessary to increase AMPA receptor currents, internalization is needed to reduce them. Transport to and from the plasma membrane of spines therefore influences the incorporation of AMPA receptors into the synapse. Interestingly, AMPA receptor internalization induced by mild synaptic activation in neuronal cultures is completely blocked by NMDA receptor inactivation (CARROLL ET AL., 1999).

The other major inducer of AMPA receptor internalization is the mGlu receptor, which is predominantly found in the rim of glutamatergic synapses and extrasynaptic locations (Figure, Microdomains and signalling modules in spines, p. 18), and has been associated with neuronal activity through synaptic 'glutamate overspill' (KANDEL AND SCHWARTZ, 2013). Nonetheless, it remains unclear in which way mGlu and NMDA receptors correlate to, synergize with, or depend on each other to activate Arf6 in glutamatergic synapses of dendritic spines.

A, 5, Thesis statement

As highlighted in the introduction, NMDA receptor to BRAG signalling might constitute a mechanism that controls synaptic Arf6 activation in cortical neurons, enabling glutamate receptors to control their own dynamics and set synaptic strength. BRAG protein regulation might respond to changes in calcium concentrations, as BRAG proteins contain IQ-like domains and might be influenced by interaction with calmodulin. The following study will take up the question how NMDA receptor complexes may convert synaptic activity into Arf6 activation. This endeavor might provide insight into synaptic Arf6 signalling and aspects about spine morphology, as well, as glutamate receptor-dependent Arf6 functions during neuronal maturation (ELAGABANI ET AL., 2016), which will be discussed.

We approached this study in a heterologous cell expression system to identify signalling pathways mediated by functional NMDA receptors and BRAG proteins. In neuronal cultures we measured NMDA receptor-triggered effects on Arf6 activity levels, and outlined the consequences of RNAi interference-induced depletion of BRAG proteins. The importance of BRAG2 for the number and morphology of dendritic spines on cortical neurons was assessed in adult mice with a genetic knockout of BRAG2 in principal neurons of the forebrain. Principles of NMDA receptor-BRAG mediated Arf6 activation are condensed in a table on p. 28. A working model of the BRAG activation mechanism is shown on p. 43. The main findings on the molecular level are sketched in Figure, *BRAG signalling in one-week-old cortical neurons* on p. 64, and Figure, *BRAG signalling in spines of three-weeks-old cortical neurons* on p. 66.

B, Materials and Methods

If not stated otherwise, the experiments were carried out by the author.

Animals

All animal procedures were in accordance with the animal protection guidelines in Directive 86/609/EEC of the European Commission and the Regional Board in Berlin (T 0269/11). Cortical neuron cultures were prepared by Ms. Dusica Briševac from E18 Wistar rat embryos or from E16.5 C57BL/6 mouse embryos. For spine analysis male littermate *Iqsec1*$^{fl/fl}$ mice (Scholz et al., 2010) were used carrying a *thy1-GFP* (line M) allele (Feng et al., 2000) and either a *NEX-Cre* allele (Goebbels et al., 2006), or no *NEX-Cre* allele. NEX-Cre mice were kindly provided by Dr. Klaus-Armin Nave (Max Planck Institute for Experimental Medicine, Göttingen, Germany).

Instruments

Bench

Diverse reaction tubes (Sarstedt)
Micropipettes (Gilson)
Micropipette tips (Sarstedt)
Pipetteman (Brand)
Pipetteman pipettes (Sarstedt)
Table-top centrifuge 5417R (Eppendorf)
Shaker 3019 (GFL)
Dri-Block Heater (Techne)
Vortex-Genie (Scientific Industries)
Butane/Propane Mix C 206 (Campingaz)
Bunsen burner Labogaz (Campingaz)
Water Bath (Julabo)
Incubator B6 (Heraeus)
Thermomixer comfort (Eppendorf)
Balance CP3202S (Sortorius)
Analytical balance MC1 (Sortorius)
Incubator hood TH30 (Edmund Bühler GmbH)
Centrifuge Multifuge 3L-R (Heraeus)
Diverse freezers (at -20°C or -80°C) and fridges (at 4°C)
Densitometer Ultrospec 2100 pro (GE Healthcare)
Spectrophotometer ND-1000 (NanoDrop)
Gel UV imager BioDoc Analyze (Biometra)

Cloning

Agarose UltraPure (Invitrogen)
Ethidium bromide (Sigma)
PCR cycler (Biometra)

Western Blotting

BCA protein assay reagent kit (Pierce)
Microplate Reader iMark (BioRad)
Power supply Power Pack B25T (Biometra)
Gelelectrophoresis chamber Hoefer SE260 (Isogen Life Sciences)
Blotting chamber (Peqlab)
Gel blotting paper (Carl Roth)
PVDF membrane Immobilion-P (Merk Millipore)
Blot imager Fusion FX7 (Vilber Lourmat)

Cell culture

Diverse cell culture plates (Sarstedt)
Biolumino HeraSafe (Heraeus)

Chemicals

bromphenol blue (Carl Roth)
calcium chloride (Merk)
Coomassie (Serva)
disodium hydrogen phosphate (Carl Roth)
dithiothreitol (AppliChem)
EDTA (Carl Roth)

EDTA-free protease inhibitor mix (Roche)
ethanol (Herbeta Arzneimittel)
glacial acetic acid (Carl Roth)
glucose (AppliChem)
glycine (Serva)
glycol (Carl Roth)
HEPES (Carl Roth)
magnesium chloride (Merk)
methanol (Carl Roth)
Nonidet P-40 (AppliChem)
phenylmethane sulfonyl fluoride (AppliChem)
potassium chloride (Carl Roth)
potassium dihydrogen phosphate (Carl Roth)
sodium chloride (Carl Roth)
sodium deoxycholate (AppliChem)
sodium dihydrogen phosphate (Carl Roth)
sodium dodecyl sulphate (Serva)
sucrose (AppliChem)
Tris (Carl Roth)
Triton X-100 (Sigma)

Solutions

Phosphate buffered saline (PBS), for work at the bench

1.37 M sodium chloride (Carl Roth), 27 mM potassium chloride (Carl Roth), phosphate buffer: 100 mM disodium hydrogen phosphate (Carl Roth) and 200 mM potassium dihydrogen phosphate (Carl Roth)

DTT buffer

100 mM Tris (Carl Roth) pH 6.8, 200 mM dithiothreitol (AppliChem), 4% sodium dodecyl sulphate (Serva), 0.2% bromphenol blue (Carl Roth) 20% glycol (Carl Roth)

Lämmli buffer

120 mM Tris (Carl Roth) pH 6.8, 0.1% bromphenol blue (Carl Roth), 6.25% sodium dodecyl sulphate (Serva), 20% glycol (Carl Roth)

Plasmids

DNA encoding the appropriate protein segments was amplified by PCR from cDNA or from validated plasmids using the high-fidelity DNA Polymerase Precisor (Bio Cat), digested using restriction endonucleases and inserted into appropriate vectors using T4 Ligase (New England Biolabs). Other inserts were cloned from validated plasmids (see Table, *Plasmids for protein expression*, p. 16). Sequence accuracy was validated by LGC Genomics through Sanger sequencing. Plasmids were amplified using *E.coli* XL1 blue (Stratagene) as host organism.

Bakterial expression

Coomassie staining solution

0.1% Coomassie (Serva), 50% methanol (Carl Roth), 7.5% glacial acetic acid (Carl Roth)

Coomassie de-staining solution

20% methanol (Carl Roth), 7.5% glacial acetic acid (Carl Roth)

The cDNAs encoding various segments of the cytosolic C-terminal stretches of rat GluN2A and GluN2B were inserted into pGEX (GE Healthcare) and expressed as GST fusion proteins using *E.coli* BL21 (Stratagene) as expression host. 1mM Isopropyl ß-D-1-thiogalactopyranoside (AppliChem) was added to

E.coli BL21 cultures in lysogeny broth medium (Invitrogen) to induce GST fusion protein expression, which was performed at 37°C for 2.5 hours.

For the binding of active Arf6 in quantitative activity assays, as described by SANTY AND CASANOVA, 2001, a GST fusion protein version of rat Gga3 producing GGA3 aa 1-313 followed by a stop codon, encoding its N-terminal Vps27/Hrs/Stam and Arf-GTP binding GGA and Tom1 domain, was over-expressed in the same way. GST-GluN2ACT200a (aa 838-1037) was recovered from inclusion bodies by guanidine treatment and ethanol precipitation (PALMER AND WINGFIELD, 2004).

Expression of GST-coupled proteins was validated on Roti-Blue (Carl Roth) or Coomassie-stained SDS-polyacrylamide gels. GST-coupled proteins were always freshly purified by glutathione sepharose (GE Healthcare) before being used for pulldown assays.

Mammalian expression

For Arf6 activity assays performed in over-expression system HEK293, rat Arf6 ending C-terminally with the sequence LE and the haemagglutinine (HA)-tag YPYDVPDYA was inserted into the bicistronic plasmid pBud (Invitrogen) expressed under the control of a CMV-promotor. Cytosolic peptides assayed for their BRAG-GEF activity-enhancing properties were expressed with an N-terminal palmitoylation site of rat neuromodulin under the control of an EF1a promoter in pBud. In these experiments rat BRAG1 and BRAG2 containing a C-terminal eGFP-tag to allow visual estimation of their expression were transiently expressed under the control of a CMV promoter. 40 aa-long GluN2A C-terminal peptides, meant to compete with GluN2A-containing receptors for binding BRAG proteins, contained eGFP-tags for the same reason.

Alternatively, functional NMDA receptors containing the rat GluN2A, mouse GluN2B subunit, or mutants with deletions in GluN2A aa 1078-1117 or GluN2B aa 1115-1154, were expressed along with rat GluN1 isoform 1a under the control of a CMV-promotor in co-expression with Arf6-HA in pcDNA3 (Invitrogen).

To investigate physical interactions BRAG1 and BRAG2, or segments between their amino-terminus and the catalytic domain, were over-expressed with an N-terminal FLAG octapeptide-tag DYKDDDDK in HEK293 cells to be pulled down by bacterial GST-coupled proteins or resin-coupled calmodulin. All proteins were expressed for 48 hours in vitro after transfection.

Table, *Plasmids for protein expression*

Insert	Vector	Construction/Source
Arf6HA	pcDNA3	*
Arf6HA	pBudCE4.1	fragment from pcDNA-Arf6HA, *Hind*III/*Xba*I ligation
BRAG1 (aa 1-1154)	pEGFP	*
BRAG2 (aa 1-947)	pEGFP	*
BRAG2 R146A (aa 1-947)	pEGFP	*

* not constructed by the author

BRAG1 (aa 1-1154)	CMV expression vector [x] containing FLAG	*
BRAG2 (aa 1-947)	CMV expression vector [x] containing FLAG	*
BRAG1 N-terminus (aa 1-752)	CMV expression vector [x] containing FLAG	*
BRAG2 N-terminus (aa 1-507)	CMV expression vector [x] containing FLAG	*
GluN1-1a (aa 1-938)	CMV expression vector [x]	+
GluN2A (aa 1-1464)	CMV expression vector [x]	+
GluN2A-ΔB2BD	CMV expression vector [x]	*
GluN2B (aa 1-1482)	CMV expression vector [x]	+
GluN2B-ΔB1BD	CMV expression vector [x]	*
GluN2ACT200 (aa 1038-1237)	pGBT	PCR, *Not*I/*Sal*I ligation
GluN2A-CT100a (aa 1038-1137)	pGBT	PCR, *Not*I/*Sal*I ligation
GluN2A-CT100b (aa 1138-1237)	pGBT	PCR, *Not*I/*Sal*I ligation
palm-GluA1CT (aa 827-907)	pBud-Arf6HA	PCR, *Not*I/*Sal*I ligation
palm-GluN2ACT (aa 838-1464)	pBud-Arf6HA	PCR, *Not*I/*Sal*I ligation
palm-GluN2BCT (aa 839-1482)	pBud-Arf6HA	PCR, *Not*I/*Sal*I ligation
palm-GluN2ACT200 (aa 1038-1237)	pBud-Arf6HA	fragment from pGBT-GluN2ACT200, *Not*I/*Sal*I ligation
palm-GluN2A-CT100a (aa 1038-1137)	pBud-Arf6HA	fragment from pGBT-GluN2ACT100a, *Not*I/*Sal*I ligation
palm-GluN2A-CT100b (aa 1138-1237)	pBud-Arf6HA	fragment from pGBT-GluN2ACT100b, *Not*I/*Sal*I ligation
GGA3 (aa 1-313)	pGEX-6P1	*
GluN2ACT200a (aa 838-1037)	pGEX-6P1	*
GluN2ACT200b (aa 1038-1237)	pGEX-6P3	fragment from pBud-AHA-palm-GluN2ACT200b, *Not*I-*Eco*RI-linker-*Not*I/*Sal*I ligation
GluN2ACT200c (aa 1238-1464)	pGEX-6P3	fragment from pBud-AHA-palm-GluN2ACT200c, *Not*I-*Eco*RI-linker-*Not*I/*Sal*I ligation

[x] SCHALL ET AL., 1990

\+ kindly provided by Dr. Peter H. Seeburg

* not constructed by the author

GluN2A-CT100a (aa 1038-1137)	pGEX-6P3	fragment from pBud-AHA-palm-GluN2ACT100a, *Not*I-*Eco*RI-linker-*Not*I/*Sal*I ligation
GluN2A-CT100b (aa 1138-1237)	pGEX-6P3	fragment from pBud-AHA-palm-GluN2ACT100b, *Not*I-*Eco*RI-linker-*Not*I/*Sal*I ligation
GluN2A-CT40a (aa 1058-1097)	pGEX-6P1	*
GluN2A-CT40b (aa 1078-1117)	pGEX-6P1	*
GluN2A-CT40c (aa 1098-1137)	pGEX-6P1	*
GluN2BCT200 (aa 1036-1243)	pGEX-6P2	*
GluN2B-CT40a (aa 1115-1154)	pGEX-6P1	*
GluN2B-CT40b (aa 1135-1174)	pGEX-6P1	*
GluN2B-CT40c (aa 1155-1194)	pGEX-6P1	*
GluN2A-CT40a (aa 1058-1097)	pEGFP-C2	*
GluN2A-CT40b (aa 1078-1117)	pEGFP-C2	*
GluN2A-CT40c (aa 1098-1137)	pEGFP-C2	*

Lentivirus plasmids

Packaging of virus constructs and targeted interference of BRAG1 and BRAG2 expression in primary cortical neuron cultures from Wistar rat E18 pups was performed by Ms. Dusica Briševac as previously described (ELAGABANI ET AL., 2016). Lentiviral constructs used in infections for RNA interference (RNAi) of BRAG1 and BRAG2, and for the BRAG-RNAi control, (RNAi-B1, -B2, -ctrl, respectively) encoded the following short hairpin RNAs (5'-3'):

GGAAGCUAUCUAUCGGGAUAAGUGAAGCCACAGAUGUUAUCCCGAUAGATAGCUUCC (RNAi-B1),

GCAUUGUGCUGUCCAACAUGAGUGAAGCCACAGAUGUCAUGUUGGACAGCACAAUGC (RNAi-B2) (SCHOLZ ET AL., 2010), and

GCAGCUAAUGGCCUUUCAUGAGUGAAGCCACAGAUGUCAUGAAAGGCCAUUAGCUGC

(RNAi-ctrl, scrambled version of RNAi-B2)

For knockout experiments, neuron cultures of *Iqsec1*$^{fl/fl}$ mice were infected with FCKiGW-Cre (SCHOLZ ET AL., 2010) or an empty vector at 15 days in vitro.

Cell line culture and transfection by calcium precipitation

Extracellular solution (ECS) pH 7.4

25 mM HEPES (Carl Roth), 140 mM sodium chloride (Carl Roth), 5.4 mM potassium chloride (Carl Roth), 1.3 mM calcium chloride (Merk), 33 mM glucose (AppliChem)

* not constructed by the author

HEPES-buffered saline (HBS) pH 7.0

50 mM HEPES (Carl Roth), 280 mM sodium chloride (Carl Roth), 10 mM potassium chloride (Carl Roth), 1.5 mM sodium dihydrogen phosphate (Carl Roth), 12 mM glucose (AppliChem)

Procedure

HEK293 cells were cultured in serum-free Dulbecco's modified eagle media (DMEM) with 4.5 g/l D-glucose (DMEM + GlutaMAX, Gibco), 100 units/ml penicillin (Gibco), 100 µg/ml streptomycin (Gibco) and 10% fetal bovine serum (FBS, Biochrome) for up to 50 passages at 37°C, 5% atmospheric CO_2 and a top cell density of approximately $7x10^6$ cells per 100 mm cell culture plate (Sarstedt) before transfection. HEK293-BRAG1- and HEK293-BRAG2-Flp-In (Thermo Scientific) cell lines (HEK-BRAG1, HEK-BRAG2) were produced by colleagues in the laboratory (Scholz et al., 2010; Elagabani et al., 2016). Between seeding and passaging or transfection of Flp-In cell lines 150 µg/ml hygromycin (Invitrogen) was added to the media to maintain cell line purity. For transfection, HEK-BRAG2 cells were seeded on poly-L-lysine coated culture plates.

13.5 µg of plasmid DNA were transfected by adding transfection solutions as HEPES-buffered saline in the presence of 12 mM calcium and 25 µM chloroquine (Sigma). The media with transfection-mix was exchanged after 6 hours. Transfected cells were kept for additional 48 hours in culture before harvest on ice. To express functional NMDA receptors in active Arf6 assays, plasmids for the expression of GluN1-1a, GluN2 subunits, or Arf6-HA were transfected in the ratios: 1:2:1.

HEK293 cells prepared for fluorescence microscopy were seeded on 20 mm Fluorodishes (World Precision Instruments) and cultured in serum-free DMEM + GlutaMAX, 100 units/ml penicillin, 100 µg/ml streptomycin and 10% FBS for 2 days to a number of approximately $9x10^5$. Cells were transfected as described above (GluN1-1a, GluN2, Arf6-HA, BRAG expression plasmid ratio: 1:2:1:1).

Stimulation of cell line- and neuronal cell cultures in vitro

Extracellular solution (ECS) pH 7.4

25 mM HEPES (Carl Roth), 140 mM sodium chloride (Carl Roth), 5.4 mM potassium chloride (Carl Roth), 1.3 mM calcium chloride (Merk), 33 mM glucose (AppliChem)

To examine the effect of NMDA receptor-expression on Arf6 activity in BRAG-HEK293 cell cultures, or the effect of NMDA receptor-expressing HEK293-BRAG cell cultures responding to glutamate stimuli on Arf6 activity or BRAG localization, transfected cell cultures were starved from glutamate for 1 hour at 37°C in ECS after removing media from the plates and washing once with PBS pH 7.5 (Gibco) at 37°C. If indicated, 3 µM ifenprodil was added during starvation. For stimulations an equal volume of ECS or ECS/glutamate was applied to cells adding up to an end concentration of 0 or 1 mM L-glutamate and gently swirled. In cellular Arf6 activation assays after 5-minute incubations at 37°C, the supernatant was quickly discarded and plates put on ice for harvest.

Primary cortical neuron cultures from Wistar rat E18 pups were prepared by Ms. Dusica Briševac as previously described (Elagabani et al., 2016). To examine neuronal responses to pharmaceuticals affecting NMDA receptor signalling, drugs were adjusted in conditioned Neurobasal media (Gibco) with

B-27 serum-free supplement (Invitrogen), 5,000 units/ml penicillin (Invitrogen), 5,000 units/ml streptomycin (Invitrogen), 2 mM GlutaMAX (Invitrogen) and equilibrated for 10 minutes at 37°C and 5% CO_2. Neurons were stimulated with 100 µM NMDA, 100 µM D-AP5, 100 µM MK-801, 3 µM ifenprodil, 1 µM TTX, 300 nM Zn^{2+}, or combinations thereof in conditioned media. Stimulated neurons were washed with 1 ml Dulbecco's phosphate buffered saline (Gibco) on ice and harvested. Lysates of cell cultures for the analysis on Western blots were harvested in a 2 mM EDTA, 1% Triton X-100, 1x protease inhibitor (Roche) containing PBS-buffer and prepared by denaturation for 5 minutes at 95°C in Lämmli buffer.

Drugs

L-glutamic acid

This drug was produced by AppliChem. Also known as L-glutamate, it has a molecular mass of 147.13 g/mol. It is the primary excitatory neurotransmitter and endogenous ligand of AMPA-type, NMDA-type, and kainite ionotropic as well as metabotropic glutamate receptors.

NMDA

This drug was produced by Tocris, and the name is abbreviated from N-methyl-D-aspartate. It has a molecular mass of 197.1 g/mol. NMDA was initially used to distinguish between the activity of non-NMDA-type and NMDA-type glutamate receptors, the latter of which it can specifically activate.

D-AP5

This drug was produced by Tocris. D-2-amino-5-phosphonopentanoate has a molecular mass of 147.1 g/mol. It is a fast-active isomer of AP5 and competitive ligand for the glutamate binding site. D-AP5 can selectively inhibit NMDA-type glutamate receptor activation in micromolar concentrations but has a different affinity towards the different NMDA receptor subunits.

Dizocilpine

This drug was produced by Tocris. Also known as MK-801, it has a molecular mass of 221.3 g/mol. It can bind inside the ion channel of NMDA receptors and block their ion influx once the channel has been opened. Other targets of dizocilpine are nicotinic acetylcholine receptors and serotonin and dopamine transporters.

Ifenprodil

This drug was produced by Sigma-Aldrich. Ifenprodil has a molecular mass of 325.4 g/mol. It is a highly selective inhibitor of heterodimeric GluN1/2B-receptors at concentrations of a few micromolar by binding to the N-terminal leucine/isoleucine/valine-binding protein (LIVBP)-like domain of GluN2B. Triheteromeric GluN2B-containing receptors are also partially inhibited after ifenprodil binding, which in either case promotes locking of GluN2B subunits in a closed conformation. The selectivity for the GluN2B subunit decreases with increasing ifenprodil concentrations.

Zinc

Zinc chloride was produced by AppliChem, which generates Zn^{2+} ions in water with a molecular mass of 65.4 g/mol. It is a highly selective inhibitor of heterodimeric GluN2A-containing receptors at less than micromolar concentrations by binding to the N-terminal LIVBP-like domain of GluN2A. Ifenprodil and zinc share similar binding mechanisms.

Tetrodotoxin

This drug was produced by Tocris and is abbreviated to TTX. It has a molecular mass of 319.27 g/mol and is produced by symbiotic bacteria residing in Tetraodontiformes. TTX prevents firing of neuronal action potentials by blocking voltage-gated sodium channels. It is therefore a potent neurotoxin.

SDS-polyacrylamide gel electrophoresis (PAGE) and quantitative western blotting

Stacking gel buffer pH 6.8

250 mM Tris (Carl Roth), 20% sodium dodecyl sulphate (Serva)

Resolving gel buffer pH 8.8

750 mM Tris (Carl Roth), 20% sodium dodecyl sulphate (Serva)

Running buffer pH 8.4

125 mM Tris (Carl Roth), 1.25 M glycine (Serva), 0.5% sodium dodecyl sulphate (Serva)

Transfer buffer pH 8.4

125 mM Tris (Carl Roth), 1.25 M glycine (Serva), 0.5% sodium dodecyl sulphate (Serva), 20% ethanol (Herbeta Arzneimittel)

Phosphate buffered saline with Tween (PBS/Tween)

1.37 M sodium chloride (Carl Roth), 27 mM KCl (Carl Roth), phosphate buffer: 100 mM disodium hydrogen phosphate (Carl Roth) and 200 mM potassium dihydrogen phosphate (Carl Roth), 0.05% Tween (AppliChem)

Procedure

Protein extracts and pulldown elutions were separated under denaturing conditions in pH 8.8 gel buffer by SDS-PAGE (6%, 10% or 15% acryl amide) and transferred to PVDF membrane (Millipore) in SDS-containing transfer buffer by wet blotting. Membranes were washed in PBS/Tween, blocked for 1 hour in 5% milk powder (Carl Roth) in PBS/Tween and incubated in primary antibody diluted in 1% milk-PBS/Tween overnight at 4°C to recognize the designated protein. Membranes were then washed intensively with PBS/Tween and incubated for 1 hour in horse raddish peroxidase-conjugated secondary species-Fc-specific antibody diluted in PBS/Tween.

Secondary antibodies

donkey anti-mouse IgG (Dinova)

donkey anti-rabbit IgG (Dinova)

donkey anti-goat IgG (Dinova)

Finally, membranes were incubated for 1 minute in enhanced luminol (Perkin Elmer) before being imaged in Fusion FX7 (Vilber Lourmat) and filmed on chemiluminescence film Amersham Hyperfilm ECL (GE Healthcare). Filmes were then scanned (LG) and .tifs prepared by Photoshop.

Primary antibodies

epitope	species	working dilution	company
Haemagglutinine HA.11	mouse, monoclonal	1 : 1,000	Covance
FLAG octapeptide F7425	rabbit, monoclonal	1 : 1,000	Sigma
FLAG octapeptide M2	mouse, monoclonal	1 : 10,000	Sigma
Arf6 ab49931	mouse, monoclonal	1 : 1,000	Abcam
NR2A 07-632	rabbit, polyclonal	1 : 1,000	Millipore
NR2B sc-9057	rabbit, polyclonal	1 : 1,000	Santa Cruz
BRAG2 P	rabbit, polyclonal	1 : 1,000	in-house
BRAG1 sc-168198	goat, polyclonal	1 : 500	Santa Cruz
βIII-tubulin TUJ1	mouse, monoclonal	1 : 5,000	Covance
α-tubulin DM 1A	mouse, monoclonal	1 : 5,000	Sigma

GST-pulldown assays

Homogenization buffer

320 mM sucrose (AppliChem), 4 mM HEPES pH 7.5, 2 mM EDTA and 1x EDTA-free protease inhibitor mix (Roche)

Triton solution

1x PBS (Carl Roth) pH 7.5, w/ or w/o 5.6 mM EDTA (Carl Roth) or calcium chloride (Merk) for f.c. of 2 mM calcium, 2.8 mM phenylmethane sulfonyl fluoride (AppliChem), 2.8% Triton X-100 (Sigma), 1x EDTA-free protease inhibitor mix (Roche)

Triton buffer

PBS pH 7.5, 0.1% Triton X-100 (Sigma), 1x EDTA-free protease inhibitor mix (Roche)

Procedure

N-terminally FLAG-tagged segments of BRAG1 or BRAG2 were over-expressed in HEK293 cells and purified. Briefly, after lysis of washed cells by sonication in PBS pH 7.5, lysates were clarified at 1,000 g for 10 minutes and another time at 100,000 g for 30 minutes at 4°C. 9 volumes of supernatant were diluted with 5 volumes of Triton solution to reach a final concentration of 1% Triton. To reduce non-specific interactions, diluted lysate supernatants were incubated with 1.5 volumes of a mixture of glutathione and GST-bound glutathione sepharose for 2 hours at 4°C. Diverse GST-fusion protein-bound glutathione-sepharose was then incubated with purified lysate supernatants for 2 hours at 4°C. Samples from the purified supernatants were denatured for 5 minutes at 95°C in DTT buffer or Lämmli buffer. After incubation, the sepharose was washed three times with Triton buffer, and bound proteins were eluted for 10 minutes at 95°C in DTT buffer or Lämmli buffer. Alternatively, the washed sepharose was diluted in 9 volumes of Triton buffer and 1 volume of 10x-calcium stocks to reach the indicated final concentrations for calcium elutions, and incubated for 1 hour at 4°C before being washed again three times with Triton buffer. Finally, bound proteins were prepared as western blot samples as described above. Samples from the clarified supernatants and pulldowns were assayed for immunoreactivity of FLAG on Western blot.

Co-immunoprecipitation

Homogenization buffer

320 mM sucrose (AppliChem), 4 mM HEPES pH 7.5, 2 mM EDTA and 1x EDTA-free protease inhibitor mix (Roche)

deoxycholate (DOC) buffer

50 mM Tris (Carl Roth) pH 9.0, 150 mM sodium chloride (Carl Roth), 1% sodium deoxycholate (Serva), 1x EDTA-free protease inhibitor mix (Roche)

RIPA-buffer

50 mM Tris (Carl Roth) pH 7.5, 150 mM sodium chloride (Carl Roth), 1% Triton X-100 (Sigma),
0.5% sodium deoxycholate (AmpliChem), 0.1% sodium dodecyl sulphate (Serva), 1x EDTA-free protease inhibitor mix (Roche)

Dialysis buffer

50 mM Tris pH 7.5, 150 mM sodium chloride, 0.1 % Triton X-100, 1x EDTA-free protease inhibitor mix (Roche)

Triton buffer

PBS pH 7.5, 0.1% Triton X-100 (Sigma), 1x EDTA-free protease inhibitor mix (Roche)

Procedure

One adult rat brain without olfactory bulbs and cerebellum was homogenized in homogenization buffer by 12 strokes with Potter S (Sartorius) at 900 rpm and 4°C. A S1 sample was collected from the supernatant after 10 minutes centrifugation at 1,400 g 4°C. S2 and P2 samples were collected from the supernatant and pellet after 10 minutes centrifugation at 14,000 g 4°C. P2 pellets were then solubilized in DOC buffer overnight at 4°C. Lysates were centrifuged for 10 minutes at 16,000 g and supernatants then dialyzed against dialysis buffer overnight at 4°C. Visking dialysis tubings 27/32 with exclusion limit of 14,000 Dalton

(Serva) were first washed with distilled water and used for this purpose. Dialyzed extracts with 100 µg of total protein – determined by Pierce BCA Protein Assay (Thermo Scientific) – were then incubated with 4 µg BRAG2-specific or control IgG (Santa Cruz) for 2.5 hours at 4°C. Antibody complexes were precipitated by Protein A agarose (Roche) for 2 hours at 4°C. Samples form the supernatants were denatured for 5 minutes at 95°C in DTT buffer or Lämmli buffer. The agarose was washed three times with Triton buffer. Finally, bound proteins were eluted for 10 minutes at 95°C in DTT or Lämmli buffer.

Calmodulin pulldown

Triton buffer

50mM Tris (Carl Roth) pH 7.5, 0.1% Triton X-100 (Sigma), 1x EDTA-free protease inhibitor mix (Roche)

Procedure

An N-terminally FLAG-tagged BRAG2 with and without an R146A mutation in the IQ motif were over-expressed in HEK293 cells and purified. After lysis of washed cells by sonication in 50 mM Tris pH 7.5, lysates were adjusted to 1% Triton and clarified at 100,000 g for 30 minutes at 4°C. Calmodulin affinity resin (Stratagene) was then incubated with supernatants for 1 hour at 4°C to allow for binding to the calmodulin affinity resin. Samples from the purified supernatant and affinity resin were denatured for 5 minutes at 95°C in DTT buffer or Lämmli buffer. Remaining affinity resin was then separated into fresh tubes. Pulled-down BRAG2 was eluted from resin-bound calmodulin by adding 50mM Tris pH 7.5 with 1% Triton and different calcium concentrations as indicated, and incubated for 1 hour at 4°C. After incubation, the affinity resin was washed three times with Triton buffer. Alternatively, 1 volume of 10x-calcium stocks was added to 9 volumes of 100,000 g supernatants to reach the indicated final concentrations, and directly incubated with washed affinity resins for 1 hour at 4°C, before final washing with Triton buffer. 2 mM EDTA were used to chelate calcium in calcium-free controls. Bound proteins were always eluted for 10 minutes at 95°C in DTT buffer or Lämmli buffer. Samples from the clarified supernatants and pulldowns were assayed for immunoreactivity of FLAG on Western blot.

Arf6 activity assays (GST-GGA3-pulldown)

Lysis buffer

50 mM Tris (Carl Roth) pH 7.5, 2 mM magnesium chloride (Merk), 100 mM sodium chloride (Carl Roth), 1% Triton X-100 (Sigma), 0.5% sodium deoxycholate (AppliChem), 0.1% sodium dodecyl sulphate (Serva), 10% glycol (Carl Roth), 1x EDTA-free protease inhibitor mix (Roche)

Wash buffer

50 mM Tris (Carl Roth) pH 7.5, 2 mM magnesium chloride (Merk), 100 mM sodium chloride (Carl Roth), 1% Nonidet P-40 (AppliChem), 10% glycol (Carl Roth), 1x EDTA-free protease inhibitor mix (Roche)

Procedure

For Arf6 activity pulldowns with GST-GGA3, as described by SANTY LC AND CASANOVA JE, 2001, Arf6-HA over-expressing HEK293-BRAG cell pellets or cortical neurons were lysed on ice in lysis buffer. Lysates were incubated for 30 minutes at 4°C and centrifuged at 100,000 g for 15 minutes. Small samples from

the supernatants were denatured for 5 minutes at 95°C in DTT buffer or Lämmli buffer. Supernatants were diluted 4-fold in lysis buffer for HEK293 cell and primary neuronal culture extracts and 2-fold for HEK293-BRAG cell extracts, and incubated with GST-GGA3-bound glutathione-sepharose (GE Healthcare) for 30 minutes at 4°C. After incubation the sepharose was washed three times with wash buffer and denatured for 10 minutes at 95°C in DTT buffer or Lämmli buffer. Samples were assayed for immunoreactivity of Arf6 or HA on Western blot.

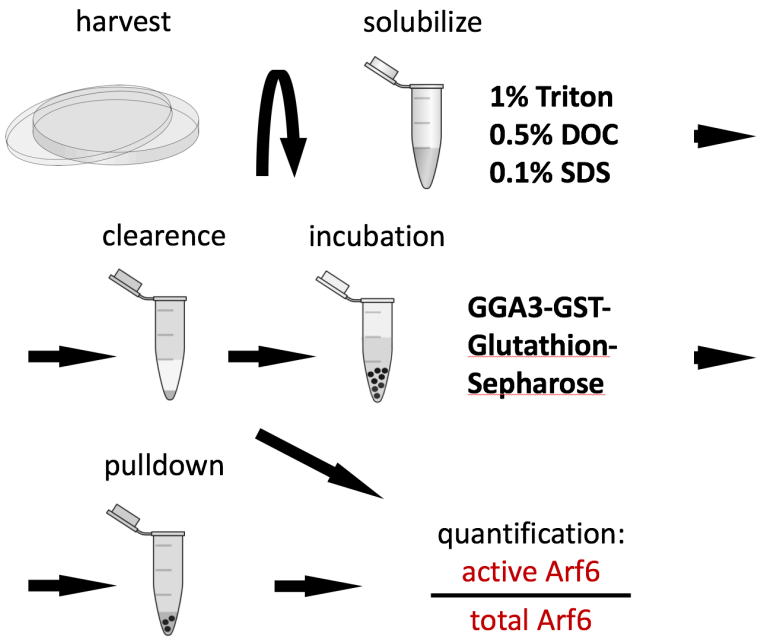

Figure, *Arf6 activity assay.*

Arf6 is extracted from cell lysates in a Triton, deoxycholate and sodium dodecyl sulfate (SDS) containing buffer. Membrane fractions are then removed by ultracentrifugation, and supernatants used as pulldown input. The amount of pulled down Arf6-GTP is compared to total cellular Arf6 levels, to yield a normalized value (pulldown-total-ratio) for the quantification of active Arf6.

Brain slices from GFP-expressing *Iqsec1*$^{fl/fl}$ mice for spinometry

Mice were anesthetized with 50 mg/kg ketamine and 5 mg/kg xylazine cocktail (Sigma) and perfused with 50 ml PBS pH 7.5 at 37°C manually via the right cardiac ventricle. While keeping equal flow speeds, PBS was replaced by 10 ml 4% acid-free formaldehyde (Carl Roth) using a 'v'-shaped valve. Brains were removed and incubated in 5 ml formaldehyde for 15 minutes at 37°C to prevent spine retraction through cooling. Perfused brains were kept overnight at 4°C, and the formaldehyde solution was replaced once with fresh solution on the next day and incubated for at least another day. Brains were embedded in 10% gelatine (AppliChem) and fixed in formaldehyde overnight at 4°C. Embedded brain blocks were then glued to a metal stage and sliced saggitally by vibratome VT 1000S (Leica) with a thickness of 100 µm. Slices were freed from gelatine, briefly dried on microscope slides (VWR), mounted with MOWIOL (Sigma) and covered with glass slips (Carl Roth). To prevent tissue damage, the slides were kept in the dark in a dry place to allow the mounting to harden. Genotypes were determined by colleagues not involved in the imaging and imaging was performed without the knowledge of the genotype of the analyzed mouse. Acquired results were matched with the genotype only after analysis was finished.

Confocal microscope imaging

For visualizing dendritic protrusion of cortical neurons, confocal images were produced from fixed tissue sections of ΔctxBRAG2- and ctrl-mice. Since they provided the clearest signals without excessive background, we decided to analyze secondary dendrites of the main apical dendrite of cortical layer 5 neurons that were branching near or into cortical layer 3. Applying Leica's software LAS AF, z-stacks of 0.2 µm to 0.5 µm step sizes were taken (to stay close to the Nyquist criterion) using a Leica SP5 inverted confocal microscope with a 1.25 numerical aperture, 63-times magnifying, oil-immersion objective. Scan excitation was done by a 488 nm argon laser. Scanned fields were acquired with an additional 5-time optical zoom and were comprised of 1,023 x 1,023 pixels. This resolution was approaching the possible maximum of the used devices. At the same time, it was supposed to avoid distortions during subsequent measurements by enabling to stack near cubic voxels with volumes around 0.3 μm^3. Further scan settings were optimized to ensure high fidelity of subsequent spine morphometry: Gain was set at 800 V. Three frame averages and two line averages proved to reduce noise to the minimum. Scan speed and pinhole size were kept at default values for not improving spine detection of our tissue properties in theory. Spine parameters were then evaluated with the spine detection software NeuronStudio, which measures spine length and spine head diameters using the Rayburst algorithm. Scanned dendrites encompassed a stretch of approximately 50 µm. The first 5-10 µm from dendritic branching points, however, were skipped to avoid systematic bias due to differences of spine numbers along dendrites of excitatory neurons in the neocortex (KATZ ET AL., 2009). After construction of the dendrite model, spines were manually corrected to remove objects recognized as spines, which were not attached to the dendrite, as apparent in the individual stack slices. Automatic recognition had an estimated fidelity of approximately 85%, and only automatically recognized spines were analyzed.

Spinning-disk live cell imaging

Extracellular solution (ECS) pH 7.4

25 mM HEPES (Carl Roth), 140 mM sodium chloride (Carl Roth), 5.4 mM potassium chloride (Carl Roth), 1.3 mM calcium chloride (Merk), 33 mM glucose (AppliChem)

Confocal image stacks of HEK293 cells expressing fluorescent BRAG1 or BRAG2 eGFP-constructs were obtained with spinning-disk confocal microscope Cell Observer (Zeiss) equipped with a 1.25 numerical aperture, 63-times magnifying, oil-immersion objective. Cells were cultured on glass-bottom dishes (World Precision Instruments) and transfected after 2 days in culture to express eGFP-tagged BRAG proteins, alternatively with functional NMDA receptors. On day 4 in culture, cells were washed with PBS pH 7.5 and starved for 1 hour from glutamate in ECS at 37°C. Cultures were then transferred to a heated incubation chamber at 37°C. Individual cells were then video recorded in 10 second-intervals, starting 1 minute before and up to 3 minutes after stimulation with either 5 µM ionomycin or 1 mM glutamate, by acquisition of 10 micron-spaced line-scanned z-stacks. Maximal projections of image stacks were generated by the supplied software (Zeiss) and adjusted by Photoshop.

Softwares

Microplate Manager (BioRad)
Nanodrop (Nanodrop Instruments)
Bio1D (Vilber Lourmat)
Fusion (Vilber Lourmat)
NeuronStudio (CNIC)
Microsoft Word (Microsoft)
Microsoft Excel (Microsoft)
Photoshop (Adobe)
Illustrator (Adobe)
Prism 5 (GraphPad)

Statistical analysis

Results from Arf6 activity assays are expressed as means of active Arf6 ratios ± standard deviation of at least three independent experiments, if not stated otherwise. Arf6 activity was quantified by comparisons of background-corrected intensity densities from active Arf6 pulldowns (pd) and Arf6 totals (in). In the case that a test group received pre-treatment, activity ratios are shown as percentages of the Arf6-GTP change compared to the untreated test group control. Values were obtained by blot imager Fusion FX7 (Vilber Lourmat) and calculated with Microsoft Excel 2003 as pd/in-ratios and percentages of the treatment effect. Graph Pad Prism version 5 was used to prepare graphs and perform statistical analysis, for the accuracy of analysis. Statistical significance of the difference between groups was evaluated by Student's t-test. Comparisons to test group controls were analyzed as dependent pairs. Differences were considered significant at p-values of less than 0.05.

C, Results

Results I, NMDA receptors recruit BRAG family members during the maturation of cortical neurons

C, 1.1, NMDA receptors containing the distinct subunits GluN2B or GluN2A stimulate BRAG1 or BRAG2 Arf6-GEF activity, respectively

In a preliminary experiment performed in a yeast two-hybrid system (not presented here) it appeared that a central region (aa 1038-1237) in the cytosolic domain (CD, aa 839-1464) of GluN2A (Figure 1A top) physically interacted with the Sec7-PH tandem-domains of the BRAG family (aa 741-1083 BRAG1; aa 496-848 BRAG2).

We planned to validate my finding by two interaction assays; a GST pulldown of over-expressed BRAG2 with GluN2A-CD segments (Figure 1A), and immunoprecipitation of endogenous BRAG2 from the brain (Figure 1B). First, I used the identified segment (GluN2ACT200b) and its surrounding segments spanning over the GluN2A-CD (GluN2ACT200a and GluN2ACT200c) to perform GST-pulldowns of BRAG2 containing an N-terminal FLAG-tag (Figure 1A top). Indeed, the segment that induced growth in the yeast two-hybrid system, efficiently and specifically pulled down BRAG2 (Figure 1A bottom).

Next, synaptic proteins were enriched in crude membrane fractionations from adult rat forebrain lysates. GluN2A was precipitated from 100 µg total protein solutions (in) by addition of 2 µg control-, anti-BRAG2- or anti-GluN2A-IgG and antibody beads (IP). Input, precipitate, and supernatant samples collected after incubation (post) were then analyzed on immunoblots (Figure 1 bottom). While control precipitation did not contain GluN2A protein, anti-GluN2A-antibody managed to precipitate GluN2A with high efficiency. Importantly, BRAG2 precipitation showed small amounts of GluN2A co-precipitation (Figure 1B).

This indicated that BRAG2 might be a part of the GluN2A-containing NMDA receptor complex. Functional interactions of NMDA receptors with BRAG proteins have not been studied before.

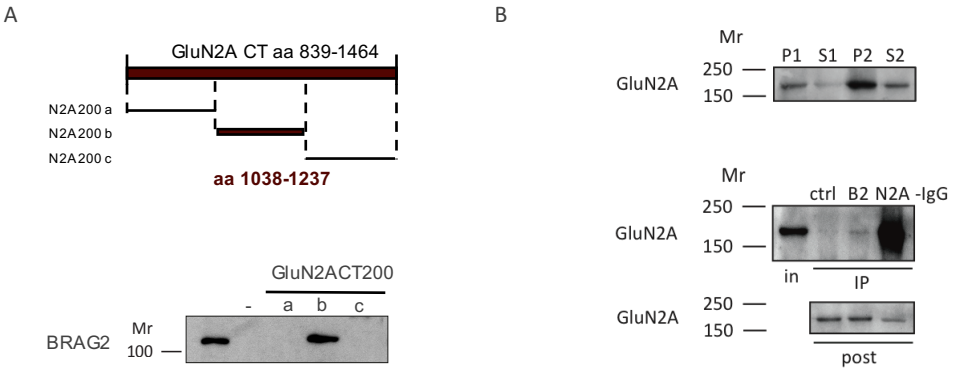

Figure 1, ***BRAG2 interacts with the GluN2A subunit of the NMDA receptor.***

(A) *BRAG2 is pulled down in GST pulldown assays by the cytosolic segment aa 1038-1237 of the rat GluN2A C-terminus.* GST-proteins GluN2ACT200a-c correspond to cytosolic segment of GluN2A aa 838-1037, aa 1038-1237, and aa 1238-1464, respectively. Shown is an immunoblot of recovered BRAG2 from pulldowns in the presence of calcium chelator EDTA. Loaded supernatant samples (in) are 5% of pulldown input.
(B) *GluN2A precipitated with BRAG2 immuo-complexes solubilized in deoxycholate.* Immunoblots of (top) endogenous GluN2A extracted from a PSD-rich fraction of whole rat forebrain (P2), and (middle) co-immunoprecipitated (IP) with an antibody to BRAG2 (B2), GluN2A (N2A) or control (ctrl) IgG. IP supernatants are shown in the blot at bottom. Input samples are 5% of immunoprecipitation input.

Human embryonic kidney (HEK)293 cells express Arf6 in detectable amounts, which can be solubilized and cleared from membranes with no apparent loss (Figure 2A). To get into a cellular system, I over-expressed N-terminally haemagglutinine (HA)-tagged Arf6 in HEK293 cells (Figure 2A) and co-expressed recombinant BRAG1 or BRAG2 to measure whether they can increase the fraction of GTP-bound Arf6 in these cells (Figure 2B).

Extracts from the different HEK293 cell cultures with solubilized Arf6 were clarified from membranes by ultracentrifugation (in, input) and subsequently used to measure their relative active-Arf6 fraction. In order to pull down activated Arf6, I prepared GST-coupled rat Golgi-localized, gamma adaptin ear-containing, ARF-binding protein 3 (GGA3). GGA3 has been used and optimized for Arf6-GTP-specific pulldown assays before (i.e. SANTY AND CASANOVA, 2001), after appearing in Arf6 interaction assays, and being identified as an Arf6 effector. This Arf6 activation assay uses GGA3's ability to bind Arf6 exclusively in its GTP-bound form, allowing the experimenter to monitor the amount of cellular Arf6 in this phase of its activation cycle.

Through incubation with clarified cell lysates, Arf6-GTP was pulled down by glutathione-coupled sepharose loaded with GST-GGA3 (pd, pulldown, Figure 2B). Comparing the Arf6 pulldown-fraction (pd) to the total cellular-fraction (t) quantifies a normalized Arf6-GTP-ratio, which is useful to report the activation state of Arf6 between different conditions. Conclusively, the ratio of active-Arf6 in the pulldown samples of the examined HEK293 cells was increased when co-expressed with either of the two BRAGs.

BRAG1 and BRAG2 over-expression induced therefore a manifold Arf6 activation in this over-expression system. Although, BRAG2 is able to activate Arf4 and Arf5, members of the Arf family class 2, due to the methods applied, the substrate in focus will exclusively be Arf6 in the following.

We decided to express functional NMDA receptors containing the regulatory subunits GluN2A or GluN2B along with Arf6 in HEK293-BRAG cells (BRAG1 or BRAG2 over-expressing HEK293 cells: HEK-BRAG1, HEK-BRAG2, see p. 19), and to assess whether there is a functional relevance behind these potential interactions. Detection of extracts on immunoblots from these cells showed that GluN2A and GluN2B in co-transfections with the GluN1-1a subunit are expressed with BRAG1 and BRAG2 in all four possible combinations (Figure 2C). Reasonably, GluN2 expression in HEK293 cells depended on how much DNA of the obligatory subunit GluN1 was transfected (Figure 2D), especially for GluN2A expression.

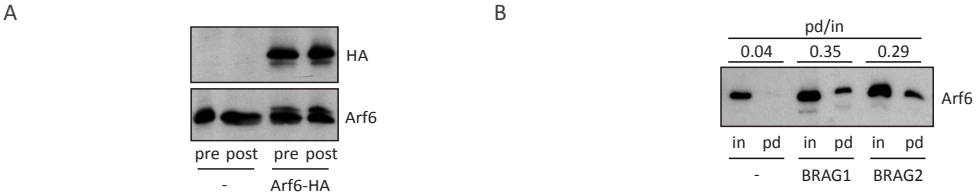

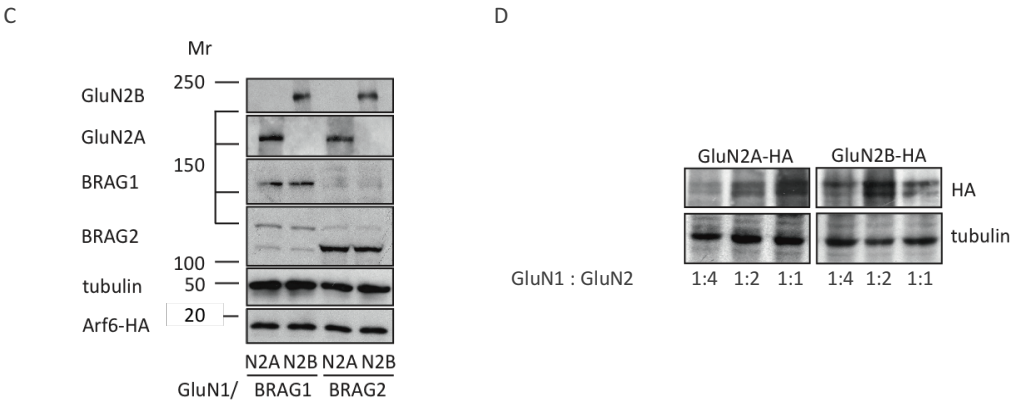

Figure 2, NMDA receptor, BRAG and Arf6 expression in HEK293 cells.

(A) *HEK293 cells express Arf6.* Endogenous Arf6 and over-expressed haemagglutinine (HA)-tagged Arf6 in HEK293 before (pre) and after (post) ultra-centrifugation, detected on immunoblots with Arf6- and HA-specific antibody.

(B) *BRAG over-expression in HEK293 cells increases amount of active Arf6.* Immunoblot-detected expression of Arf6 and its Arf6-GTP fractions after Arf6-GTP-specific pulldown assays from HEK293 cells. Cells were co-transfected with Arf6-HA (Arf6) and eGFP (-), BRAG1-eGFP (BRAG1) or BRAG2-eGFP (BRAG2) and cultivated for 48 hours before harvest. Arf6 activity levels were calculated as density ratios between Arf6-GTP and total Arf6 bands (pd/in) and indicated above the bands. *(Arf6 activity compared to empty transfection (-) in fold-changes: BRAG1: 8-fold, n=1; BRAG2: 7-fold, n=1)* Input samples are 5% of pulldown input.

(C) *Expression of Arf6-HA and NMDA receptors in HEK293-BRAG cells.* Immunoblots of functional GluN2A- and GluN2B-containing NMDA receptors in HEK-BRAG1- and HEK-BRAG2 cell lines, as detected by protein-specific antibodies.

(D) *Expression of GluN2A-containing receptors depends on GluN1 subunit.* NMDA receptor expression of GluN1/2A and GluN1/2B with increasing ratios of GluN1-1a co-expression detected on immunoblots of HEK293 cell lysates.

α-tubulin was detected as loading control. Mr, relative molecular mass.

Next, these cultures were stimulated with the endogenous NMDA receptor ligand L-glutamate. Arf6 activity assays after receptor stimulation surprisingly showed, when GluN2A and BRAG2 or GluN2B and BRAG1 were over-expressed in the cells, active-Arf6 levels were increased (Figure 3A). The increases were robust and statistically significant, although hardly passing 200%. When NMDA receptors were stimulated in the presence of BRAG proteins in the remaining two pairings (GluN2A and BRAG1 or GluN2B and BRAG2) Arf6 activity sunk below basal levels.

These results indicated that NMDA receptor subunits and BRAG family members synergized in specific pairs to induce Arf6 activation after receptor ligand binding. Opposing this, mismatching BRAG-receptor pairing seemed to cause Arf6-GTP hydrolysis. I repeated this experiment in HEK293 cells not over-expressing BRAG proteins in a constitutive manner, because it appeared plausible that other factors than BRAGs would reduce Arf6 activity upon NMDA receptor stimulation in HEK293 cells. Accordingly, active-Arf6 levels decreased again below basal levels after NMDA receptors containing the regulatory subunits GluN2A and GluN2B were stimulated (Figure 3B). BRAG protein expression was therefore not involved in Arf6-GTP hydrolysis.

Arf6-GTP hydrolysis can be explained by the activity of Arf6-GAPs. In this scenario, over-expression and stimulation of matching NMDA receptor subunits and BRAG family members would have masked a GAP-

induced drop in Arf6-GTP levels through GEF-activity. The drop in Arf6 activation would however become evident in the absence of activated BRAG proteins.

NMDA receptors are the glutamate-activated calcium channels of the central nervous system. Calcium could contribute to BRAG-mediated Arf6 activation because BRAG proteins possess calcium-free calmodulin binding IQ-like domains. To test this assumption, I stimulated HEK293-BRAG cells that co-expressed functional NMDA receptors with the identified BRAG-compatible GluN2 subunit shown in Figure 3A with glutamate, however under calcium-free conditions (Figure 3C).

When calcium was left out from the media, active-Arf6 levels showed no change between basal and stimulated HEK-BRAG1- and BRAG2. This does not only imply that BRAG1- as well as BRAG2-mediated Arf6 activation is calcium dependent, but also that the opposed process reducing Arf6-GTP levels has been obstructed upon calcium depletion. This infers the presence of an Arf6-GAP protein in HEK293 cells, and that the stimulation of NMDA receptors controls its calcium-dependent activity.

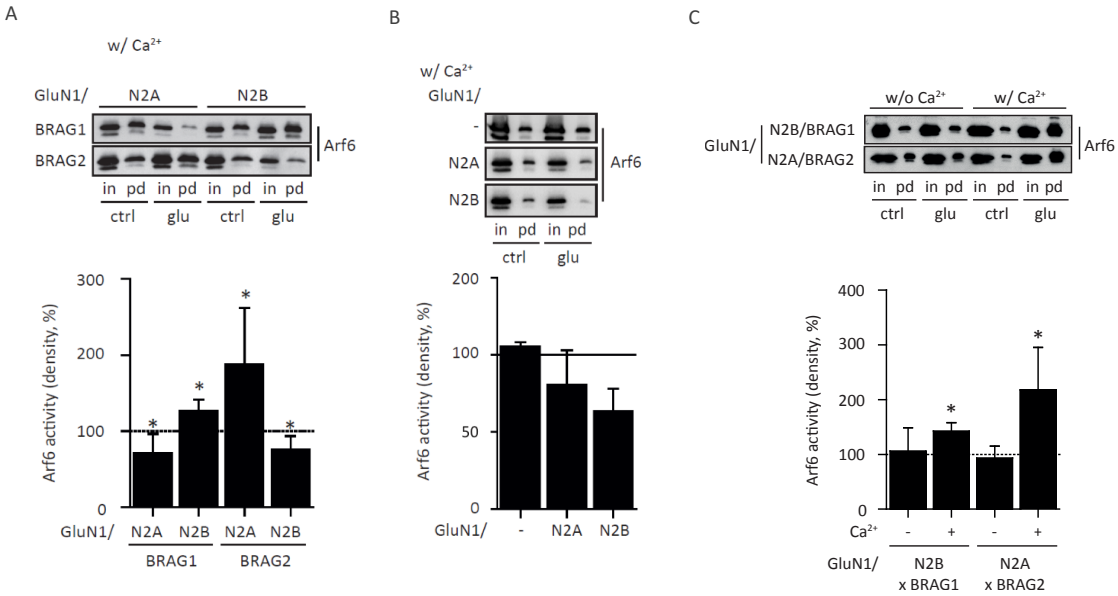

Figure 3, The GluN2A-BRAG2 and GluN2B-BRAG1 signaling axes.

(A) *BRAG1 and BRAG2 are activated by NMDA receptors containing GluN2B or GluN2A subunits.* L-glutamate stimulation (glu) of BRAG1 and BRAG2 in glutamate-deprived, NMDA receptor-expressing (GluN1/N2A or GluN1/N2B) HEK-BRAG1 or HEK-BRAG2 cells in complete extracellular solution (w/ Ca^{2+}). *(BRAG1: GluN1/N2A: 71 ±25.5%, n=9, p= 0.01; GluN1/N2B: 127 ±14.3%, n=6, p= 0.01; BRAG2: GluN1/N2A: 188 ±73.9%, n=6, p= 0.04; GluN1/N2B: 75 ±18.4%, n=6, p= 0.02)*.

(B) *NMDA receptor stimulation induces Arf6-GTP hydrolysis.* L-glutamate exposure (glu) of glutamate-deprived, NMDA receptor-expressing (GluN1/GluN1, GluN1/N2A or GluN1/N2B) HEK293 cells – notably, not over-expressing BRAG proteins – in complete extracellular solution (w/ Ca^{2+}). *(GluN1: 106 ±2.5%, n=2; GluN1/2A: 81 ±22.2%, n=2; GluN1/2B: 64 ±14.8%, n=2)*.

(C) *NMDA receptor-triggered changes in Arf6 activity require the presence of extracellular calcium.* L-glutamate stimulation (glu) of HEK-BRAG1 or HEK-BRAG2 cells in complete (w/ Ca^{2+}) or calcium (Ca^{2+})-free (w/o Ca^{2+}) extracellular solution. Cells are expressing functional GluN2A-containing (GluN1/N2A) and GluN2B (GluN1/N2B) receptors, respectively. *(BRAG1 x GluN2B: without calcium: 106 ±42.1%, n=11, p= 0.63; with calcium: 143 ±15.0%, n=6, p= 0.01; BRAG2 x GluN2A: without calcium: 94 ±21.6%, n=8, p= 0.81; with calcium: 218 ±77.3%, n=6, p= 0.01)*.

Bars depict mean percentage changes in Arf6 activity ± standard deviation after L-glutamate stimulation, calculated as density ratios between Arf6-GTP and total Arf6 (pd/in) and normalized to untreated controls (ctrl). Input samples are 2.5% of pulldown input in all experiments.

C, 1.2, GluN2B-receptors regulate BRAG1-mediated Arf6 activation in cortical neuron cultures at early stages.

The ratio of NMDA receptor subunits and the amount of synaptic AMPA receptors in relation to them are so far the most reliable indicators for synaptic maturation (Wu et al., 1999; Bellone and Nicoll, 2007; and many others). To capture a rough picture of synaptic changes, I analyzed the regulation of glutamate receptor subunit protein levels during neuron development, and compared them to those of endogenous BRAG1 and BRAG2 proteins. On immunoblots, I assessed their expression in nuclear-free supernatants of mouse forebrain lysates (Figure 4A), and in lysates of primary cortical cultures from mouse pups (Figure 4B). Since average synapse maturation takes place around two weeks after birth (Li et al., 2010), five appropriate time points for brain lysates (postnatal day (P) 1, 7, 14, 21, and adult) and two time points for neuron culture lysates (day in vitro (DIV) 8 and 22) were analyzed.

Around birth (P/DIV 1), GluN2B-receptors assist neuronal progenitor cells to mature into a network of extensive dendritic trees with functional synapses (around P/DIV 21). In later stages, they are involved in the activation of immature synapses. In forebrain lysates, GluN2B expression increased during the first two weeks of postnatal brain development. For the remaining assessed time points, GluN2B was expressed at mediocre levels comparable to the first week. In contrast, cortical cultures kept expressing GluN2B at higher levels after three weeks compared to one week in culture, and displayed a relation in expression that resembled the earlier levels in brains between one and two weeks after birth. Assuming that it is a reliable marker of immature synapses, the higher GluN2B expression may indicate that synaptogenesis or immature synapses persist for a longer period of time in cortical neuron cultures than in forebrain tissue. GluN2A expression in the brain also increased during the first two weeks after birth, but remained high until adulthood. In line with literature, after three weeks of cortical development GluN2A expression has surpassed GluN2B expression in the forebrain. Cortical cultures also showed a large increase in GluN2A expression, although the ratio of GluN2A to GluN2B did not resemble the situation in the brain. This is a strong indicator that spontaneous activity in neuronal cultures is enough to induce synaptic maturation, however, the well-described subunit switch from GluN2B- to GluN2A-dominance in NMDA receptors of cultured cortical neurons is not as evident here as that of neurons in the forebrain.

BRAG1 and BRAG2 proteins were also increasingly expressed in the forebrain throughout the life of the assessed mice. Generally, expression of BRAG1, BRAG2 and GluN2A ran in parallel, while GluN2B expression plummeted after the initial increase for two weeks after birth. In its profile, GluN2B expression resembled the expression of GluN1.

In regards to the functional Arf6 activation pathway shown in Figure 3A, GluN2A and BRAG2 expression upregulation in cortical neurons was only induced after three weeks in culture, and GluN2B and BRAG1 were both expressed at the early time point DIV 8. These expression patterns are likely to have a functional significance.

As a reference, the principal subunit of AMPA receptors GluA2 and the principle subunit of NMDA receptors GluN1 were detected in the cultures as well. Their increased expression suggested that the synapses in the assessed cultures have matured during their three weeks in vitro, as expected.

Then, the neuron cultures from embryonic rat cortices were used to measure their basal active-to-total Arf6 ratio at DIV 7 and DIV 21. I also assessed the contribution of NMDA receptor activity to the formation of basal Arf6-GTP levels by treating one group of each age for one hour with the general NMDA receptor antagonist aminophosphonovaleric acid (AP5, Figure 4B).

Arf6-GTP pulldowns showed that NMDA receptor activity elevated active-Arf6 levels, surprisingly however only in young neurons. While AP5 treatment decreased active-Arf6 levels in neurons at DIV 7, neurons on DIV 21 neurons lacked intrinsic NMDA receptor-driven Arf6 activation and was basally at comparable levels to DIV 7 neurons after NMDA receptor blockade. Contrary to Arf6-GTP, total Arf6 levels did not decrease throughout maturation in cortical neuron cultures.

Effects of Arf6 activity in dendritic spines were shown to be different depending on the age of neuron cultures (Kim et al., 2015). Here we showed that activation mechanisms of synaptic Arf6 might also differ between neuronal ages.

In NMDA receptor-expressing HEK293-BRAG cells, specific pairing between BRAGs and GluN1/2 receptors was responsible for glutamate-triggered Arf6 activation (Figure 3A). Therefore, the same signalling axes may exist in neurons. For further investigations it was necessary to exclude either of the two assessed BRAG proteins from the neuron cultures, when it was needed. We also wanted to know beforehand whether this manipulation affects the other investigated factors that might be involved in Arf6 activation. For this goal, I analyzed cortical neuron cultures depleted from BRAG1 (B1-RNAi) or BRAG2 (B2-RNAi), or both (B1/2-RNAi), by RNA interference (RNAi) at DIV 2 or 15 and detected NMDA receptor subunits GluN2A and GluN2B on immunoblots at DIV 7 or 21 respectively (Figure 4C).

This process effectively depleted neurons from BRAG proteins (Figure 4C). As control, cultures were infected with a virus carrying a scrambled shRNA version of BRAG2 (ctrl-RNAi), which did not affect BRAG protein expression. This protein expression assay showed that except to the target proteins, none of the assessed proteins was affected by the RNAi of BRAG proteins. Only when both proteins were depleted simultaneously, total levels of NMDA receptor expression (reflected by GluN1 expression) were decreased. This might implicate BRAG1 and BRAG2 in the general basal NMDA receptor turnover in neurons.

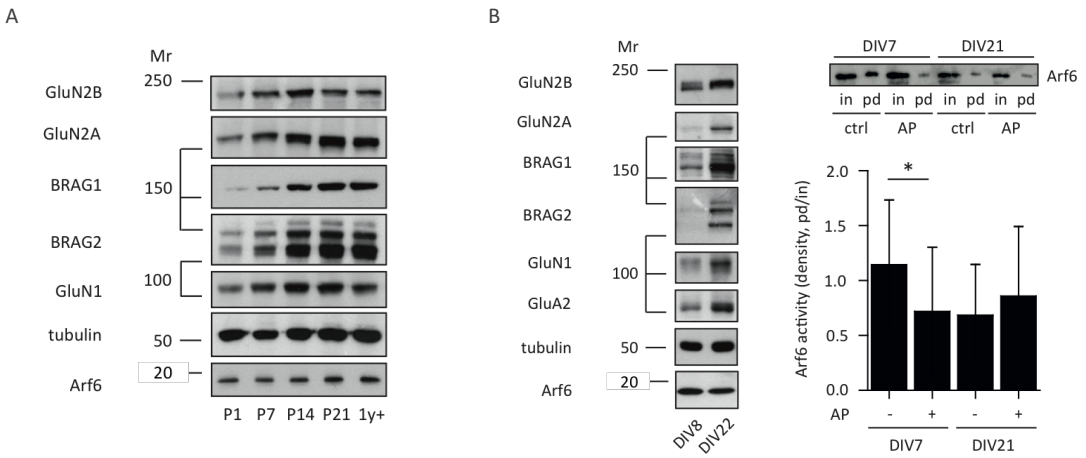

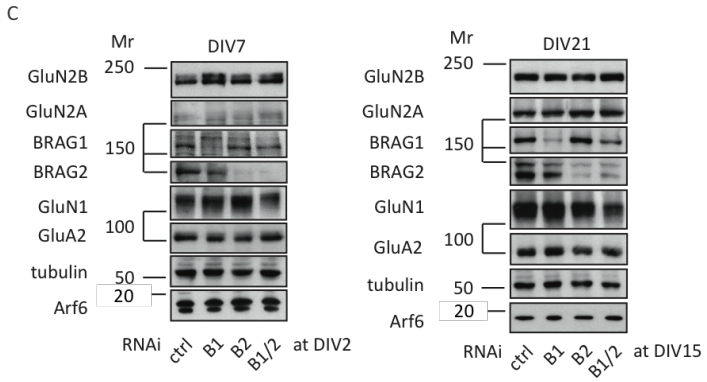

Figure 4, Arf6 activation is different in neuronal cultures before and after maturation in vitro.

(A) (B left) *Age-dependent differences in expression of endogenous BRAG1, BRAG2, Arf6 and important NMDA receptor subunits* of (A) forebrains between 1 and 21 postnatal days (P) and adult age (1y+), or (B left) cortical neuron cultures at 8 and 22 days in vitro (DIV) after isolation at fetal stage E18.
(B right) *Relative Arf6 activity is higher at DIV7 than at DIV21, and is mediated by NMDA receptors.* Endogenous Arf6 activity in one-week and three-weeks-old cortical neuron cultures with and without one-hour treatment with D-AP5 (AP). Bars illustrate means of active to total Arf6 ratios ± standard deviation, calculated as density ratios between active Arf6 ratios to total Arf6 (pd/in) *(DIV7: without AP: 1.2 ±0.59, n=8; with AP: 0.7 ±0.59, n=8; p=0.01; DIV21: without AP: 0.5 ±0.33, n=6, p=; with AP: 0.6 ±0.42, n=6, p= 0.57; DIV7 versus DIV21 p=0.04)*. Input samples are 5% of pulldown input.
(C) *RNAi of BRAG1 or BRAG2 do not change the expression of endogenous Arf6 and selected AMPA and NMDA receptor subunits. RNAi of both reduces the expression of the principal receptor subunit GluN1.* Proteins were detected on immunoblots of neuronal culture cell lysates at DIV7 or DIV21 after RNAi at DIV2 or DIV15, respectively. ß-tubulin was detected as loading control. Mr, relative molecular mass.

Since the expression analysis indicated that there is an age-dependent regulation in the expression of the two principal regulatory NMDA receptor subunits in neuron cultures, the possibility that Arf6 activation is controlled by NMDA receptors in a subtype-selective manner at different stages of cortical neuron maturation appeared realistic. NMDA receptor blockage was the simplest approach to assess if Arf6 activation in young cultures is promoted by one specific subtype. In the chapter Materials and Methods, I described frequently used pharmacology interfering with NMDA receptor activity. To isolate effects of GluN2B-receptors from receptors which also contain the GluN2A subunit, the appropriate drugs to use were ifenprodil and zinc.

Seven-days-old cultures were treated for one hour with either GluN2B-specific ifenprodil or GluN2A-specific zinc and active-Arf6 pulldowns were subsequently performed (Figure 5A). To remember, both drugs act through similar mechanisms on NMDA receptors. As expected, ifenprodil treatment significantly reduced basal Arf6 activity by blocking the highly expressed GluN2B-receptors. The functionality of GluN2B has often been connected to developmental aspects of immature synapses. Also to mention, the GluN2B subunit was detected in young neuron cultures while the GluN2A subunit was almost not detectable (Figure 4B). Active-Arf6 levels of young neurons showed a similar drop after treatment with ifenprodil, as with AP5 (Figures 3B, 4A, ca. 70% and 63% compared to the controls, respectively). This indicated that stimulation of GluN2B-receptors mediated synaptic Arf6 activation in one-week-old neuronal cultures.

To identify the responsible BRAG protein, cortical neuron cultures depleted from BRAG1 or BRAG2 were treated for one hour with ifenprodil (Figure 5B, 5C). The contribution of GluN2B-containing receptor stimulation to Arf6 activation was calculated and showed that GluN2B-triggered Arf6 activation was

missing in BRAG1-depleted neurons, pointing to a functional GluN2B-BRAG1 signalling axis that increased active-Arf6 levels in young neuron cultures (Figure 5D). As before, GluN2B activity (in the absence (-) of ifenprodil) reduced Arf6-GTP levels when the functional BRAG was missing, and we assumed that NMDA receptor-Arf6GAP signalling was responsible for this. GluN2B activity blockade also revealed that for unclear reasons Arf6-GTP levels were higher in neurons lacking BRAG1. BRAG1 expression in itself led to lower basal Arf6-GTP levels (Figure 5C), which is unusual for an Arf6-GEF and requires further study.

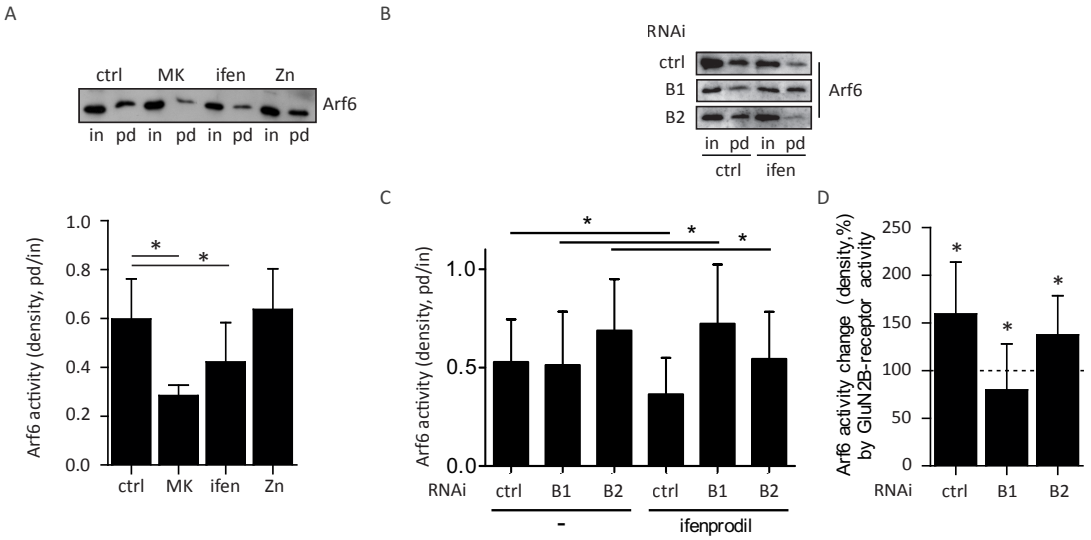

Figure 5, Functional GluN2B-BRAG1 signalling axis in young neurons.

(A) *Subunit-selective GluN2B-receptor control over Arf6 activation in young neurons.* Arf6 activity in one-week-old cortical neuron cultures after a one-hour treatment with the NMDA receptor channel blocker dizocilpine (MK) GluN2B blocker ifenprodil (ifen) or the GluN2A blocker zinc (Zn). Bars illustrate mean active Arf6 ratios ± standard deviation, calculated as density ratios between active and total Arf6 (pd/in) *(control: 0.6 ±0.17, n=8; ifenprodil: 0.4 ±0.16, n=8; zinc: 0.6 ±0.17, n=6; versus control: ifenprodil p=0.01; zinc p=0.83)*. Input samples are 5% of pulldown input.
(B,C,D) *GluN2B-mediated Arf6 activation is blocked and GluN2B-receptor activity reduces active Arf6 levels in BRAG1-depleted young neurons.* Blockade of GluN2B-containing NMDA receptor activity in one-week-old cortical neuron cultures infected with lentiviri delivering control short hairpin (sh) RNA (ctrl) or shRNAs for BRAG1 or BRAG2 (B1 or B2) RNAi after 2 days in vitro. (B) Immunoblots of active Arf6 assay with neurons treated for one hour with (ifen) or without ifenprodil (ctrl). (C) Shown are mean active Arf6 ratios ± standard deviation, calculated as density ratios between active and total Arf6 (pd/in) *(w/o ifenprodil, RNAi control: 0.53 ±0.22%, n=9; B1-RNAi: 0.52 ±0.27, n=11; B2-RNAi: 0.57 ±0.22, n=10; w/ ifenprodil, RNAi control: 0.36 ±0.19, n=9; B1-RNAi: 0.72 ±0.30, n=11; B2-RNAi: 0.45 ±0.20, n=10)*. (D) Shown are mean percent-changes in Arf6-GTP levels by GluN2B-containing NMDA receptor activity, normalized to ifenprodil-treated controls (ifen) ± standard deviation *(RNAi control: 160 ±54.1%, n=9, p=0.02; B1-RNAi: 80 ±48.2%, n=11; p=0.03; B2-RNAi: 138 ±41.0%, n=10; p=0.01)*. Input samples are 5% of pulldown input.

Finally, we tested if exposure of unstimulated GluN1/2B receptors to ifenprodil would reduce Arf6 activity. We confirmed that ifenprodil did not affect Arf6 activity in GluN1/2B receptor-expressing HEK-BRAG1 cells (not presented) ruling out off-target drug effects. Surprisingly, in the same experiment simple presence of GluN1/2B receptors caused a clear trend for Arf6 activation in HEK-BRAG1 cells, while GluN1/2A expression did not. Therefore, I repeated this experiment in all four combinations, to elucidate whether this effect was GluN2B-BRAG1-specific. Indeed, GluN2B-expressing HEK-BRAG1 cells specifically showed a higher active-Arf6 level (Figure 6), which we knew was ifenprodil-insensitive. This effect was not further tested in neuronal cultures, although it might also be present and/or modified there.

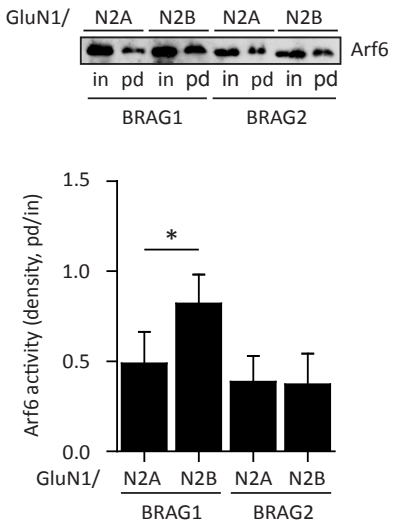

Figure 6, GluN2B-containing NMDA receptors trigger tonal Arf6 activation via BRAG1.

Arf6-GTP measurement in glutamate-deprived, GluN2A-containing or GluN2B-receptor-expressing (GluN1/N2A or GluN1/N2B) HEK- BRAG1 and BRAG2 cells in complete extracellular solution (w/ Ca^{2+}). Bars illustrate means of active to total Arf6 ratios ± standard deviation *(BRAG1: GluN1/N2A: 0.5 ±0.18%, n=7; GluN1/N2B: 0.8 ±0.16%, n=7, p= 0.01; BRAG2: GluN1/N2A: 0.4 ±0.14%, n=4; GluN1/N2B: 0.4 ±0.17%, n=4, p=0.78)*.
Input samples are 5% of pulldown input.

C, 1.3, Activated NMDA receptors stimulate BRAG2 Arf6-GEF activity in cortical neuron cultures at mature stages.

Blocking NMDA receptor activity in three-weeks-old neurons with AP5 did not decrease Arf6-GTP levels (Figure 4B), in contrast to one-week-old cultures. Therefore, we planned to elaborate if NMDA receptor-driven Arf6 activation is functional in highly BRAG1/BRAG2/GluN2A/GluN2B-expressing mature neurons. We decided to follow the crude but simple approach to stimulate three-weeks-old cortical neuron cultures with the specific agonist NMDA. Arf6-GTP levels started to accumulate three minutes after 100 µM NMDA was added to the medium (Figure 7A). This pointed to a physiological response building up GTP-exchange in Arf6, due to increased NMDA receptor stimulation.

To isolate NMDA receptor effects in this assay, I performed NMDA stimulation in the presence of tetrodotoxin (TTX), which abolishes spontaneous firing and prevents neurons from network activity carried by all glutamate receptors. After a one-hour blockage of glutamate release by action potentials, NMDA stimulation still increased Arf6-GTP levels to the same extent as in the presence of network activity (Figure 7B top).

The set up of three-weeks-old neuron cultures seemed appropriate to test further age-related differences in Arf6 activation. I started with an NMDA stimulation profiling with three, five and ten minutes time points. Only five minutes of 100 µM NMDA stimulation activated Arf6 with statistical significance (Figure 7C). Interestingly, ten-minute exposures did not show any elevation in Arf6 activity compared to unstimulated cells.

Neurons that were stimulated for five minutes with 100 µM NMDA and then kept in incubation in NMDA-free medium again, showed a sustained increase in Arf6-GTP levels at least up to ten minutes following stimulation (Figure 7D). This elevated GTP-bound Arf6 level slowly returned closer to basal only about half an hour after NMDA stimulation has stopped. Arf6-GAPs may not have been stimulated enough to cause Arf6-GTP hydrolysis, when compared to neurons that were continually stimulated with NMDA for 10 minutes. If neurons in fact expressed NMDA receptor-driven Arf6-GAPs, the balance of GEF and GAP effects at different NMDA receptor signalling conditions may have resulted into different outcomes of final Arf6-GTP levels. In specific, short boosts of NMDA receptor activity seemed to stimulate the Arf6-GEFs BRAG, and longer receptor stimulation might have additionally activated unidentified Arf6-GAPs.
Furthermore, NMDA-mediated Arf6 activation was blocked, when AP5 was mixed into the stimulation medium (Figure 7E), which identifies the NMDA receptor and its ligand binding as the initiators of the previous Arf6 reactions. NMDA stimulation of neuronal cultures in the presence of dizocilpine (see Materials and Methods), to prevent charge transfer via NMDA receptors showed no change in Arf6-GTP levels (Figure 7E), adding to the mentioned model of calcium-dependent BRAG activation, and theoretically to calcium-dependent Arf6-GAP activation. NMDA stimulation of one-week-old neurons also elevated Arf6-GTP levels (Figure 7F) that could be blocked by AP5 or dizocilpine. BRAGs seemed to share similar activation mechanisms at all stages of maturity, although NMDA receptor stimulation in mature neurons might have promoted Arf6-GTP production twice as effectively.

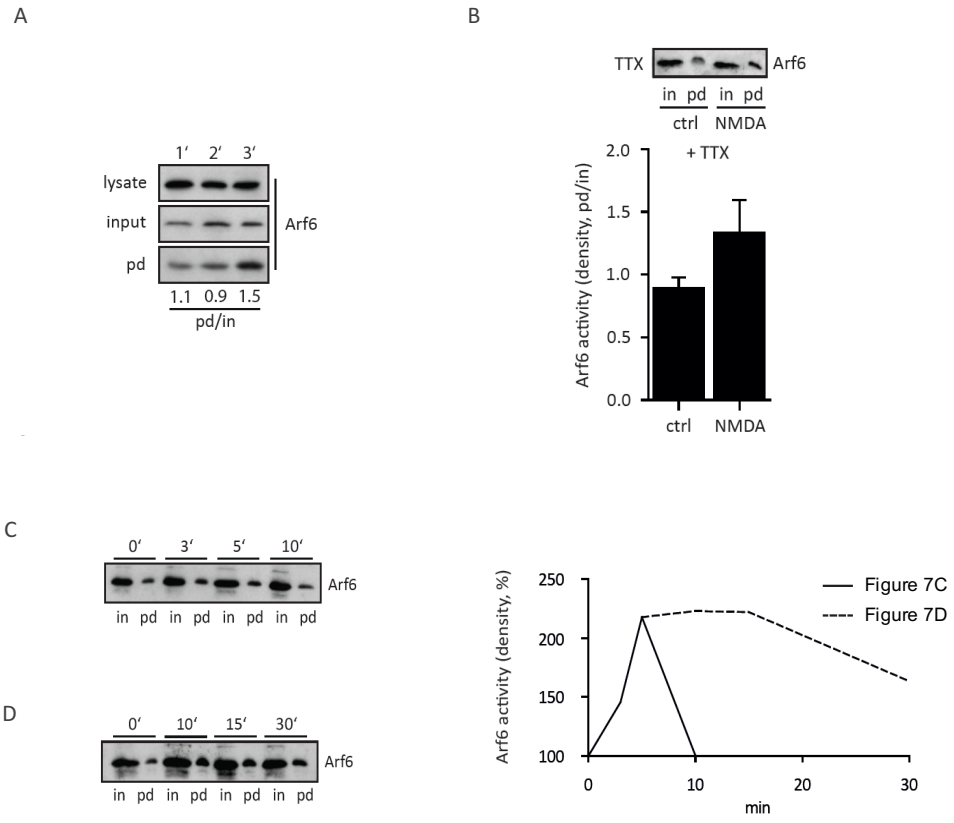

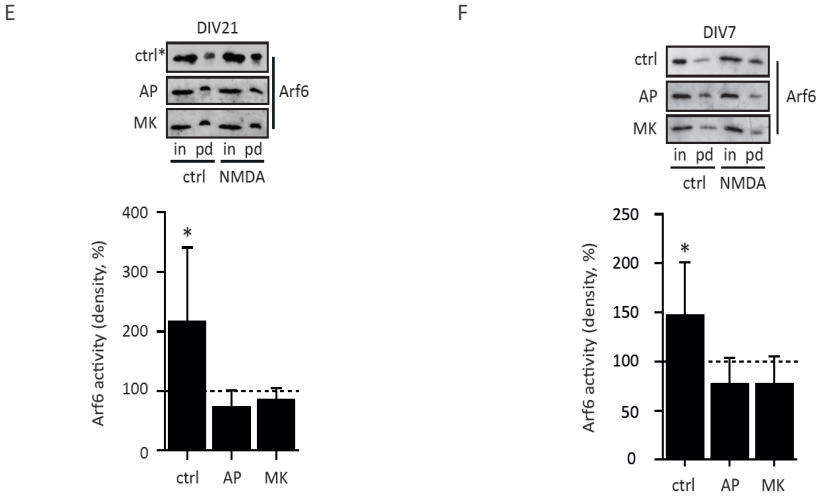

Figure 7, NMDA stimulation profile of Arf6 activation in adult cortical neurons.

(A) *Arf6 activity increases in NMDA-stimulated DIV21 cultures.* Three different neuron cultures of approximately 10^6 cells were treated for 1, 2, or 3 minutes with 100 µM NMDA. The neurons were harvested (lysate) and freed from membranes by ultra-centrifugation (inputs) before being used for the GST-GGA3 pulldowns (pd). Active to total Arf6 input ratios (pd/in) are indicated below the blots.
(B) *NMDA-triggered Arf6 activation is not related to network activity.* Neurons were stimulated with and without a one-hour pre-treatment with tetrodotoxin (TTX). Bars show average percentages of Arf6-GTP increase ± standard deviation *(TTX: without NMDA 0.9 ±0.09, n=3; with NMDA 1.3 ±0.26, n=3)*.
(C) *NMDA triggers Arf6 activation after appropriate stimulation.* Neurons were stimulated for 3, 5, or 10 minutes and normalized to untreated cells (ctrl) *(top, 3 minutes: 146 ±15.8%, n=4; 5 minutes: 218 ±121%, n=4; 10 minutes: 100 ±37.4%, n=4; bottom, 5' stimulation +5 minutes (10'): 223 ±118.6%, n=4; +10 minutes (15'): 222 ±83.9%, n=3; +25 minutes (30'): 163 ±107%, n=3)*.
(D) *Arf6 activation does not decrease abruptly after 5 minutes NMDA stimulation.* Cortical neuron cultures were stimulated for 5 minutes, washed and incubated in growth media for another 5, 10, or 25 minutes.
(C,D) The graph shows the average percentage of Arf6-GTP increase throughout the assessed time points.
(E) *NMDA exposure during ion channel or ligand-binding blockade does not increase Arf6 activity.* Three-weeks-old cortical neuron cultures were stimulated for 5 minutes with NMDA with or without the presence of NMDA antagonist D-AP5 (AP) or NMDA receptor channel blocker dizocilpine (MK). Bars depict average percentages of Arf6 activation normalized to unstimulated controls (ctrl) with the same drug treatment ± standard deviation *(DIV21: control: 217 ±124.2, n=15, p=0.01; AP: 73 ±28.0, n=9, p=0.06; MK: 85 ±19.9, n=10, p=0.06)*. (*) Quantification of control group without pre-treatment was added to the graph in Figure 8B to compare extent of Arf6 activation in the parallel experiment.
(F) *NMDA-stimulated Arf6 activation via BRAG has a similar mechanism in young neurons*. One-week-old cortical neuron cultures were stimulated with NMDA with or without the presence of NMDA antagonist D-AP5 (AP) or NMDA receptor channel blocker dizocilpine (MK). Bars illustrate average Arf6 activity (pd/in) normalized to unstimulated controls (ctrl) with the same drug treatment ± standard deviation *(control: 147 ±54.2, n=6, p=0.01; AP: 77 ±27.1, n=6, p=0.09; MK: 77 ±28.7, n=6, p=0.06)*. Input samples are 5% of pulldown input in all experiments.

Next, I stimulated mature neuron cultures with NMDA after selected BRAG depletion. In order to avoid interference with their development, neurons were infected with shRNA-containing viruses after two weeks in culture and assessed a week later (Figure 8A).

After BRAG1 depletion, neuron cultures displayed increased active-Arf6 levels upon NMDA stimulation indicating that NMDA receptors did not signal to BRAG1 to activate Arf6 anymore, after neurons have matured. Surprisingly, presence of BRAG2 was necessary to mediate NMDA receptor-mediated Arf6 activation in three-weeks-old neurons. This submitted that spontaneous activity in the cultures was sufficient to induce synaptic maturation as well as changes in their synaptic NMDA receptor expression (Figure 4B); and apparently a functional switch in BRAG signalling came along with it (Figure 8A).

Similar to BRAG1-depleted young neurons that hydrolyze Arf6-GTP by NMDA receptor activity (Figure 5B), NMDA stimulation of BRAG2-depleted mature neurons induced a significant drop in the amount of active Arf6. Consequently, Arf6-GTP hydrolysis appears to be correlated to NMDA receptor activity at all neuronal stages (Figures 4B, 7A).

When neurons were prevented from expressing BRAG1 and BRAG2 together, Arf6-GTP levels remained unaltered by stimulated NMDA receptor activity, suggesting that BRAGs are the only NMDA receptor-dependent Arf6-GEFs in cortical neurons. In the genome of viruses used for these double knockdowns, shRNA cassettes were inserted in tandem with a single promoter. Therefore, there is the possibility that this set up has reduced the knockdown efficiency (Figure 4D). Nonetheless, the double knockdown was efficient enough to block NMDA-mediated Arf6 activation, although NMDA-mediated Arf6-GTP hydrolysis was not observed either (Figure 8A). Remaining amounts of BRAG in the double knockdown might have thwarted a visible drop in Arf6-GTP levels by NMDA receptor-driven Arf6-GTP hydrolysis.

C, 1.4, GluN2A-containing NMDA receptors signal to BRAG2 to activate Arf6 and maintain the mature GluN2A-BRAG2-mediated signalling pathway at late stages.

To determine which GluN2 subunit is in charge of BRAG2 stimulation, we returned to a similar approach as applied in young neurons; specific receptor blockage. I stimulated mature neuron cultures with a combination of NMDA and ifenprodil or zinc because (1) NMDA receptor-dependent Arf6 activation in mature neurons only became visible after stimulation with NMDA, and (2) ifenprodil and zinc would help to distinguish between subtype-specific NMDA receptor effects by isolating their activities (Figure 8B).

Presence of ifenprodil during NMDA stimulation had no adverse effect on Arf6 activation. Zinc on the other side blocked Arf6-GTP production, inferring that neurons at this stage had switched to GluN2A-BRAG2 signalling to control Arf6 activation. Again, Arf6-GTP was hydrolyzed when the functional pathway, i.e. GluN2A signalling, was blocked during NMDA-stimulation.

Moreover, global reduction in NMDA receptor activity for one hour, i.e. by the treatment of AP5 or dizocilpine, in three-weeks-old cultures induced a slight trend for active-Arf6 build-up. Specific blockage of GluN2A-containing receptors by zinc however caused a clear increase in active-Arf6 levels, whereas ifenprodil did not (Figure 8C).

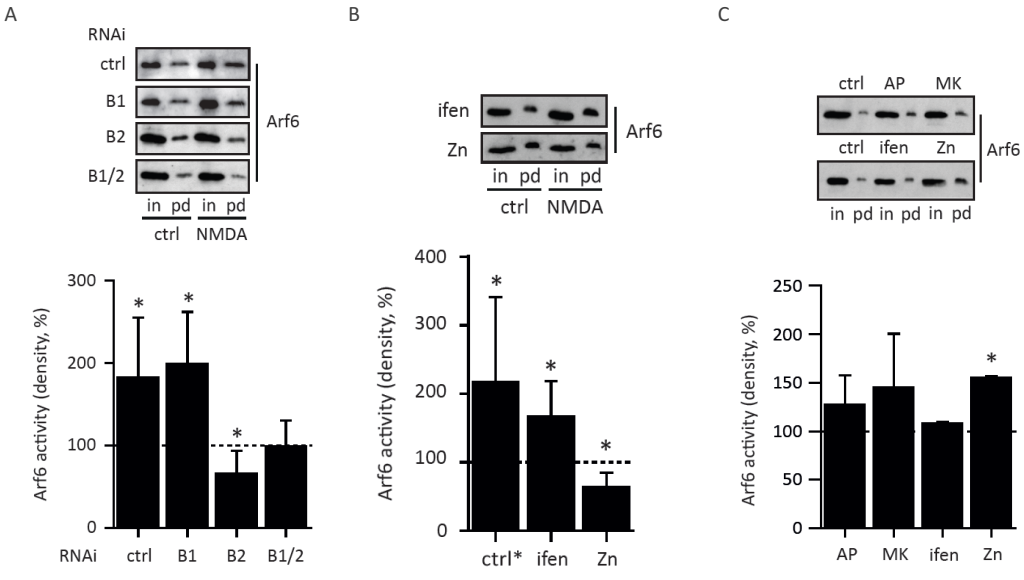

Figure 8, Functional GluN2A-BRAG2 signalling axis in adult neurons.

(A) *NMDA receptor stimulation triggers Arf6 activation via BRAG2 in adult cortical neurons.* NMDA receptor-mediated Arf6 activity was assessed in three-weeks-old cortical neuron cultures infected with lentiviri delivering control short hairpin (sh) RNA (ctrl) or shRNAs for BRAG1 (B1), BRAG2 (B2) or BRAG1 and BRAG2 (B1/2) RNAi after 15 days in vitro. Neurons were treated for 5 minutes with NMDA. Arf6 activity was calculated as the ratio of pulled down Arf6 to total Arf6 (pd/in) at three weeks in vitro. Bars illustrate averaged percentages of NMDA effects after normalization to untreated controls (ctrl) of the RNAi-treated group ± standard deviation *(RNAi control: 183 ±72.7%, n=17, p=0.01; B1-RNAi: 224 ±74.1%, n=8; p=0.01; B2-RNAi: 65 ±24.5%, n=12; p=0.04; B1/2-RNAi: 99 ±31.1%, n=9; p=0.35)*.
(B) *Arf6 activation in adult cortical neurons is stimulated by GluN2A-containing receptors.* Three-weeks-old cortical neuron cultures were stimulated for 5 minutes with NMDA in the presence or absence of the GluN2B blocker ifenprodil (ifen) or the GluN2A blocker zinc (Zn). Bars show averaged active Arf6 ratios (pd/in) normalized to unstimulated controls (ctrl) with the same drug treatment in percent ± standard deviation *(control: 217 ±124.2, n=15, p=0.01; ifenprodil: 167 ±51.4, n=10, p=0.01; zinc: 63 ±21.7, n=10, p=0.01)*. Input samples are 5% of pulldown input. (*) Quantification of control group without drug pre-treatment was added to the graph to compare extent of Arf6 activation in the parallel experiment previously shown in Figure 7E.
(C*) Prolonged NMDA receptor blockage with zinc specifically increases Arf6-GTP levels.* Three-weeks-old cortical neuron cultures were blocked with NMDA antagonist D-AP5 (AP) or NMDA receptor channel blocker dizocilpine (MK) and with GluN2B antagonist ifenprodil (ifen) or GluN2A antagonist zinc (Zn) for one hour. Bars depict average Arf6 activity (pd/in) normalized to unstimulated controls (ctrl) ± standard deviation *(AP: 127 ±30.3, n=2; MK: 145 ±55.4, n=2; ifenprodil: 108 ±1.1, n=2; zinc: 155 ±2.1, n=2)*.

Given that GluN2A-containing NMDA receptor stimulation (Figure 8B) promoted the same effect on Arf6 activity as their blockage (Figure 8C), Arf6 activation in mature neurons was showing a contradiction in itself. In an attempt to explain this, we assumed that the high Arf6-GTP level in mature neurons after GluN2A blockade was generated differently than by NMDA stimulation. More specifically, the endogenously elevated Arf6-GTP levels after GluN2A blockade may share similarities with the tonal GluN2B-BRAG1-mediated Arf6 activation in young neurons (Figure 5A).

To elaborate on this, I consecutively blocked GluN2A- and GluN2B-receptors in mature neurons with the hope to observe a switch in the characteristics of Arf6 activation by BRAG signalling. Three-weeks-old neuron cultures were treated with or without zinc for one hour, washed, and treated with or without ifenprodil for another hour (Figure 9A). In a further approach, zinc-induced Arf6-GTP up-regulation was examined in control or BRAG1 shRNA-infected mature neurons to elucidate BRAG1's role in this process (Figure 9B). Blocking GluN2A-containing receptors with zinc induced a significant increase in Arf6-GTP levels that was reverted by blocking GluN2B-receptors with ifenprodil (Figure 9A). At the same time, BRAG1 RNAi abolished zinc-induced Arf6-GTP up-regulation in mature neurons (Figure 9B). Neurons after GluN2A blockade have therefore returned to GluN2B-BRAG1 signalling, as it was seen in one-week-old neuron cultures.

Surprisingly, late depletion of BRAG2 also increased active-Arf6 levels in mature cultures (Figure 9C). This elevated active-Arf6 level could be reverted by blocking GluN2B-receptors with ifenprodil. Preventing expression of BRAG1 and BRAG2 in mature cultures did not re-install high Arf6-GTP levels via GluN2B-receptor activity, in contrast to the single BRAG2 knockdown. These results confirm that – for undefined reasons – mature neurons re-install GluN2B-BRAG1 signalling resulting in elevated Arf6-GTP levels comparable to young neurons (Figure 4B), when GluN2A-BRAG2 signalling in mature neurons is interfered with.

To characterize the activation of Arf6 after GluN2B-BRAG1 re-installation, I assessed whether NMDA-triggered Arf6 activation was changed after a one-hour pre-treatment with ifenprodil or zinc (Figure 9D). As expected, long GluN2B-blockade remained ineffective in inhibiting NMDA-driven active-Arf6 production. More importantly however, zinc-blocked cultures also persisted to fail to increase Arf6-GTP levels, regardless of the re-installation of GluN2B-BRAG1-mediated Arf6 activation. In contrast to young neurons (Figure 7F), Arf6-GTP was hydrolyzed when NMDA receptors were stimulated in zinc-blocked cultures after the return to GluN2B-BRAG1 signalling.

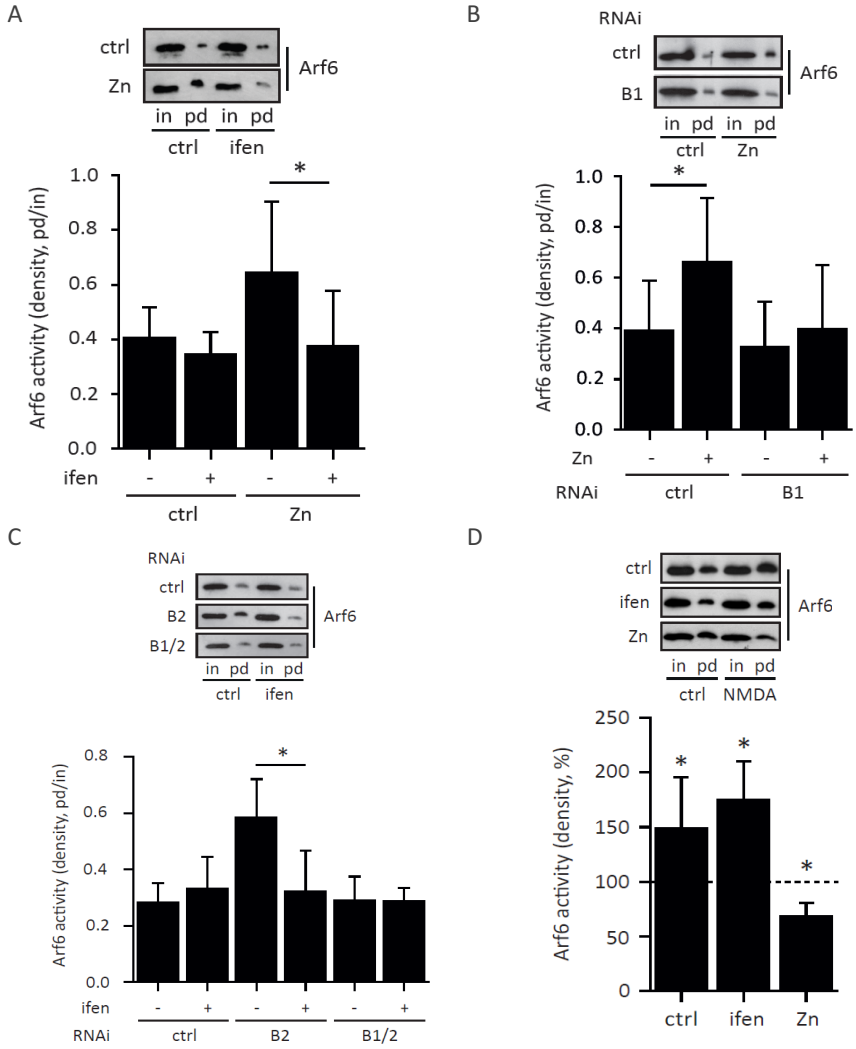

Figure 9, GluN2A-BRAG2 signalling maintains the mature Arf6 activation pathway at late stages in cortical neuron cultures.

(A) Three-weeks-old cortical neurons were treated for one hour with medium containing zinc (Zn) or medium alone (ctrl), before another treatment of half of each group with medium containing ifenprodil (ifen) or medium alone *(control: without ifenprodil: 0.4 ±0.11, n=10, with ifenprodil: 0.3 ±0.08, n=6, p=0.47; zinc: without ifenprodil: 0.6 ±0.26, n=10, with ifenprodil: 0.4 ±0.21, n=10, p=0.01; control versus zinc without ifenprodil: p=0.01)*.

(B) *BRAG1 is required to re-install the GluN2B-mediated tonal signalling in zinc-blocked mature cultures.* Three-weeks-old cortical neuron cultures had been infected with lentiviri delivering a control short hairpin (sh) RNA (ctrl) or shRNA for BRAG1 (B1) RNAi at 15 days in vitro. Neurons were treated for one hour with (Zn) or without zinc (ctrl) *(RNAi control: w/o ifenprodil: 0.4 ±0.20, n=9, with ifenprodil: 0.7 ±0.25, n=10, p=0.01; BRAG1-RNAi: w/o ifenprodil: 0.3 ±0.18, n=8, with ifenprodil: 0.4 ±0.25, n=10, p=0.56; RNAi control versus BRAG1-RNAi without ifenprodil: p=0.75)*.

(C) *BRAG2 depletion re-installs the GluN2B-BRAG1-mediated tonal Arf6 stimulation of young cortical neuron cultures.* Three-weeks-old cortical neurons had been infected with lentiviri delivering control short hairpin (sh) RNA (ctrl), shRNAs for BRAG2 (B2) RNAi or for BRAG1 and BRAG2 (B1/2) RNAi at 15 days in vitro. Neurons were treated for one hour with media containing ifenprodil (ifen) or media alone (ctrl) and cultures were then assessed for the active Arf6 fraction. *(RNAi control: w/o ifenprodil: 0.3 ±0.07, n=10, with ifenprodil: 0.3 ±0.11, n=11, p=0.20; BRAG2-RNAi: w/o ifenprodil: 0.6 ±0.14, n=13, with ifenprodil: 0.3 ±0.14, n=12, p=0.01; BRAG1/2-RNAi: w/o ifenprodil: 0.3 ±0.09, n=6, with ifenprodil: 0.3 ±0.05, n=6, p=0.89; RNAi control versus BRAG2-RNAi without ifenprodil: p=0.01; RNAi control versus BRAG1/2-RNAi without ifenprodil: p=0.86)*.
(A,B,C) Arf6 activities were calculated as Arf6-GTP to total Arf6 ratios (pd/in) and illustrated as averaged activity ratios ± standard deviation.
(D) *GluN2B-BRAG1 signalling re-installation in mature neurons does not allow NMDA-triggered Arf6 activation.* Three-weeks-old cortical neuron cultures were blocked with GluN2B antagonist ifenprodil (ifen) or GluN2A antagonist zinc (Zn) for one hour, and subsequently stimulated for 5 minutes with NMDA in the presence or absence of ifenprodil (ifen) or zinc (Zn), respectively. Bars show average active Arf6 ratios (pd/in) normalized to unstimulated controls (ctrl) with the same drug treatment in percent ± standard deviation *(control: 149 ±46.8, n=22, p=0.01; ifenprodil: 175 ±35.6, n=6, p=0.01; zinc: 68 ±12.7, n=11, p=0.01)*.
Input samples are 5% of pulldown input in all experiments.

In summary, the activity of GluN2A-containing NMDA receptors regulated Arf6 GDP/GTP exchange in three-weeks-old neurons (Figure 8B), and their basal activity ensured the maintenance of the mature GluN2A-BRAG2 signalling pathway (Figure 9A). Arf6-GTP levels in cortical neurons decreased during maturation, because the basal NMDA receptor activity did not lead to Arf6 activation in mature neurons with a functional GluN2A-BRAG2 signalling (Figure 4B). This change has likely occurred in a gradual manner from synapse to synapse during maturation, as it had been proposed for the NMDA subunit composition (Sobczyk et al., 2005). The following table summarizes the NMDA receptor-dependent Arf6 activation principles of this dissertation.

	DIV7	**DIV21**
basal Arf6 activity	high	low
basal NMDAR-BRAG signalling	GluN2B-BRAG1	GluN2A-BRAG2
GluN2B-blockade	Arf6-GTP drop	no effect
GluN2A-blockade	no effect	GluN2B-BRAG1 signal re-installation
GluN2B-stimulation	Arf6 activation	no Arf6 activation
GluN2A-stimulation	not available	Arf6 activation
B2-RNAi	no effect	GluN2B-BRAG1 signalling
B1-RNAi	GluN2B signalling uncoupled from Arf6 activation	GluN2B signal re-installation is missing

Table, Principles of NMDA receptor-BRAG mediated Arf6 activation.

The studied NMDA receptor-BRAG signalling takes place in predictable ways, summarized here as Arf6 activation principles. Basal Arf6-GTP levels and Arf6 activation pathways are different between one-week and three-weeks-old neurons. Their response to the blockade of the functional pathways via specific NMDA receptor blockers is altered between young and mature neurons, as well. While BRAG2 depletion only affects mature neurons, BRAG1 depletion displayed different unexpected effects at all stages.

Results II, BRAG1 and BRAG2 play different roles in the maturation of Arf6 regulation

C, 2.1, BRAG1 depletion during neuronal development affects NMDA receptor-mediated Arf6 activation also at late stages in cortical neuron cultures.

In the previous Arf6 activation measurements of mature neurons, RNAi-mediated BRAG-depletion was performed after two weeks in culture, in order to avoid any interferences in the development of the cells (Figure 8A). In a different approach, RNAi of BRAG protein expression was performed early at DIV 4, and Arf6 activity with and without NMDA-stimulation was measured at three weeks in culture.

NMDA-triggered Arf6 activation was abolished in these neurons when BRAG2, but also when BRAG1, had been knocked down (Figure 10A). Additionally, all knockdown groups showed elevated Arf6-GTP levels compared to control-infected neurons (Figure 10B).

Approaching with the same rational as before, I treated early BRAG-depleted neuron cultures for one hour with ifenprodil to see whether GluN2B activity was involved in their phenotype. Remarkably, cortical neurons did not decrease Arf6-GTP levels in response to blockade of GluN2B after knockdown of BRAG1. The Arf6-GEF that activated Arf6, independent of NMDA receptors in neurons missing BRAG1 expression during their maturation, was not identified in this study, and should first be screened for amongst Arf6-GEFs expressed throughout the lifetime of cortical neurons. As with late RNAi at DIV 15, BRAG2-depleted neurons expectedly showed elevated Arf6-GTP that depended on GluN2B-receptor activity. These results pronounced that BRAG2 GEF-functions might only be significant at advanced stages of neuronal development. It could be that these neurons remain in the GluN2B-BRAG1 signaling state throughout their lifetime.

Assuming that BRAG1-depleted mature neurons still expressed BRAG2 and GluN2A-containing receptors, it was unclear why NMDA-stimulated Arf6 activation was missing. Synaptic Arf6 activation was possibly saturated in this situation, and general alterations of synaptic development could have also been the cause. For unspecified reasons however, blocking GluN2B-containing receptor activity prior to NMDA stimulation enabled Arf6 activation, without Arf6-GTP levels having to return to basal levels (Figure 10C). This may imply two things. First, that BRAG1 depletion was involved in unexpected effects of GluN2B, perturbing Arf6 activation throughout a cortical neuron's lifetime (Figure 10B). Secondly, synapses still switched to GluN2A-BRAG2 signaling during maturation, regardless of the absence or presence of BRAG1, making NMDA-triggered Arf6 activation possible in BRAG1-depleted mature neurons, if GluN2B-receptors were blocked (Figure 10C).

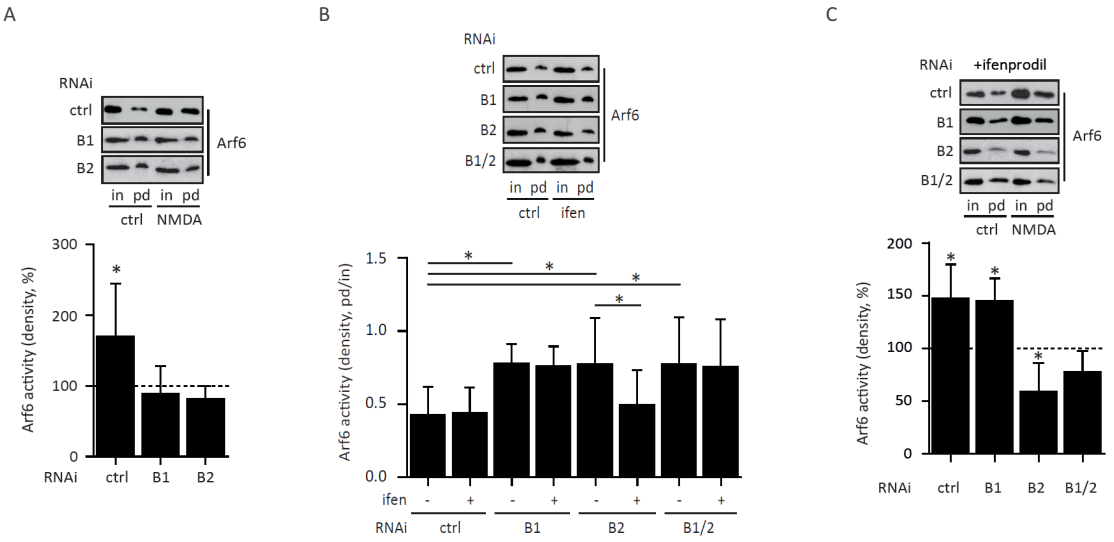

Figure 10, BRAG1 depletion during postnatal development perturbs NMDA receptor-regulated Arf6 activity throughout cortical neurons' lifetimes.

(A) *BRAG depletion during development un-couples NMDA receptor control over Arf6 activity in adult neurons.* Three-weeks-old cortical neurons had been infected with lentiviri delivering a control short hairpin (sh) RNA (ctrl), or shRNAs for BRAG1 or BRAG2 (B1 or B2) RNAi after 4 days in vitro. Neurons were stimulated for 5 minutes with NMDA. *(RNAi control: 170 ±75.1, n=11, p=0.01; BRAG1-RNAi: 89 ±38.9, n=7, p=0.47; BRAG2-RNAi: 81 ±19.1, n=7, p=0.05)*.

(B) *BRAG1 depletion leads to Arf6 activation without the contribution of GluN2B-NMDA receptors.* Three-weeks-old cortical neurons infected with control short hairpin (sh) RNA (ctrl) or shRNAs for BRAG1 or BRAG2 (B1 or B2) RNAi after 4 days in vitro were treated for one hour with the GluN2B blocker ifenprodil. All bars show averaged active Arf6 ratios (pd/in) ± standard deviation *(RNAi control: w/o ifenprodil: 0.4 ±0.20, n=10, with ifenprodil: 0.4 ±0.17, n=9, p=0.65; BRAG1-RNAi: w/o ifenprodil: 0.8 ±0.14, n=9, with ifenprodil: 0.8 ±0.13, n=9, p=0.71; BRAG2-RNAi: w/o ifenprodil: 0.8 ±0.32, n=8, with ifenprodil: 0.5 ±0.24, n=8, p=0.01; BRAG1/2-RNAi: w/o ifenprodil: 0.8 ±0.32, n=8, with ifenprodil: 0.8 ±0.32, n=7, p=0.54; RNAi control versus: BRAG1-RNAi w/o ifenprodil: p=0.01, BRAG2-RNAi w/o ifenprodil: p=0.01, BRAG1/2-RNAi w/o ifenprodil: p=0.01)*.

(C) *GluN2B activity after BRAG1 depletion prevents the activation of the mature GluN2A-BRAG2-mediated pathway.* Three-weeks-old cortical neurons had been infected with lentiviri delivering a control short hairpin (sh) RNA (ctrl), shRNAs for BRAG1, BRAG2 (B1 or B2) or BRAG1 and BRAG2 (B1/2) RNAi after 4 days in vitro. Neurons were treated for one hour with media containing ifenprodil (ifen) and then stimulated for another 5 minutes with NMDA in the presence of ifenprodil *(RNAi control: 147 ±32.2, n=14, p=0.02; BRAG1-RNAi: 145 ±21.1, n=16, p=0.01; BRAG2-RNAi: 59 ±26.9, n=13, p=0.01; BRAG1/2-RNAi: 77 ±20.2, n=6, p=0.07)*.

(A,B) Bars illustrate averaged percentages of NMDA effects after normalization to untreated controls (ctrl) of the RNAi-treated group ± standard deviation.

Input samples are 5% of pulldown input in all experiments.

C, 2.2, BRAG2 depletion during neuronal maturation affects the mature phenotype of dendritic spines in adult mice.

We investigated whether BRAG2 has effects on spine numbers and morphology, which are considered to be indicators for neuronal development. To this end, I used mice that have been genetically manipulated to lack BRAG2 specifically in projection neurons of the forebrain and to label a subset of neurons with GFP. These mice were generated by inter-breeding *Iqsec1*$^{fl/fl}$ mice (SCHOLZ ET AL., 2010), *NEX-Cre* mice (GOEBBELS ET AL., 2006) and thy1-GFP line M mice (FENG ET AL., 2000).

In SCHOLZ ET AL., 2010, gene targeting in embryonic stem cells was used to introduce loxP sites flanking exon 2 of the BRAG2 gene, generating *Iqsec1*$^{fl/fl}$ mice. According to previous analyses, Cre-mediated

deletion of exon 2 in *Iqsec1* drastically reduces BRAG2 expression; however, since the sequence encoding the catalytic Sec7 domain is not located on exon 2, aberrant transcripts might lead to residual BRAG2 activity. Neuronal basic helix-loop-helix proteins, or Nex, are transcription factors that are only expressed in certain parts of the brain, i.e. projecting neurons of the hippocampi and neocortex, as well as in beta-pancreatic cells and enteroendocrine cells. In *Nex-Cre*-positive *Iqsec1*$^{fl/fl}$ mice the BRAG2 knockout is restricted to Nex-expressing cells. *Thy1*-GFP line M mice, as described in FENG ET AL., 2000, and produced in the laboratory of Dr. Joshua Sanes, express GFP under the Thy1 promotor, which controls CD90 expression and is active in a unique pattern of a small subset of mature principal neurons. For the spine analysis, I used *Iqsec1*$^{fl/fl}$, *Thy1*-GFP-positive and Nex-Cre-positive (ΔctxBRAG2) or -negative (ctrl) male littermates.

In these mouse lines, hundred micron-thick brain sections displayed no particular malformation of hippocampal or cortical gross structures (not presented). GFP-positive neurons in the cortex were sparse and were also found in cortical layer 5 (Figure 11A). For their easy identification, I investigated these fluorescent principal neurons, first by evaluating the spine density of secondary branches on the apical dendrite. 1917 spines on approximately 40 dendrites of 4 neurons per cortex in 4 mice per genotype were analyzed. Spine density in adult mice was significantly increased in ΔctxBRAG2- compared to ctrl-mice (Figure 11B).

Besides aberrations in the shape of spines found in brains of patients with neurodegenerative diseases, the dimensions of spines are often used as indicators for spine maturity and the strength of their synaptic transmission. Generally, large body length of spines is associated with weak immature connections, and large head diameters are linearly correlated to synaptic strength (HARRIS ET AL., 1992; ARELLANO ET AL., 2007). To elaborate on the maturity of spines in the two genotypes, I looked for differences in spine morphology. Software analysis after spine recognition showed that BRAG2 depletion caused dendritic spines in cortical layer 5 neurons to decrease spine head diameters about 13% in average (Figure 11D). Analysis of the density of the spine head diameter bins revealed that the spine population with diameters up to 0.6 µm showed an increase in numbers (Figure 11E, Figure 11F). By calculating the ratio between spine head diameter (dh) and spine body length (ls) of individual spines, I determined an arbitrary maturation index (dh/ls), which also shifted for the entire spine population towards less mature spines in adult ΔctxBRAG2-mice (Figure 11G).

To show that the effects of the conditional BRAG2 knockout are related to the effects of BRAG2 depletion by RNAi, Arf6 activation was measured in neuronal cultures of *Iqsec1*$^{fl/fl}$-mice infected with viruses carrying the coding region of Cre or empty viruses. Cre-expressing cultures were effectively depleted from BRAG2 and showed a higher relative Arf6-GTP level (Figure 11H).

In summary, BRAG1 and BRAG2 seemed to play a role in the maturation of synapses of cortical neurons. BRAG1 coordinated NMDA receptor-mediated Arf6 activity (1) with persistent changes in Arf6 activation when depleted during an early critical period in developing neurons (Figure 10), and (2) reduced plasticity of BRAG signalling when missing in matured neurons (Figure 9C). At the end of synaptic maturation, BRAG2 appeared to take up control over NMDA receptor-mediated Arf6 activation (Figure 4B, Figure 8A), which is important for morphological aspects of spine modulation in adult brains (Figure 11).

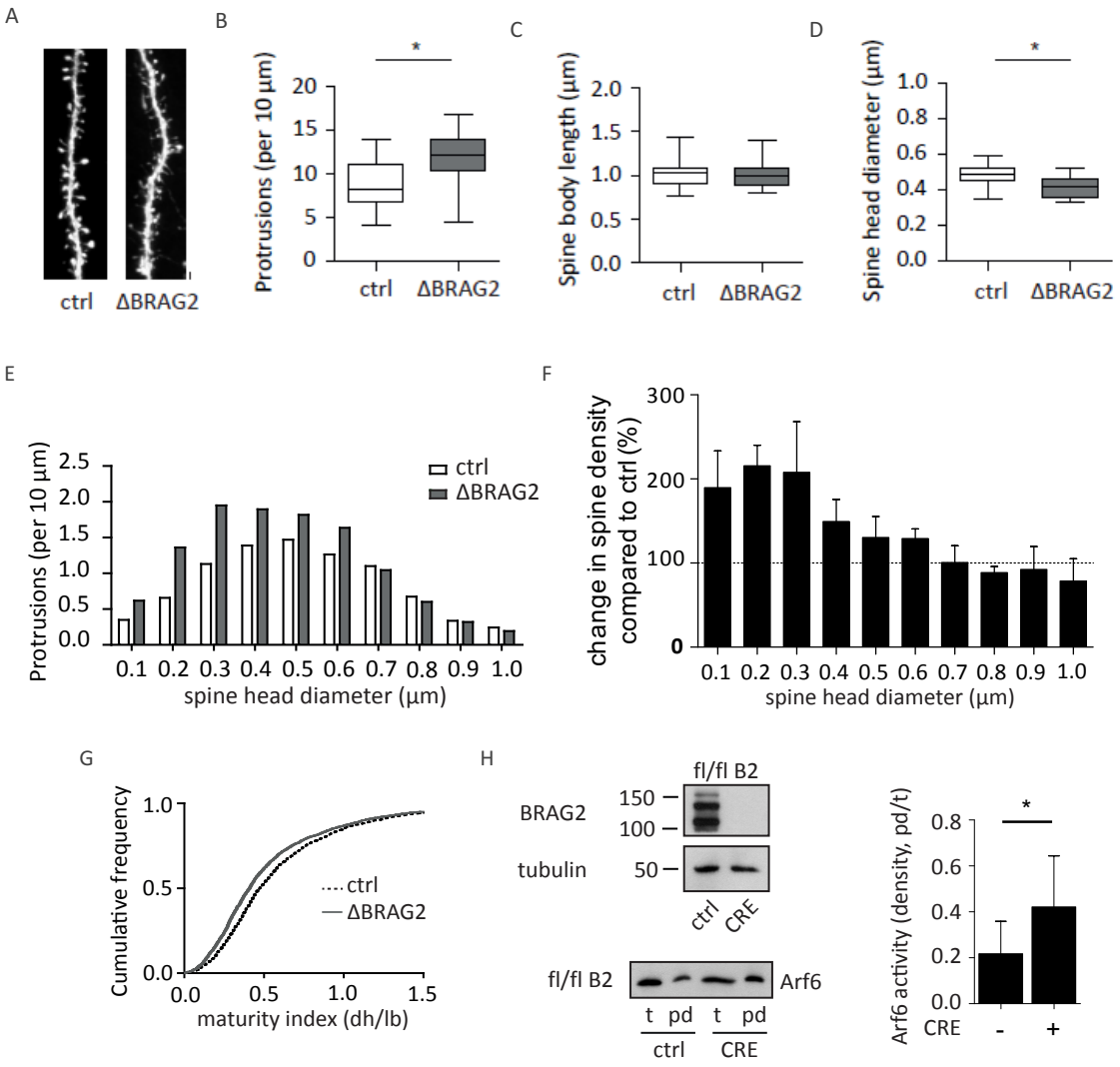

Figure 11, BRAG2 depletion affects the mature phenotype of dendritic spines in adult mice.

(A) Fluorescence images of secondary branch segments of the apical dendrite of layer 5 neurons in brain slice preparations of adult ctrl- and ΔctxBRAG2-mice (ΔBRAG2).

(B) *Principal neurons of the cortical layer 5 increase their spine density upon BRAG2 depletion.* Mean density of dendritic protrusions of *Iqsec1*$^{fl/fl}$ control (ctrl) and Cre-expressing Nex-Cre *Iqsec1*$^{fl/fl}$ knockout mice (ΔBRAG2), as recognized and counted by NeuronStudio and shown as protrusion per 10^{-5} metres (10 µm) *(ctrl: 8.6 ±2.51 spines per 10 µm, ΔctxBRAG2: 11.6 ±2.67 spines per 10 µm; n=39-47 dendrites)*.

(C) Measurements of spine body length in µm as evaluated by NeuronStudio.

(D) *Dendritic spines of cortical neurons have reduced average spine head diameters in BRAG2 knockout mice (ΔBRAG2).* Measurements of spine head diameter in µm as evaluated by NeuronStudio *(head diameter: ctrl: 0.48 ±0.06 µm, ΔctxBRAG2: 0.42 ±0.06 µm; spine length: ctrl: 1.01 ±0.138 µm, ΔctxBRAG2: 1.01 ±0.137 µm; n=1917 spines)*.

(E,F) *BRAG2 knockout mice (ΔBRAG2) have an increased number of spines with small spine heads compared to control mice.* (E) Shown are the densities of spines grouped into head diameter bins of 0.1 µm. (F) Bars show the percentual changes ± standard deviation in spines numbers per 10 µm dendrite of 0.1 µm head diameter bins (ΔBRAG2 versus ctrl-mice, 4 neurons of 4 mice per genotype, with 2-3 dendrites per neuron).

(G) Cumulative spine frequencies of ctrl- or ΔBRAG2-mice over their maturity index (dh/ls) calculated as the ratio of spine head diameter (dh) to spine body length (ls).

(H) *BRAG2 knockout in neuron cultures causes elevated Arf6-GTP levels.* Three-weeks-old cortical neurons from *Iqsec1*$^{fl/fl}$ mice were infected with empty viruses (Cre -) or viruses carrying the encoding region for Cre (Cre +) after 15 days in vitro. (top) Immunoblots of infected neuron cell lysates. Bars show averaged active Arf6 ratios (pd/in) ± standard deviation *(-CRE: 0.22 ±0.14; +CRE: 0.42 ±0.22; n= 5; p= 0.009)*. Input samples are 5% of pulldown input in all experiments.

C, 3.1, BRAG1 preferably binds at the stretch aa 1115-1154 in the C-terminus of GluN2B, and BRAG2 preferably binds at the stretch aa 1078-1117 in the C-terminus of GluN2A.

The interaction assays presented in the introductory result chapter pointed to interactions between BRAG proteins and a central region inside the GluN2A cytosolic domain (CD) stretching from amino acid (aa) 1038 to aa 1237 of GluN2A. I used this and the homologous segment of the GluN2B-CD, i.e. aa 1036-1243 in GluN2B, to perform GST-pulldowns with BRAG1 and BRAG2 proteins containing N-terminal FLAG-tags (Figure 12A). Interestingly, both GluN2 segments were able to pulldown either BRAG protein without apparent specificity. To simulate an approximate response to NMDA receptor signaling, the pulldowns were also performed in the presence of calcium. Surprisingly, BRAG proteins showed preferred binding to the compatible GluN2-CD (Figure 3A) when calcium has been added to the pulldowns, i.e. GluN2B-CD preferentially bound BRAG1 and GluN2A-CD selectively bound BRAG2. The human form of BRAG1 (hBRAG1) is longer than the assessed form of rats (rBRAG1) and might have different features. Therefore, I repeated the same assay with hBRAG1, which also selectively bound to the GluN2B-CD in the presence of calcium, however with higher specificity than the shorter rodent form. Diverging binding properties might result in different features for GEF-activation. However, glutamate-stimulation of NMDA receptor-expressing HEK293 cells resulted in equivalent Arf6-activation by hBRAG1 as with rBRAG1 (Figure 12B).

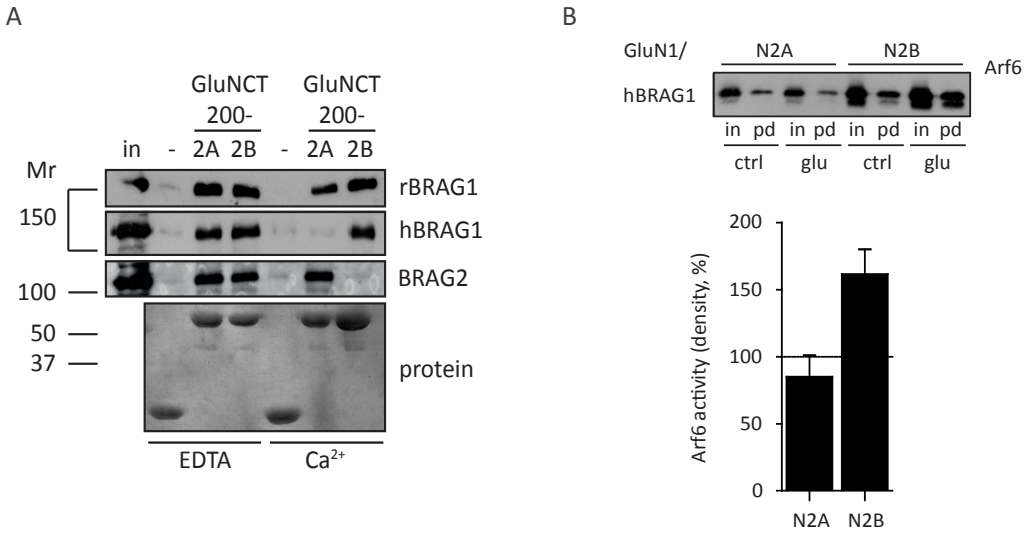

Figure 12, Calcium increases physical NMDA receptor-BRAG pairing.

(A) *BRAG-constructs bind to central segments of cytosolic domains (CD) of both GluN2 subunits. In the presence of 2mM calcium a preferential binding between GluN2BCD-BRAG1 and GluN2ACD-BRAG2 can be observed.* Immunoblots of N-terminally FLAG-tagged recombinant (1) rat BRAG1 and BRAG2 (rBRAG), and (2) human BRAG1 (hBRAG1) containing an extended C-terminal region, over-expressed in HEK293 cells and recovered by GST-pulldown with GST fused to the middle third CD regions of GluN2A and GluN2B. NMDA receptor regions comprise amino acids (aa) 1038-1237 of GluN2A (GluNCT2002A) or aa 1036-1243 of GluN2B (GluNCT2002B) in presence of 2mM EDTA or calcium (Ca^{2+}).

(B) *L-glutamate stimulation (glu) of human BRAG1 (hBRAG1) in glutamate-deprived, NMDA receptor-expressing (GluN1/N2A or GluN1/N2B) HEK293 cells in complete extracellular solution.* Bars depict mean percentage changes in Arf6 activity ± standard deviation, calculated as density ratios between Arf6-GTP and total Arf6 (pd/in) and normalized to untreated controls (ctrl) *(hBRAG1: N2A: 85 ±15.9%, n=2; N2B: 161 ±18.4%, n=2; rBRAG1r: N2A: 71 ±25.5%, n=9; N2B: 127 ±14.3%, n=6, see p. 48 for results of Figure 3A)*. Input samples are 2.5% of pulldown input in all experiments. Mr, relative molecular mass.

I continued with GST-pulldowns to further map the interaction sites between GluN2-CDs and BRAG proteins. Using shorter fragments of the identified 200 aa-long stretches of the GluN2-CDs, in the presence of calcium the interactions appeared to be confined to the sequences aa 1078-1117 in GluN2A for BRAG2 and aa 1115-1154 in GluN2B for BRAG1 (Figure 13A, Figure 13B).

Surprisingly, FLAG-tagged fragments of the amino-terminus (NT) of BRAG1 and BRAG2, containing regions upstream of the Sec7-PH tandem domain, also bound to 40 aa-stretches of their compatible GluN2-CDs, even in the absence of calcium and with higher selectivity (Figure 13C). Conclusively, the N-terminal fragments of BRAG proteins lacking the Sec7-PH domain interacted subtype-specifically with GluN2-CDs, while BRAG1 and BRAG2 Sec7-PH domains bound GluN2-CDs indiscriminately, according to the preliminary results from the yeast two-hybrid system. In the full length proteins, regions in the Sec7-PH domains may therefore reduce the selective binding of the BRAG-NTs to GluN2-CDs in the absence of calcium. Sec7PH-GluN2 interactions might also induce BRAG protein conformations that lead to catalytic inactivity under certain conditions, i.e. the absence of calcium.

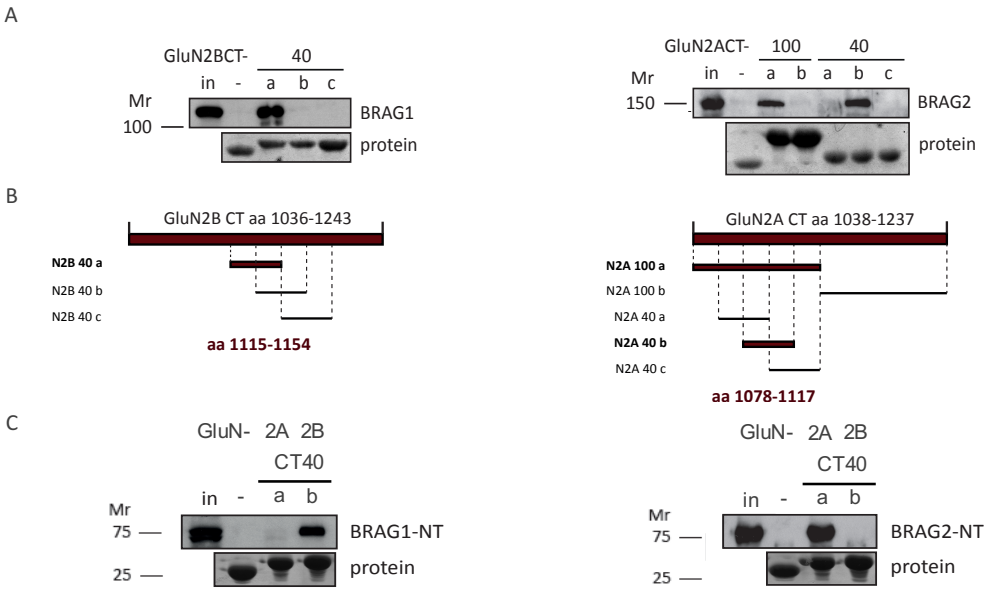

Figure 13, GluN2A and GluN2B cytosolic domains at the stretches aa 1078-1117 and aa 1115-1154 interact with N-termini of BRAG2 and BRAG1, respectively.

(A) *GluN2A aa 1078-1117 binds BRAG2 and GluN2B aa 1115-1154 binds BRAG1.* Shown are representative immunoblots of N-terminally FLAG-tagged BRAG1- and BRAG2-constructs containing Sec7-PH domains and complete N-terminal regions, pulled down in the presence of 2mM calcium by specific binding to GST fusion-segments of (1) GluN2B aa 1115-1154 (GluN2B-CT 40a), aa 1135-1174 (GluN2B-CT 40b) and aa 1155-1194 (GluN2B-CT 40c), or (2) GluN2A aa 1038-1137 (GluN2A-CT 100a), aa 1138-1237 (GluN2A-CT 100b), aa 1058-1097 (GluN2A-CT 40a), aa 1078-1117 (GluN2A-CT 40b) and aa 1098-1137 (GluN2A-CT 40c), respectively.

(B) Schematic map of tested GluN2 cytosolic segments and conclusions from (A).

(C) *BRAG proteins show specific binding to GluN2-CDs via segments between N-terminus and Sec7 domain.* Segments of BRAG1 and BRAG2 upstream of the Sec7-PH domain (BRAG-NT) can specifically bind to identified 40 aa-long segments of GluN2A (to GluN2A-CT 40b) and GluN2B (GluN2B-CT 40a) after calcium depletion by 2mM EDTA, respectively. Input samples are 2.5% of pulldown input.

Next, the functional significance of the identified binding regions in GluN2A and GluN2B for Arf6 activation were assessed. In GluN2A-expressing HEK-BRAG2 and GluN2B-expressing HEK-BRAG1 cells, glutamate-stimulated Arf6 activation was completely abolished, if the specific BRAG-binding site was deleted from the CD of the receptors (ΔBD, Figure 14B).

Expression of these mutant receptors was not different from the wild type receptor (Figure 14A). Over-expression of 40 aa-long competitive peptides, containing the sequences of the specific BRAG2-binding site and of two other regions around it as depicted in Figure 13B, had the same effect in GluN2A-BRAG2-expressing HEK293 cells; when competitive peptides spanned over the first 20 amino-terminal aa of the identified BRAG2 binding site, NMDA receptor-triggered Arf6 activation was abolished (Figure 14C).

These results substantiate the crucial role of physical interaction in the receptor complex for NMDA receptor-mediated BRAG-dependent Arf6 activation.

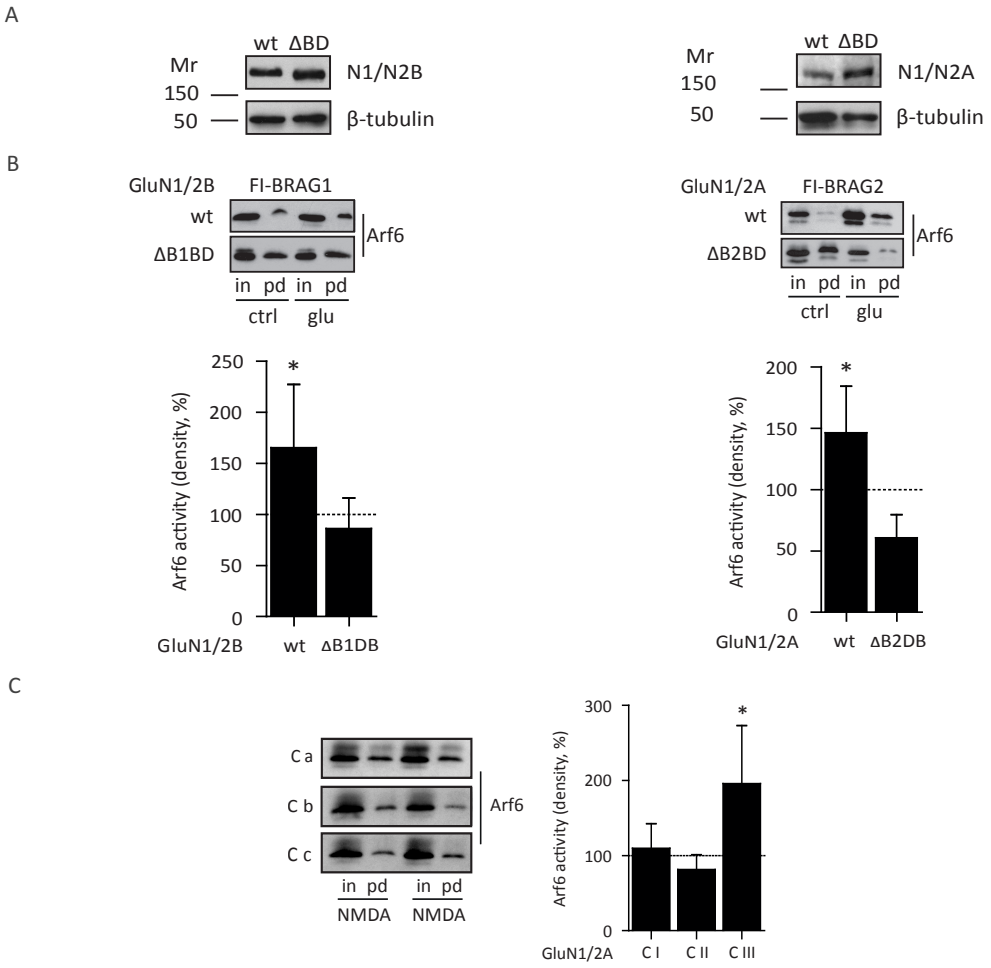

Figure 14, Arf6 activation via GluN2A and GluN2B requires physical interactions with BRAG1 and BRAG2.

(A) Immunoblots of functional GluN2A-containing (GluN1/2A) and GluN2B (GluN1/2B) receptors with deletions of the identified BRAG protein binding regions from cell lysates of HEK-BRAG1 and HEK-BRAG2 cell lines, as detected by protein-specific antibodies.

(B) *BRAG stimulation via NMDA receptors requires physical interaction at distinct GluN2 sites.* L-glutamate stimulation (glu) of NMDA receptors in glutamate-deprived HEK293-BRAG cells in complete extracellular solution. HEK-BRAG2 cells were transfected with a functional GluN1/2A receptor with a deletion at the stretch amino acids (aa) 1078-1117 (ΔB2BD), and HEK-BRAG1 cells with a functional GluN1/2B receptor with a deletion at the stretch amino acids (aa) 1115-1154 (ΔB1BD) *(BRAG2 x GluN2A: wt: 146 ±37.9%,*

n=14, p= 0.01, ΔB2BD: 61 ±18.9%, n=7, p= 0.03; BRAG1 x GluN2B: wt: 165 ±62.2%, n=14, p= 0.01, ΔB1BD: 86 ±30.0%, n=8, p= 0.14).
(C) *BRAG stimulation via NMDA receptors is blocked by physical competition at distinct interaction sites.* HEK-BRAG2 cells were co-transfected with functional GluN1/2A receptor and eGFP-tagged peptides with sequences of the identified BRAG-binding regions *(CI (=GluN2A-CT 40a): 110 ±32.7%, n=5, p= 0.35, CII (=GluN2A-CT 40b): 81 ±19.7%, n=7, p= 0.04, CII (=GluN2A-CT 40c): 196 ±77.2%, n=7, p= 0.01)*. Expression of the peptides was confirmed visually by fluorescence microscopy.
(B,C) Bars depict mean percentage changes in Arf6 activity ± standard deviation, calculated as density ratios between Arf6-GTP and total Arf6 (pd/in) and normalized to untreated controls (ctrl). Input samples are 2.5% of pulldown input.

C, 3.2, GluN2A and GluN2B cytosolic domains stimulate BRAG2 and BRAG1 through physical interaction involving calmodulin.

I tested whether BRAG2 follows the same behavior towards calmodulin and calcium concentrations as BRAG1 (Myers et al., 2012), and found that BRAG2 was binding to calcium-free calmodulin (Figure 15A). After clarification of over-expressed BRAG2 via ultracentrifugation, calmodulin was able to pull down BRAG2 from the supernatant. This interaction was strongly reduced when calcium concentration was increased to 100 µM free calcium, compared to when EDTA was added. To confirm that this interaction was mediated by the IQ motif, I repeated the calmodulin pulldown with BRAG2 containing a point mutation at R146 in the IQ motif, which effectively decreased calmodulin binding in calcium-free conditions, while the wild type responded to the absence or presence of calcium (Figure 15B).
Since the presence of calcium promoted the specific interactions of the functional receptor-BRAG pairings (Figure 12A), we investigated whether increase in calcium concentration leading to the release of calmodulin from BRAG2 (Figure 15A) can also lead to the destabilization of the non-functional receptor-BRAG complex, in comparison to the functional receptor-BRAG complex (Figure 15B). After purifying the complex of BRAG2 with the central 200 aa-long fragments of the cytosolic domain of GluN2A and GluN2B in a GST-pulldown, EDTA or increasing amounts of calcium were added to the pulldown sepharose. After the incubation in the presence of 100 µM calcium, BRAG2 was released from the GluN2B complex, while the GluN2A-BRAG2 complex was less influenced by calcium. This suggests that the presence of calcium and the consequent release of calmodulin from the complex can weaken the interaction of the non-functional BRAG2-GluN2B pairing. In the opposite case under low calcium conditions, calmodulin binding might promote conformational changes in BRAG proteins (Myers et al., 2012) that stabilize its non-functional receptor binding and/or its catalytic inactivity.

The involvement of calmodulin binding in BRAG2 GEF-activity was further addressed in an active Arf6 assay conducted in HEK293 cells expressing BRAG proteins and membrane-bound constructs of the GluN2-CDs. The CD-constructs were stabilized at membranes by adding a palmitoylation site to their NTs. The GluN2B-CD specifically increased BRAG1 GEF-activity (compare functional GluN2B-receptor expression shown in Figure 6). In contrast to this, BRAG2 could not be stimulated by the GluN2A-CD (Figure 15C). Since BRAG2 interaction with the GluN2A-CD is responsive to the presence of calcium and is generally less active under basal conditions in neuron cultures, we speculated whether BRAG2 GEF-activity might be functionally more sensitive to calmodulin binding than BRAG1. I repeated the experiment with the above-mentioned point mutant, which renders BRAG2 less capable of binding to calmodulin

(Figure 15D). Interestingly, the GluN2A-CD was able to stimulate BRAG2 R146A GEF-activity. This suggested that physical interaction of calmodulin-free BRAG proteins with the NMDA receptor CDs was indispensable for Arf6 activation, and points to a central role of calcium and calmodulin for the catalytic regulation of BRAG. According to these experiments, release from calmodulin is a step in BRAG2-GEF activation. This might also take place in neurons when calcium concentrations increase after NMDA receptor stimulation.

In a last approach, we planned to look for an indication that BRAG2-GEF activation required the controlled influx of calcium through NMDA receptors. Therefore, HEK293 cells expressing GluN1/2A receptors and BRAG2 were treated with ionomycin for 3 minutes, which creates calcium-permeable pores in plasma membranes that mediate calcium influx. In GluN1/2A-expressing HEK-BRAG2 cells, I compared Arf6-GTP levels after adding ionomycin or glutamate. Ionomycin treatment failed to increase active-Arf6 levels (Figure 15E). Previous results suggested that calcium influx by NMDA receptors also stimulated Arf6-GTP hydrolysis in certain contexts (Figure 3B). Differences in the amount of calcium influx might decide whether Arf6-GTP levels are increased or decreased. These results indicate that BRAG2 stimulation was intimately connected to physical interactions as well as calcium ion conductance of NMDA receptors, and that regulated stimulation conditions were necessary to guarantee increased GEF-activity of BRAG proteins.

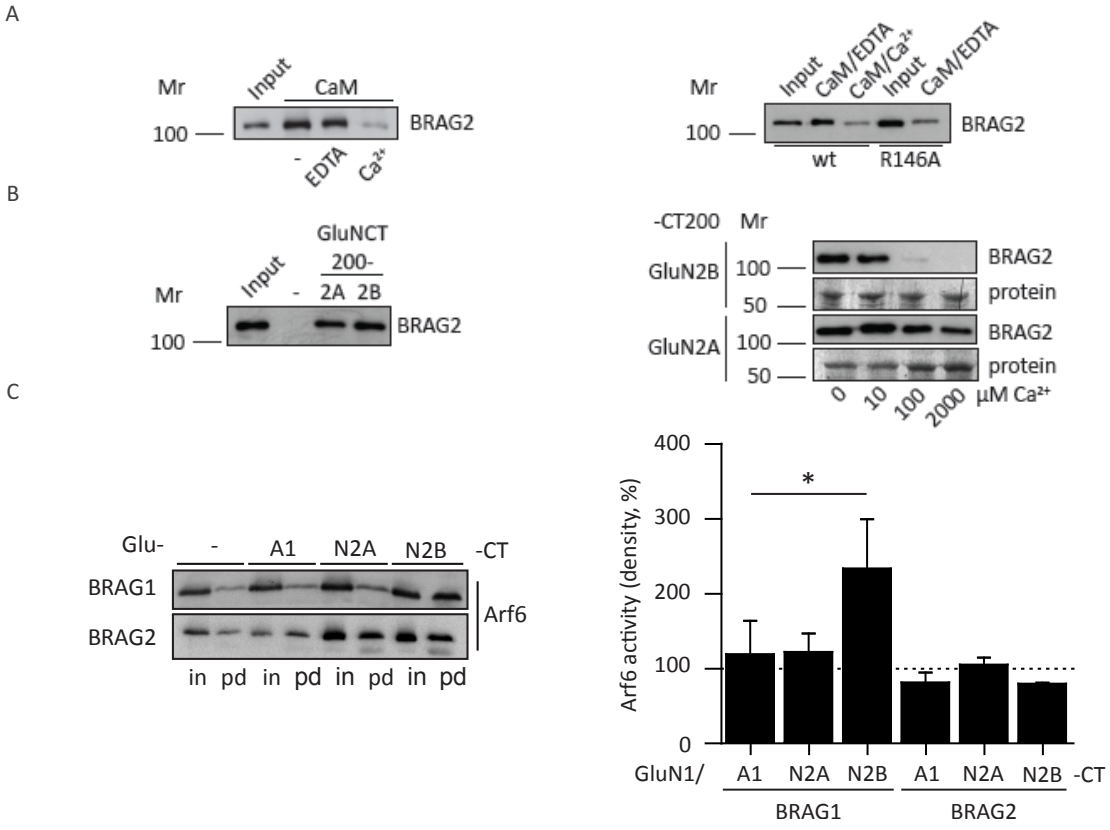

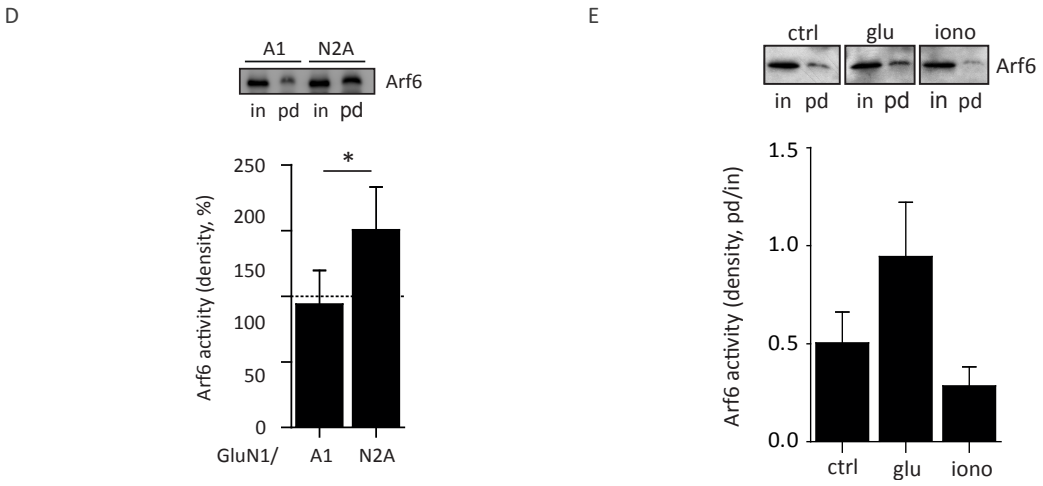

Figure 15, BRAG2 GEF-activity modulation requires controlled calcium influx and binding to calcium-free calmodulin via its IQ motif.

(A) (left) *BRAG2 can bind calmodulin in the absence of calcium, and be released in the presence of calcium.* Immunoblot of BRAG2, recovered from calmodulin pulldowns. BRAG2 (Input) was purified with calmodulin-resin (CaM) and consequently eluted by 2 mM EDTA or 100 µM calcium (Ca^{2+}). Loaded supernatant samples estimate to 1.25% of pulldown input.
(right) *IQ-like motif of BRAG2 mediates calcium sensitive binding to calmodulin.* Immunoblot of BRAG2 and BRAG2 R146A, recovered from calmodulin pulldowns. BRAG2 (Input, wt) was pulled down in the presence of 2 mM EDTA or 2 mM calcium (Ca^{2+}), and BRAG2 R146A (Input, R146A) in the presence of 2 mM EDTA. Input samples are 1.25% of pulldown input.
(B) *Increase in calcium concentration destabilizes the non-functional GluN2B-BRAG2 interaction.* (left) Immunoblot of over-expressed BRAG2 (Input) recovered from GST-pulldown with cytosolic regions of GluN2A and GluN2B. NMDA receptor regions comprise amino acids (aa) 1038-1237 of GluN2A (GluNCT2002A) or aa 1036-1243 of GluN2B (GluNCT2002B). (right) After purification of the recovered BRAG2 proteins, the pulldowns were incubated with increasing concentrations of calcium.
protein, coomassie-stainings of GST-GluNCT2002A or -GluNCT2002B samples from the used sepharose.
(C) *GluN2BCT-BRAG1 signalling increases Arf6 activity in HEK293 cells.* Shown are a representative immunoblots of Arf6GTP-specific pulldown assays from HEK293 cells expressing Arf6-HA, BRAG1- or BRAG2-eGFP and membrane-bound constructs of the GluA1 C-terminus (CT), GluN2ACT or GluN2BCT *(BRAG1 x CT: GluA1: 119 ±44.5%, n=8, GluN2A: 122 ±24.5%, n=6, GluN2B: 234 ±65.5%, n=6; versus GluA1CT: GluN2A p=0.88, GluN2B p=0.01; BRAG2 x CT: GluA1: 81 ±13.3%, n=7, GluN2A: 105 ±9.5%, n=2, GluN2B: 80 ±1.1%, n=2; versus GluA1CT: GluN2A p=0.05, GluN2B p=0.90).*
(D) *GluN2ACT can only activate calmodulin-free BRAG2 (BRAG2 R146A)*. Arf6 activity assays were performed from HEK293 cells expressing Arf6-HA, BRAG2 R146A-eGFP and membrane-bound constructs of the GluA1 (A1) and GluN2A C-termini (N2A) *(BRAG2RA x CT: GluA1: 94 ±25.5%, n=3, GluN2A: 151 ±32.6%, n=6, p=0.04)*.
(C,D) Bars depict mean percentage changes in Arf6 activity ± standard deviation, calculated as density ratios between Arf6-GTP and total Arf6 (pd/in) and normalized to controls without co-transfection of a membrane bound peptide or untreated control (-). Input samples are 1.25% of pulldown.
(E) *BRAG2-mediated Arf6 activation requires calcium influx via GluN2A-containing NMDA receptors.* Stimulation with 1 mM L-glutamate (glu) or 5 µM ionomycin (iono) of Arf6 in glutamate-deprived GluN2A-containing NMDA receptor-expressing HEK-BRAG2 cells in complete extracellular solution for 3 minutes. Input samples are 2.5% of pulldown input *(GluN1/2A x BRAG2: control: 0.5 ±0.16, n=8, glu: 1.0 ±0.28, n=2, iono: 0.3 ±0.10, n=8; iono versus control: p=0.01)*.
Bars depict mean Arf6 activity ± standard deviation, calculated as density ratios between Arf6-GTP and total Arf6 (pd/in).

C, 3.3, BRAG1 and BRAG2 precipitate when mismatched NMDA receptor partners are activated

BRAG proteins are a substantial part of the PSD. All BRAG family members possess a PDZ-ligand domain that might be responsible for the interaction of BRAGs with glutamatergic synapses. As reported, I found that the Sec7-PH tandem domain and N-terminal sections of BRAG proteins might be involved in interactions with NMDA receptors and activity regulation of BRAGs. In MYERS ET AL., 2012, BRAG1 was suggested to bind calmodulin in calcium-free conditions, where they might exist as soluble monomers in complex with calmodulin. In the presence of calcium, BRAG1 multimerized with other BRAG1 proteins via a coiled-coil domain in their NT upstream of the IQ motif. BRAG1 in spines of neuronal cultures stimulated with NMDA formed aggregates in extrasynaptic regions.

As final experiment we intended to explore how the BRAG activation described here might relate to the activation mechanism proposed in MYERS ET AL., 2012. To this end, I expressed eGFP-tagged BRAG1 and BRAG2 in HEK293 cells, to test if BRAG proteins form precipitates upon an increase in intracellular calcium concentration, which in the case of BRAG1 was reported to activate Arf6. Confirming this, treatment of BRAG-eGFP-expressing cells with ionomycin induced the formation of intracellular puncta, with both BRAG1 and BRAG2 (Figure 16A).

Since glutamate-stimulation of NMDA receptor-expressing cells has led to Arf6-GTP up-regulation (Figure 3A), I tested how fluorescent BRAG proteins behave after receptor stimulation in similar situations as analyzed before, and compared how this might correlate to the measured Arf6 activities (Figure 16B). Surprisingly, BRAG proteins responded contrary to what was expected, and did not form puncta when compatible NMDA receptor-BRAG combinations were activated by glutamate. In cases, when Arf6 activation and NMDA receptor-BRAG pairing had been observed, the fluorescent signal appeared to be more diffuse. Interestingly, BRAG proteins precipitated only when NMDA receptors and BRAG proteins did not match. Then, increases in localized fluorescence signals became visible, with the consequence that the fluorescent multimers seemed to represent the inactive form of BRAG. BRAG proteins precipitated therefore in conditions of elevated calcium concentration (Figure 16A) and absence of their receptor-binding partners (Figure 16B). Conclusively, the active forms of BRAG proteins may have been physically associated to the compatible receptors, which might have prevented BRAG proteins from condensation into inactive membrane-proximal precipitates.

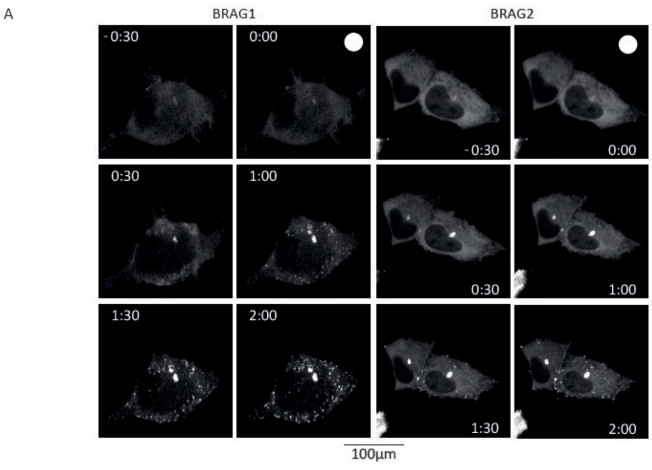

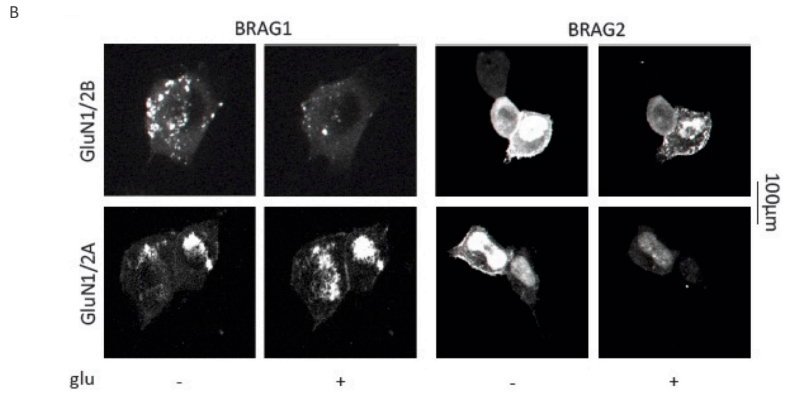

Figure 16, BRAG multimerization competes with NMDA receptor interaction to regulate BRAG GEF-activity.

BRAG proteins form inactivating multimers, when intracellular calcium is increased. The formation of fluorescent puncta in BRAG-eGFP-expressing HEK293 cells (2-4 cells per test group) correlates with states of low Arf6 activity. Shown are fluorescence images of
(A) BRAG-eGFP-expressing HEK293 cells treated for 5 minutes with 3 µM ionomycin in complete extracellular solution. The white circle indicates the time point of ionomycin stimulation.
(B) HEK293 cells were transiently transfected with BRAG-eGFP, and functional GluN1/2A or GluN1/2B receptors, deprived from glutamate and treated with 1 mM L-glutamate (glu). Live images were taken by a spinning-disk confocal microscope in 10 seconds intervals in a heating chamber at 37°C with 5% CO_2
1 minute before and 2 minutes after addition of L-glutamate.

As for the precipitates observed in the perisynaptic regions of neuronal spines in MYERS ET AL., 2012, if confirmed, this inactivating self-interaction of BRAG proteins might represent a mechanism by which BRAG activity is confined to synaptic regions, where interacting receptors are present. In cases where no activating binding partner is present, increase in intracellular calcium might induce BRAG protein condensation into inactive aggregates, as opposed to a closed inactive form bound to calmodulin in low-calcium conditions. A preliminary working model of the BRAG activation mechanism is shown below, and requires further testing.

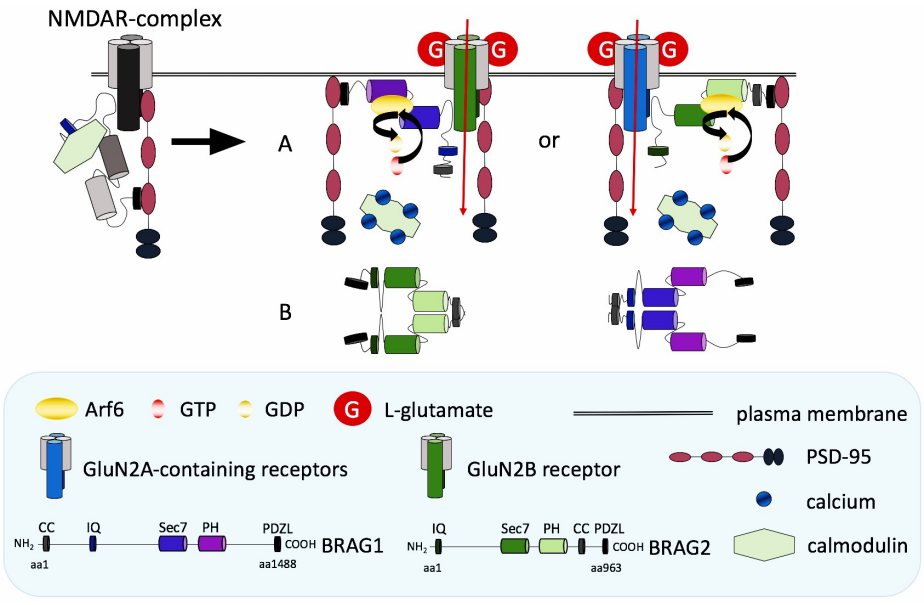

BRAG-mediated Arf6 activation.

BRAG proteins incorporate into the PSD via PDZ interactions as calmodulin-bound inactive monomers. When calcium releases calmodulin, BRAG proteins (A) become activated by specific cytosolic receptors domains or (B) multimerize via CC-CC interactions.

Results in Brief

- BRAG1 and BRAG2 are constituents of the NMDA receptor complex
- BRAG1 interacts with GluN2B and BRAG2 interacts with GluN2A at central regions of the cytosolic C-terminal receptor segments in a functional context
- N-terminal BRAG protein segments mediate subtype-selective binding to GluN2
- GluN2-BRAG interactions are sensitive to ambient calcium concentrations
- BRAG functional regulation is tied to multimerization and interaction with calmodulin
- GluN2-BRAG interactions reflect the importance of BRAG at different functional stages of synapse development: GluN2B signals to BRAG1 at early culture stages, GluN2A signals to BRAG2 at late culture stages
- GluN2-BRAG signalling shows indications of plasticity: GluN2A-BRAG2 signalling replaces GluN2B-BRAG1 signaling during maturation of neuronal cultures; when GluN2A-BRAG2 signalling is interfered with, GluN2B-BRAG1 signaling is re-installed
- Presence of BRAG1 in one-week-old neuronal cultures installs GluN2B-dependent control over Arf6 activation; in the absence of BRAG1, GluN2B stimulation induces Arf6-GTP hydrolysis
- Presence of BRAG2 after the second week in culture enables GluN2A (1) to replace tonic GluN2B-BRAG1 signalling and (2) to prevent its re-installation
- Matured neuron cultures increase Arf6-GTP levels after (5 min) NMDA-stimulation via GluN2A-BRAG2 signalling; (1) prolonged stimulation (> 5 min), (2) stimulation during GluN2A blockade or (3) during absence of BRAG2 induces Arf6-GTP hydrolysis
- Absence of BRAG1 during development changes the principles of neuronal Arf6 activation
- Absence of BRAG2 increases spine density on secondary branches of apical dendrites in cortical layer 5 neurons, and creates a surplus of morphologically more immature spines

D, Discussion

D, 1, Glutamate receptor complexes regulate Arf6 signalling

D, 1.1, NMDA receptors stimulate BRAG-GEF activity

This investigation deals with NMDA receptor signalling that leads to neuronal small GTPase Arf6 activation via BRAG proteins. Arf6-GTP levels were measured by a GST-pulldown assay with the Arf6 effector GGA3 (Figure 2B). After ligand binding (Figures 2A, 3A, 6), calcium influx via NMDA receptors promoted the Arf6 GDP/GTP-exchange by BRAG1 in young, and by BRAG2 in mature neuron cultures (Figures 2C, 4B, 7A; *DIV 7*, B, p. 60; *DIV 21*, C, p. 61). NMDA receptor signalling undergoes changes during the development of the forebrain, by a subunit switch through increased GluN2A expression in glutamatergic synapses (Paoletti et al., 2013). In consistency with the gathered results, I submit, that the NMDA receptor signalling switch finds its continuation in the consecutive recruitment of GluN2B-to-BRAG1 and GluN2A-to-BRAG2 signalling that regulated Arf6 activation of cortical neurons in the course of their maturation in culture (Figures 2A, 3A, 4A, 7A, 10; Elagabani et al., 2016). In mature neuron cultures, both pathways were

functional. BRAG2-GEF activity by NMDA stimulation switched back to BRAG1-GEF activity in response to compromised GluN2A-containing NMDA receptor signalling (Figures 7C, 8A-C; *DIV 21*, E, p. 61). The specificity in the signalling pathways correlated with the physical interactions of GluN2-BRAG signalling partners under elevated calcium concentration (Figure 12A), as it would occur after NMDA receptor stimulation. Calcium weakened the physical interactions of BRAG proteins with calmodulin and the mismatched receptor subunits (Figures 13A-D). After calmodulin release, BRAG proteins became active while remaining strongly attached to the regulatory subunit of the matching NMDA receptor at the identified sites in their cytosolic segments (Figures 12A, 12B, 12G-I, 13B-D). Unfortunately, technical difficulties prevented us from examining GluN2-CD binding to the catalytic Sec7-PH domains of BRAG1 and BRAG2 in GST pulldown assays. It would be interesting to know whether BRAG Sec7-PH domain bind to GluN2-CDs in a stable manner and/or in a calcium-sensitive manner. We were surprised to learn that the crucial binding site for the selective GluN2-BRAG interactions lied outside of the catalytic domains of BRAG proteins (Figure 13C). These N-terminal binding sites of BRAG proteins were required for the NMDA receptor-mediated BRAG-GEF activation mechanism (Figure 13G-I), which had to be factored into my proposed working model suggesting that calmodulin release can expose Sec7-PH domains of receptor-attached BRAG proteins in order to perform Arf6 GDP/GTP exchange functions. The interaction assays used here are not a proof of direct interaction. Expression of NMDA receptor and BRAG mutants affecting (a) the BRAG GEF activity, (b) the BRAG calmodulin binding, or (c) the BRAG-GluN2 interactions in neurons could reveal more details about this novel signalling pathway. Comparisons of BRAG function during expression of wild type and catalytically dead BRAG proteins after BRAG protein depletion, could reveal possible GEF-independent functions of the multi-domain BRAG proteins (also see Brown et al., 2016).

D, 1.2, NMDA and mGlu receptor signalling hierarchy in BRAG-mediated Arf6 activation in mature neurons

Besides NMDA receptor activity, Arf6 activation has been linked to AMPA and mGlu receptor activity via BRAG2 (Scholz et al., 2010). BRAG2 can interact with the cytosolic terminus of GluA2 subunits of the AMPA receptor, after AMPA and mGlu receptors are activated, which increases BRAG2 Arf6-GEF activity. The resulting Arf6 activation leads to the endocytosis of AMPA receptors. NMDA receptor-BRAG-mediated Arf6 activation too, induces endocytosis of AMPA receptors (Elagabani et al., 2016). Arf6 activation by NMDA receptors might work with a pool of BRAG proteins that is anchored to the PSD and enters into physical interaction with NMDA receptors, awaiting activation (Figure *DIV 21*, A, p. 61). The NMDA receptor-BRAG signalling however might be bypassed by mGlu receptors, which increase intracellular calcium concentrations. This promotes (1) phosphatase activity, which removes the phosphorylation on the GluA2 subunit of AMPA receptors that blocks interaction with BRAG2, and (2) calmodulin release from inactive BRAG2 (Figure *DIV 21,* D, p. 61). It is unclear whether these activation routes of Arf6 have different functional time spans or consequences. If the mGlu and the NMDA receptor mediated BRAG activation pathways are not independent of each other, a hierarchy of these pathways to activate Arf6 might exist. A major difference between these two glutamate receptor-mediated Arf6 activation mechanisms is that NMDA receptor-triggered Arf6 activation did not require phosphatase

activity. Depending on (1) the features of the stimulation, (2) the involved glutamate receptor subunits and (3) glutamate receptor complex localization, the signalling outcome of Arf6 activation might differ.

D, 1.3, Consequences of parallel NMDA and mGlu receptor signalling in mature neurons

NMDA-triggered Arf6 activation in the presence of TTX inactivating neuron network activity indicated that NMDA receptors can trigger Arf6 activation without spontaneous firing of neuron cultures. The experiments that outlined the GluN2-BRAG signalling pathways were performed in the over-expression system of HEK293 cells to ensure isolated conditions from the prevalent glutamate receptor signalling in neurons. The combined effect of NMDA, mGlu and AMPA receptor activity on synaptic BRAG activation remains an open question. NMDA as well as mGlu receptor-mediated LTD induction at Schaffer collaterals in the hippocampus of mice was obstructed after targeted BRAG2 knockout of hippocampal neurons (Scholz et al., 2010). It is not known whether mGlu receptors can trigger BRAG1 GEF-activity; presumably mGlu receptor-BRAG signalling could also take place during distinct phases of neuron development and maturation. While NMDA receptors were observed to trigger BRAG-mediated AMPA receptor endocytosis (Elagabani et al., 2016), the steps between NMDA stimulation and the internalization event are not fully clear. Downstream effects of Arf6 have been investigated before (discussed in last the paragraph, p. 63). In Myers et al., 2012, BRAG-c-Jun N-terminal Kinase-Ras signalling was suggested to induce AMPA receptor endocytosis. Many known signalling proteins rely on phosphorylation for their activation. Measuring phosphorylation levels of important signalling molecules could reveal whether, or not, and at which time points during maturation, BRAG1 and BRAG2 can induce a specific signalling pathway involved in AMPA receptor internalization upon NMDA receptor stimulation. Because of their atypical PH domain, BRAG proteins might locate to different kinds of membrane compartments. It is possible that BRAG proteins co-localize with certain GTPases or their regulators after NMDA receptor stimulation and influence the trafficking of internalized AMPA receptors. It is also not known whether BRAG proteins stay attached to, and are trafficked with, AMPA receptors that are internalized upon their activation.

D, 2, Arf6 activation and deactivation by NMDA receptor activity

D, 2.1., Self-inactivation of BRAG proteins

BRAG proteins that are controlled by NMDA receptor activity might be controlled by sequestration to the PSDs. Outside of synapses, where NMDA receptors are not as densely clustered as in PSDs and their cytosolic segments are not as readily available, BRAG proteins might (1) exist as inactive monomers in complex with calmodulin or, as suggested by the preliminary observations in the live imaging of fluorescent BRAG proteins (Figure 16), (2) form inactive BRAG multimers in the close proximity of membranes when (a) the calcium level rises (Figure 16B) and presumably when (b) AMPA receptor binding sites remain blocked in the absence of mGlu receptor activity (Scholz et al., 2010). The synaptic sites of BRAG GEF-activation might therefore differ between the two signalling routes. In adult neurons, BRAG GEF-activity might even be restricted to synaptic sites, as a result of self-inactivation of BRAGs under the above-mentioned conditions, i.e. while extrasynaptic mGlu receptor signalling is not active (Figure *DIV 21*, B, C, p. 61). Visual approaches using fluorescence or chemiluminescence resonance energy transfer have

the necessary spatial resolution to locate BRAG proteins in living neurons at different synaptic sites of the plasma membrane of spines (PATTERSON AND YASUDA, 2011). Fluorescent Arf6 effectors could be designed and used to gather information about the location of BRAG activation in neurons (KIMPLE ET AL., 2003; ITO AND UEDA, 2014).

D, 2.2., NMDA receptor-dependent Arf6GAP activity

NMDA receptor signalling affected Arf6 activation and inactivation (Figures 2A, 2B). In either case, calcium influx was the trigger (Figures 2C, 6). In instances when BRAG-mediated Arf6 activation would have occurred, but the required BRAG-GluN2 signalling was interfered with, NMDA receptors induced Arf6-GTP hydrolysis (Figures 4B, 7A). NMDA receptor stimulation in HEK293 cell cultures, which did not over-express BRAG proteins, also induced Arf6-GTP hydrolysis (Figure 3B). Arf6 GTPase-activating processes that are dependent on NMDA receptors have previously been reported (OKU AND HUGANIR, 2013). BRAG-Arf6GAP, e.g. AGAP3, interactions in NMDA receptor complexes might mediate the control of glutamate receptors over Arf6 activation, according to the demands of spine development and the synaptic input of spines. The absence of one regulator may lead to changes in NMDA receptor complex signalling of co- and counteracting regulators. Pairs of synaptic GEFs and GAPs for small GTPase regulation have been reported before (UM ET AL., 2014), and they might adjust GTPase activity in coordination with regulator pairs of other GTPases to control more complex processes. Ras and Rap for instance, have different sets of regulators, promote and counteract cell proliferation respectively, and antagonize each other during synaptic plasticity (BOS, 1998; BOS ET AL., 2001). While Ras enhances synaptic transmission, Rap diminishes it; respectively through insertion or removal of synaptic AMPA receptors (ZHU ET AL., 2002). The understanding about the synergy of two or more GTPases is at preliminary stages but could be expanded by investigation of broader GTPase signalling networks. Interactions between Arf6 and regulators of other GTPases, as well, as other GTPases with Arf6 regulators were shown to affect endosomal recycling (ALLAIRE ET AL., 2013). Interactions of activated BRAG proteins with other regulatory proteins than the discovered partners were not explored, but could be elucidated by genome-wide interaction screenings. The influence of Arf6 and other GTPases on each other's activation can be assessed with similar assays, as the pulldown with a GTPase effector that was applied here.

While calcium transients are conveyed in the timescale of milliseconds, signal molecules in spines that respond to changes in calcium concentration can extend their signalling over minutes (HARVEY ET AL., 2008; MURAKOSHI ET AL., 2011). After the signals are integrated by molecular machineries, changes in a dendritic spine can be stabilized for hours and days (KANDEL AND SCHWARTZ, 2013). Similar to the activation timescales of other GEFs and GAPs that signal in dendritic spines (HARVEY ET AL., 2008; MURAKOSHI ET AL., 2011), Arf6 activation by NMDA receptor stimulation became measurable after a few minutes (Figure 7A). Arf6 activation peaked at five minutes after application of 100 µM NMDA. Arf6-GTP levels remained high; up to more than 15 minutes after the stimulation. Longer than five-minute stimulations caused Arf6-GTP hydrolysis (Figures 6C, 6D). The balance in NMDA receptor-triggered Arf6-GEF and Arf6-GAP activity might therefore be regulated by different conditions of NMDA receptor stimulation, which gives NMDA receptors the possibility of full control over the tuning of synaptic Arf6-

GTP levels. The existence of an Arf6GAP that explains the observed behavior of NMDA receptor dependent Arf6 regulation is entirely hypothetical at this point and needs to be identified. Arf6GAPs expressed in cortical neurons that bind calmodulin and respond to NMDA receptor stimulation in an over-expression system could be primary candidates. Protein fractionation also needs to show that spines contain this Arf6GAP, and possibly a modulator protein that mediates the interactions of Arf6 regulators e.g. from the (1) Arf GAP with Rho GAP, ankyrin repeat, PH domains family or (2) Arf GAP with Src homology3, ankyrin repeat, PH domains family (Jaworski, 2007; Myers and Casanova, 2008). For the development of novel tools to investigate Arf6 activation in neurons, the description of the panel of Arf6GAPs, Arf6 GEFs and Arf6 activation modulators that specifically localize to spines might be of great value. Like for BRAG proteins, there might be different Arf6GAPs becoming functional at different time points of neuronal development. Their activation might show NMDA receptor subunit specificity as well. The suspected Arf6GAP in HEK293 cells, shown in figures 2A and 2B, might also be different to the neuronal Arf6GAPs, presented in figures 4B and 7A. Investigation of Arf6GAPs could be performed with similar approaches as presented here. Enzymes that characteristically respond to changes in calcium concentration are especially interesting.

D, 3, BRAG-mediated Arf6 activation changes, as glutamate receptor complexes mature

D, 3.1., BRAG functions before the NMDA receptor subunit switch

Signalling complexes in synapses convert neuronal activity patterns into changes of the PSD architecture surrounding them, which remains elusive in respect to its molecular mechanisms. Synaptic changes include incorporation of different receptor subunits into the glutamate receptor complexes themselves; a trait AMPA and NMDA receptor complexes share alike. By extending large protein segments from the membrane into the cytosol, glutamate receptors, and NMDA receptors in particular, serve as specialized PSD binding platforms for signalling proteins inside the cell. As binding platforms, they recruit different sets of signalling molecules into the receptor complex via physical protein interactions. Consequently, the composition of glutamate receptor complexes that incorporate into the plasma membrane of spines defines how neurotransmission beyond ion currents is orchestrated. The assembly of different sets of signalling proteins via receptor complexes has been shown to change intracellular signalling (Kennedy, 2000, Lamprecht and LeDoux, 2004).

In Adesnik et al., 2008, it was proposed that once structural stability of newly formed synapses is established, incorporated GluN2B-NMDA receptors keep AMPA receptors from accumulating in the synapse. To achieve this, GluN2B-NMDA receptors in immature synapses might recruit pathways that induce LTD in mature synapses. In these immature synapses, GluN2B-mediated signalling is also necessary for a synapse to detect correlated neuronal activity that can overcome the depressive effect of GluN2B-receptors. Eventually, when the switch to GluN2A-containing receptors is promoted, mature NMDA receptor subtypes take control over AMPA receptor trafficking and activity-dependent synapse strengthening (Adesnik et al., 2008; Gray et al., 2011). The consecutive installation of BRAG signalling regulated by different NMDA receptor subtypes might enable neurons to regulate Arf6-GTP levels during synaptic maturation. BRAG1 signalling that activates Arf6 upon early synaptic activity might

be connected to the depressing function of GluN2B-NMDA receptors in young neurons (Figure 5B, see ADESNIK ET AL., 2008). At a stage when neurons had more stable synapses, BRAG2 signalling required NMDA stimulation to activate Arf6 (Figure *DIV 21*, B, C, p. 61). This plays into the notion that only strong stimuli can provoke relevant responses at the end of the neuronal maturation (YASHIRO AND PHILPOT, 2008).

Through the way in which the measurements of relative Arf6 activation were deployed here, local and temporal changes in active Arf6 levels and Arf6 activation mechanisms might have been missed. The physiological meaning of the decrease in Arf6-GTP levels in comparison to the total amount of cellular Arf6 has to be further described, and might be misleading at this moment, considering the scope of the applied methods. The consequences of the developmental change in Arf6-GTP levels also remain to be described and correlated to the very structures where synaptic activity dependent BRAG activation takes place.

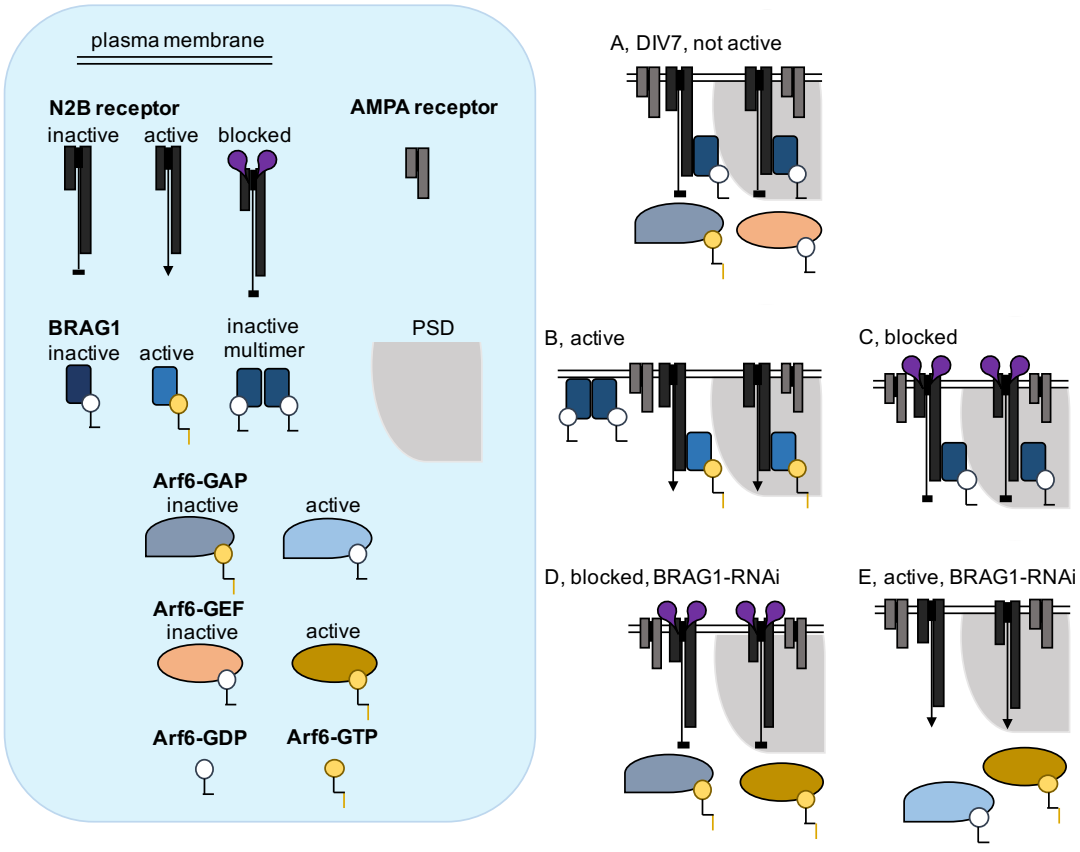

Figure, *DIV 7, BRAG signalling in one-week-old cortical neurons.*

A, Young neurons express synaptic BRAG1, which enhances synaptic transmission and replaces NMDA receptor independent Arf6 activation mechanisms. Note that young neurons might express Arf6-GEFs that are controlling Arf6 activation prior to BRAG expression in spines. B, BRAG1 expression installs NMDA receptor-triggered Arf6 activation. C, BRAG1 signalling is sensitive to GluN2B-receptor blockade. D, Depletion of BRAG1 reveals NMDA receptor independent Arf6 activation. E, After depletion of BRAG1, GluN2B-receptor activity induces the hydrolysis of Arf6-GTP.

D, 3.2., Changes in Arf6 activation principles by BRAG signalling

In cultured neurons, Arf6 activation by BRAGs shifted from a GluN2B- to a GluN2A-dominated signalling (Figures 2A, 3A, 4A, 7A, 10; *DIV 7*, B, C, p. 60; *DIV 21*, B, C, p. 61). After BRAG2 depletion, neurons were not able to enter into the mature GluN2A-mediated Arf6 activation pathway (Figures 8C; *DIV 21*, F, p. 61). After early depletion of BRAG1, GluN2B-NMDA receptors were not able to activate Arf6 anymore (Figure 5B). Loss of BRAG1 at DIV 2-4 (1) caused persistently elevated Arf6 activation, by an early NMDA receptor-BRAG-independent pathway (Figures 9B; *DIV 7*, D, p. 60; *DIV 21*, G, H, p. 61), (2) changed NMDA receptor signalling cascades in young neurons towards hydrolyzing active Arf6 (Figure *DIV 7*, E, p. 60) and (3) interfered with the BRAG2 signalling pathway at mature stages via GluN2B-receptor activity (Figures 9C; *DIV 21*, H, p. 61). After considering the presented results, I propose that BRAG1 expression induces a process that allows GluN2B-NMDA receptors to replace NMDA receptor-independent Arf6 activation mechanisms before synaptic maturation (Figure *DIV 7*, A, p. 60). One or more Arf6GEFs that are active in developing neurons (Figure 5B, 9C), EFA6A for instance (Choi, 2006) might cause a tonal Arf6 activation at the beginning of their maturation. By the start of BRAG1 signalling, these Arf6-GEFs might be blocked, and Arf6 activation in young neurons would become responsive to synaptic activity only when GluN2B-receptors are activated. In a similar event, BRAG2-dominated signalling might replace BRAG1 signalling to help synapses to stabilize through a robust reduction of active Arf6 levels (Figure 8A).

Another consequence of this is that, given the tonally elevated levels of Arf6-GTP after BRAG1 depletion and GluN2B-receptor inactivation through ifenprodil treatment (Figure 5B; *DIV 7*, D, p. 60), young neurons might have less active Arf6 at basal levels, when BRAG1 is expressed in synapses and NMDA receptors are inactive (Figure *DIV 7*, A, p. 60). In Brown et al., 2016, it was shown that the interaction of BRAG1 with the PSD enhances synaptic transmission even by catalytically dead mutants of BRAG1. Increased AMPA receptor insertion by incorporation of BRAG1 into the PSD was favored to explain the strengthening of synapses; i.e. over the possibility of a curbed AMPA receptor removal from synapses caused by synaptic BRAG1 expression. As initially indicated in Brown et al., 2016, synaptic BRAG1 expression may nonetheless increase AMPA receptor density by regulating and reducing Arf6 activation (Figure *DIV 7*, A, p. 60) and AMPA receptor internalization at resting conditions of neurons, e.g. by forming and recruiting an Arf6-GEF/GAP-complex to synapses, or stabilizing Arf6GEF modulators at synapses, et cetera. Later in development, when GluN2A-containing receptors were increasingly expressed, cortical neuron cultures displayed robustly lowered Arf6-GTP levels, even at conditions when NMDA receptors were stimulated by network activity (Figures 3B; *DIV 21*, B, p. 61). Installation of BRAG2 signalling might also be responsible for this; possibly through a similar mechanism as the ones mentioned above for BRAG1 (see Figure 9C). Interfering with GluN2A-containing NMDA receptor signalling in mature neurons induced a return to GluN2B dependent Arf6 activation (Figures 8A; *DIV 21*, E, p. 61). When BRAG1 was depleted from adult neurons, this reversion was not possible anymore (Figure 9B). Cortical neurons might show this functional plasticity of BRAG signalling in the brain as well. A visual assay in living neurons to report BRAG activation has not been established so far. If interaction between fluorescent BRAG proteins with modified fluorescent Arf6 effectors could generate distinct signals to report BRAG GEF-activity, changes in the time point and location of BRAG1 or BRAG2 signalling might be able to be visualized on the level of individual dendritic spines, and neurons.

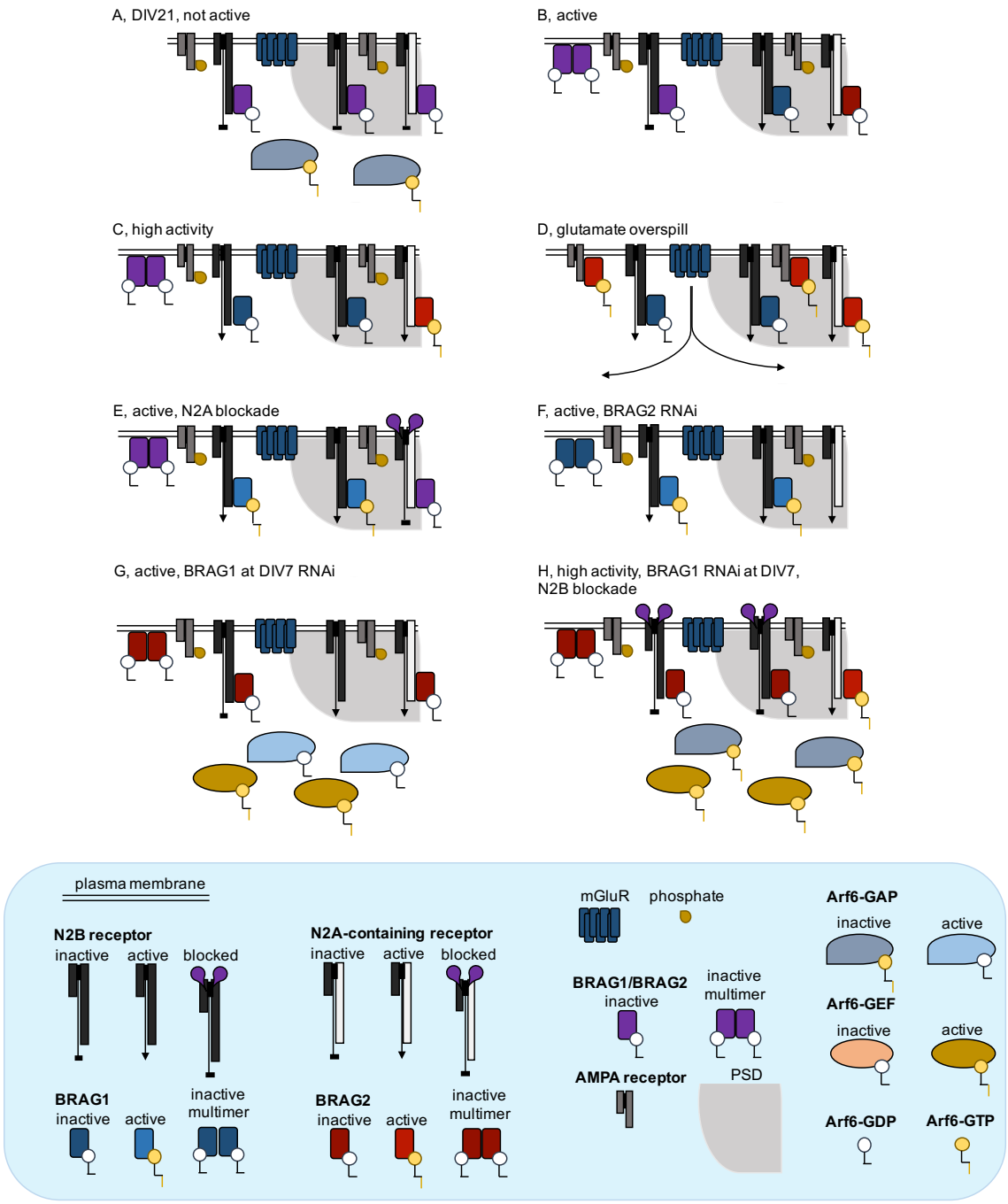

Figure, ***DIV 21, BRAG signalling in spines of three-weeks-old cortical neurons.***

A, In mature neurons, BRAG1 and BRAG2 form complexes with NMDA receptors after incorporation into the synapse. An unknown mechanism mediates NMDA receptor dependent Arf6 hydrolysis. B, Spontaneous network activity in neuron cultures can activate NMDA receptors but does not induce NMDA receptor-triggered Arf6 activation. Tonal GluN2B-BRAG1 signalling is not present. C, A strong stimulus like NMDA treatment can induce GluN2A-containing receptor-mediated Arf6 activation. D, The relationship between AMPA receptor- and NMDA receptor-mediated Arf6 activation is unclear. The mGlu and NMDA receptor Arf6 activation pathways might have distinct characters and functionalities and could take place in parallel. E, Impairment of the activity of GluN2A-containing NMDA receptor signalling installs tonal GluN2B-BRAG1 signalling. F, Depletion of BRAG2 installs tonal GluN2B-BRAG1 signalling. G, BRAG1 depletion installs tonal NMDA receptor independent Arf6 activation and a GluN2B-receptor dependent mechanism that blocks NMDA-stimulated Arf6 activation. H, NMDA-stimulated GluN2A-BRAG2 signalling takes place in early BRAG1-depleted neurons but is only measurable after the negative tone of GluN2B-receptor activity is blocked.

D, 4, Small GTPase signalling in glutamate receptor complexes remodel spines and their synapses – an outlook

D, 4.1., Signalling cascades of Arf6 in spines

Components of small GTPase signalling pathways interact with cytosolic glutamate receptor extensions to couple neuronal activity to synaptic changes (Schwechter et al., 2013; Um et al., 2014; Oku and Huganir, 2013). Arf6 combines two aspects of synaptic plasticity, i.e. spine remodelling (Choi, 2006; Kim et al., 2015) and neurotransmitter receptor trafficking (Macia et al., 2004; Scholz et al., 2010; Myers et al., 2012; Piguel et al., 2014). Arf6 regulates vesicle biogenesis by shifting cytoskeletal dynamics, modifying lipids at (Krauss et al., 2003) and recruiting coat-forming proteins to the plasma membrane (Paleotti O, 2005). The main effects of Arf6 activity at the plasma membrane are mediated by phosphatidylinositol 4-phosphate 5-kinase (PIP5K) and phospholipase D, which produce phosphoinositol 4-5-bisphosphate and phosphatic acid, respectively (Randazzo et al., 2000). Their lipid biogenesis displays regulation loops created by affecting each other's production rate; i.e. phosphatic acid activates PIP5K, and phospholipase D is affected by regulators controlled by phosphoinositol 4-5-bisphosphate (as reviewed in Randazzo et al., 2000). Phosphoinositol 4-5-bisphosphate and phosphatic acid signalling at membranes targets different sets of effectors. In this and other ways, the signals from active Arf6 regulate the outcome of other small GTPase signalling cascades. Small GTPase signalling pathways generally cross after a few reaction steps with the assistance of a large selection of modulators that assemble and position them with other regulators (Myers and Casanova, 2008). By confining the place of these reactions like in dendritic spines, robust local signalling cascades of synaptic signalling proteins that contain regulatory loops might be created (Grant and O'Dell, 2001).

D, 4.2., Synergy of Arf6 and related small GTPases to regulate the cytoskeleton

In immature neurons up to two weeks in culture, Arf6 activation is controlled by NMDA receptor activation via BRAG1 (Figure 5B) and promotes dendritic spine formation with the involvement of Rac1 (Bongmba et al., 2011; Kim et al., 2015). At this stage, neuronal Rac1 expression is at its highest point and was shown to affect spines at the level of the filopodia-to-spine transition (Raemaekers et al., 2012), while synaptic glutamatergic activity is dominated by GluN2B-NMDA receptors. Arf6 activity was suggested to control Rac signalling not only as effector, but also by regulating its localization to the plasma membrane by activating phospholipase D to generate phosphatic acid (Randazzo et al., 2000). At later stages, neuronal excitatory synapses are dominated by GluN2A-containing NMDA receptors that control Arf6 activity via BRAG2 (Figure 8A) and increasingly activate RhoA (Kim et al., 2015). RhoA antagonizes Rac1 signaling to regulate the maintenance of spines in mature neurons. Arf6 might therefore be activated by NMDA receptors to induce different signalling outcomes that regulate cytoskeletal dynamics at different time points of dendritic spine maturation. Loss of BRAG2 by genetic depletion in cortical cultures displayed elevated Arf6-GTP levels presumably by remaining in the GluN2B-BRAG1 signaling modality in culture. Loss of BRAG2 in *Iqsec*$^{fl/fl}$ mice forebrains resulted in the occurrence of more immaturely shaped spines on principal neuron dendrites in the parietal neocortex, when compared to wild type brains (Figure 11E-H). The effects brought by the change in BRAG-mediated Arf6 activation therefore affected the cytoskeletal dynamics in spines. Increased Arf6 activation by the continuation of GluN2B-BRAG1 signaling

in adult neuron cultures would coincide with a reduced number of synapses and amplitudes of evoked NMDA and AMPA receptor currents in BRAG2-depleted neurons (Elagabani et al., 2016). Weakened synaptic transmission by reduced AMPA and NMDA receptor currents in BRAG2-depleted neurons (Elagabani et al., 2016) might have induced the outgrowth of immature spines as a compensatory mechanism (Kirov and Harris, 1999). Notably, cortical neuron dendrites of infants with an inherited form of intellectual disability display an excess of thin spines, which disappears by the time of puberty resulting in decreased spine densities (Purpura, 1974). Mutations in Brag1 have later been proposed to cause X-chromosome-linked intellectual disability (Shoubridge et al., 2010). Alterations in the number and shape of dendritic spines can be caused by altered synaptic signalling and can have severe physiological effects on brain functions. An unusual increase in the amount of active Arf6 levels might be one cause for this (Figure 11H). It is possible that gene therapy or functional manipulation to regulate Arf6-GTP levels in these affected brains at the right time span might promote normal brain development. On a similar note, efforts to control the role of Arf6 in the invasiveness of cancer cells are already in progress (Sabe, 2003; Valderrama and Ridley, 2008).

D, 4.3., NMDA receptors trigger BRAG mediated Arf6 activation to regulate AMPA receptor trafficking

To date, the molecular foundation to induce the reduction of AMPA receptors during LTD remains short of a simplified description, although several have been proposed. AMPA and NMDA receptor trafficking and capturing inside spines and their plasma membrane play a crucial role in LTD and metaplasticity mechanisms in principal neurons of the neocortex, and Arf6-regulated vesicular transport might be involved in their adjustment. While single knockdowns showed no effect, simultaneous depletion of BRAG1 and BRAG2 reduced the amount of NMDA receptors in cortical cultures for reasons that were not determined here (Figure 4C). The combined lack of BRAG proteins might have altered trafficking-dependent rates of NMDA receptor synthesis and degradation in the affected cells. Unlike for NMDA receptors, changes in AMPA receptor trafficking after the depletion of BRAG proteins have been shown, and correlated with Arf6-GTP levels (Elagabani et al., 2016). Mature neurons after RNAi-mediated BRAG2 depletion have fewer and smaller synapses and show higher rates of AMPA receptor endocytosis, which did not respond to NMDA stimulation as it did in control or BRAG1-shRNA infected neurons.

Arf6 activation in adult neurons can (1) reduce GluA1-containing AMPA receptor currents via NMDA receptor activity (Myers et al., 2012), and (2) induce LTD via NMDA and mGlu receptor-dependent AMPA receptor internalization (Scholz et al., 2010). Both processes are mediated by BRAGs and require regulated AMPA receptor trafficking that might be affected by the Arf6 activation principles suggested in this dissertation. It remains unclear if BRAG-mediated Arf6 activation dictated by glutamate receptor activation takes part in the vesicular AMPA receptor trafficking out of spines (Zheng et al., 2015), or trafficking towards degradation and recycling back to the plasma membrane (Ehlers, 2000), or other processes involved in NMDA receptor-dependent LTD. NMDA receptor stimulation activates calcineurin and protein phosphatase 1 which target PIP5K. Once dephosphorylated, PIP5K interacts with AP-2 that is recruited to membranes. This stimulates PIP5K to produce phosphoinositol 4-5-bisphosphate, which prompts the recruitment of the endocytic machinery and promotes the assembly of the endocytic machinery that endocytoses AMPA receptors by interacting with the receptors' endocytic motifs (Unoki

ET AL., 2012). Arf6 also stimulates PIP5K to produce phosphoinositol 4-5-bisphosphate (KRAUSS ET AL., 2003).

We recently showed AMPA receptor miniature events in mice forebrains infected with adeno-associated viruses delivering shRNA for BRAG1 or BRAG2 RNAi to their hippocampi (ELAGABANI ET AL., 2016). In cases when BRAG depletion induced elevated Arf6-GTP levels, i.e. BRAG1 knockdown in young neurons and BRAG2 knockdown in mature neurons, the loss of BRAG proteins reduced the frequency of spontaneous AMPA receptor currents in CA1 neurons of the hippocampus, and therefore the number of their functional synapses. This indicates that the identified NMDA receptor-BRAG-Arf6 signalling pathways regulate the stability of CA1 synapses during the development of the hippocampus. Since the conditional knockout of BRAG2 in the forebrain of mice led to compromised AMPA receptor as well as NMDA receptor currents, the exact consequences of BRAG-mediated Arf6 activation, and the specificity of its effects, need further elaboration.

The gathered results and proposed mechanisms of NMDA-triggered BRAG-GEF activity might help to put the role of Arf6 activation during neuronal development into new perspectives. Further insight in the interaction of BRAG proteins with calmodulin, glutamate receptors and synaptic proteins might help to understand the fine-tuning of synaptic Arf6 activation by BRAGs. Targeted interference with the identified BRAG-GluN2 interactions by sequence mutations or competitive peptides might eventually become useful in further studies to tune NMDA receptor dependent Arf6 activation in neurons and possibly alter neuronal connectivity of principal neurons of the neocortex. Finally, through elucidation of the molecular mechanisms controlling Arf6 activation and synaptic BRAG functions, we might understand how BRAG proteins stabilize or destabilize synapses of neurons in the neocortex and other regions in the brain during their development.

E, References

1. Abrahamsson, T., Gustafsson, B., and Hanse, E. (2008). AMPA silencing is a prerequisite for developmental long-term potentiation in the hippocampal CA1 region. J. Neurophysiol. *100*, 2605–2614.
2. Adesnik, H., Li, G., During, M.J., Pleasure, S.J., and Nicoll, R. a (2008). NMDA receptors inhibit synapse unsilencing during brain development. Proc. Natl. Acad. Sci. U. S. A. *105*, 5597–5602.
3. Aizel, K., Biou, V., Navaza, J., Duarte, L. V., Campanacci, V., Cherfils, J., and Zeghouf, M. (2013). Integrated Conformational and Lipid-Sensing Regulation of Endosomal ArfGEF BRAG2. PLoS Biol. *11*, 1–12.
4. Allaire, P.D., Seyed Sadr, M., Chaineau, M., Seyed Sadr, E., Konefal, S., Fotouhi, M., Maret, D., Ritter, B., Del Maestro, R.F., and McPherson, P.S. (2013). Interplay between Rab35 and Arf6 controls cargo recycling to coordinate cell adhesion and migration. J. Cell Sci. *126*, 722–731.
5. Andrásfalvy, B.K., and Magee, J.C. (2004). Changes in AMPA receptor currents following LTP induction on rat CA1 pyramidal neurones. J. Physiol. *559*, 543–554.
6. Antonny, B. (2006). Membrane deformation by protein coats. Curr. Opin. Cell Biol. *18*, 386–394.
7. Araya, R., Nikolenko, V., Eisenthal, K.B., and Yuste, R. (2007). Sodium channels amplify spine potentials. Proc. Natl. Acad. Sci. U. S. A. *104*, 12347–12352.
8. Arellano, J.I., Benavides-Piccione, R., Defelipe, J., and Yuste, R. (2007). Ultrastructure of dendritic spines: correlation between synaptic and spine morphologies. Front. Neurosci. *1*, 131–143.
9. Ascher, P., and Nowak, L. (1988). Quisqualate- and kainate-activated channels in mouse central neurones in culture. J. Physiol. *399*, 227–245.
10. Bellone, C., and Nicoll, R.A. (2007). Rapid bidirectional switching of synaptic NMDA receptors. Neuron *55*, 779–785.
11. Ben-Ari, Y. (2002). Excitatory actions of gaba during development: the nature of the nurture. Nat. Rev. Neurosci. *3*, 728–739.
12. Bito, H. (2010). The chemical biology of synapses and neuronal circuits. Nat. Chem. Biol. *6*, 560–563.
13. Bliznyuk, A., Aviner, B., Golan, H., Hollmann, M., and Grossman, Y. (2015). The N-methyl-D-aspartate receptor's neglected subunit - GluN1 matters under normal and hyperbaric conditions. Eur. J. Neurosci. *42*, 2577–2584.
14. Bongmba, O.Y.N., Martinez, L.A., Elhardt, M.E., Butler, K., and Tejada-Simon, M. V (2011). Modulation of dendritic spines and synaptic function by Rac1: a possible link to Fragile X syndrome pathology. Brain Res. *1399*, 79–95.
15. Bonifacino, J.S., and Lippincott-Schwartz, J. (2003). Coat proteins: shaping membrane transport. Nat. Rev. Mol. Cell Biol. *4*, 409–414.
16. Bos, J.L. (1998). All in the family? New insights and questions regarding interconnectivity of Ras, Rap1 and Ral. EMBO J. *17*, 6776–6782.
17. Bos, J.L., de Rooij, J., and Reedquist, K.A. (2001). Rap1 signalling: adhering to new models. Nat. Rev. Mol. Cell Biol. *2*, 369–377.
18. Boyer, C., Schikorski, T., and Stevens, C.F. (1998). Comparison of hippocampal dendritic spines in culture and in brain. J. Neurosci. *18*, 5294–5300.
19. Brown, J.C., Petersen, A., Zhong, L., Himelright, M.L., Murphy, J.A., Walikonis, R.S., and Gerges, N.Z. (2016). Bidirectional regulation of synaptic transmission by BRAG1/IQSEC2 and its requirement in long-term depression. Nat. Commun. *7*, 11080.
20. Cajal, S. y R. (1899). Textura del sistema nervioso del hombre y de los vertebrados. (Imprenta y Librería de Nicolás Moya, Madrid).
21. Carroll, R.C., Beattie, E.C., Xia, H., Lüscher, C., Altschuler, Y., Nicoll, R.A., Malenka, R.C., and von Zastrow, M. (1999). Dynamin-dependent endocytosis of ionotropic glutamate receptors. Proc. Natl. Acad. Sci. U. S. A. *96*, 14112–14117.
22. Cash, S., and Yuste, R. (1999). Linear summation of excitatory inputs by CA1 pyramidal neurons. Neuron *22*, 383–394.
23. Chesneau, L., Dambournet, D., MacHicoane, M., Kouranti, I., Fukuda, M., Goud, B., and Echard, A. (2012). An ARF6/Rab35 GTPase cascade for endocytic recycling and successful cytokinesis. Curr. Biol. *22*, 147–153.
24. Choi, S. (2006). ARF6 and EFA6A Regulate the Development and Maintenance of Dendritic Spines. J. Neurosci. *26*, 4811–4819.
25. Collingridge, G.L., Isaac, J.T.R., and Wang, Y.T. (2004). Receptor trafficking and synaptic plasticity. Nat. Rev. Neurosci. *5*, 952–962.
26. Cox, R., Mason-Gamer, R.J., Jackson, C.L., and Segev, N. (2004). Phylogenetic analysis of Sec7-domain-containing Arf nucleotide exchangers. Mol. Biol. Cell *15*, 1487–1505.

27. D'Souza-Schorey, C., and Stahl, P.D. (1995). Myristoylation is required for the intracellular localization and endocytic function of ARF6. Exp. Cell Res. *221*, 153–159.
28. D'Souza-Schorey, C., Van Donselaar, E., Hsu, V.W., Yang, C., Stahl, P.D., and Peters, P.J. (1998). ARF6 targets recycling vesicles to the plasma membrane: Insights from an ultrastructural investigation. J. Cell Biol. *140*, 603–616.
29. Donaldson, J.G. (2003). Multiple Roles for Arf6: Sorting, Structuring, and Signaling at the Plasma Membrane. J. Biol. Chem. *278*, 41573–41576.
30. Donaldson, J.G., and Jackson, C.L. (2011). ARF family G proteins and their regulators: roles in membrane transport, development and disease. Nat. Rev. Mol. Cell Biol. *12*, 362–375.
31. Dumas, T.C. (2005). Developmental regulation of cognitive abilities: modified composition of a molecular switch turns on associative learning. Prog. Neurobiol. *76*, 189–211.
32. Dunphy, J.L., Moravec, R., Ly, K., Lasell, T.K., Melancon, P., and Casanova, J.E. (2006). The Arf6 GEF GEP100/BRAG2 regulates cell adhesion by controlling endocytosis of beta1 integrins. Curr. Biol. *16*, 315–320.
33. Dupuis, J.P., Feyder, M., Miguelez, C., Garcia, L., Morin, S., Choquet, D., Hosy, E., Bezard, E., Fisone, G., Bioulac, B.H., et al. (2013). Dopamine-Dependent Long-Term Depression at Subthalamo-Nigral Synapses Is Lost in Experimental Parkinsonism. J. Neurosci. *33*, 14331–14341.
34. Ehlers, M.D. (2000). Reinsertion or Degradation of AMPA Receptors Determined by Activity-Dependent Endocytic Sorting. Neuron *28*, 511–525.
35. Elagabani, M.N., Briševac, D., Kintscher, M., Pohle, J., Köhr, G., Schmitz, D., and Kornau, H.-C. (2016). Subunit-Selective NMDA Receptor Signaling through BRAG1 and BRAG2 during Synapse Maturation. J. Biol. Chem. *291*, 9105–9118.
36. Endele, S., Rosenberger, G., Geider, K., Popp, B., Tamer, C., Stefanova, I., Milh, M., Kortum, F., Fritsch, A., Pientka, F.K., et al. (2010). Mutations in GRIN2A and GRIN2B encoding regulatory subunits of NMDA receptors cause variable neurodevelopmental phenotypes. Nat Genet *42*, 1021–1026.
37. Erreger, K., Dravid, S.M., Banke, T.G., Wyllie, D.J.A., and Traynelis, S.F. (2005). Subunit-specific gating controls rat NR1/NR2A and NR1/NR2B NMDA channel kinetics and synaptic signalling profiles. J. Physiol. *563*, 345–358.
38. Fan, X., Jin, W.Y., and Wang, Y.T. (2014). The NMDA receptor complex: a multifunctional machine at the glutamatergic synapse. Front. Cell. Neurosci. *8*, 160.
39. Feldman, D.E., and Knudsen, E.I. (1998). Experience-dependent plasticity and the maturation of glutamatergic synapses. Neuron *20*, 1067–1071.
40. Feng, W., and Zhang, M. (2009). Organization and dynamics of PDZ-domain-related supramodules in the postsynaptic density. Nat. Rev. Neurosci. *10*, 87–99.
41. Feng, G., Mellor, R.H., Bernstein, M., Keller-Peck, C., Nguyen, Q.T., Wallace, M., Nerbonne, J.M., Lichtman, J.W., and Sanes, J.R. (2000). Imaging neuronal subsets in transgenic mice expressing multiple spectral variants of GFP. Neuron *28*, 41–51.
42. Ferreira, J.S., Schmidt, J., Rio, P., Águas, R., Rooyakkers, A., Li, K.W., Smit, A.B., Craig, A.M., and Carvalho, A.L. (2015). GluN2B-Containing NMDA Receptors Regulate AMPA Receptor Traffic through Anchoring of the Synaptic Proteasome. J. Neurosci. *35*, 8462–8479.
43. Foster, K. a, McLaughlin, N., Edbauer, D., Phillips, M., Bolton, A., Constantine-Paton, M., and Sheng, M. (2010). Distinct roles of NR2A and NR2B cytoplasmic tails in long-term potentiation. J. Neurosci. *30*, 2676–2685.
44. Fukaya, M., Kamata, A., Hara, Y., Tamaki, H., Katsumata, O., Ito, N., Takeda, S., Hata, Y., Suzuki, T., Watanabe, M., et al. (2011). SynArfGEF is a guanine nucleotide exchange factor for Arf6 and localizes preferentially at post-synaptic specializations of inhibitory synapses. J. Neurochem. *116*, 1122–1137.
45. Funakoshi, Y., Hasegawa, H., and Kanaho, Y. (2011). Regulation of PIP5K activity by Arf6 and its physiological significance. J. Cell. Physiol. *226*, 888–895.
46. Goebbels, S., Bormuth, I., Bode, U., Hermanson, O., Schwab, M.H., and Nave, K.-A. (2006). Genetic targeting of principal neurons in neocortex and hippocampus of NEX-Cre mice. Genesis *44*, 611–621.
47. Grant, S.G.N. (2016). The molecular evolution of the vertebrate behavioural repertoire. Philos. Trans. R. Soc. Lond. B. Biol. Sci. *371*, 20150051.
48. Grant, S.G.N., and O'Dell, T.J. (2001). Multiprotein complex signaling and the plasticity problem. Curr. Opin. Neurobiol. *11*, 363–368.
49. Gray, E.G. (1959). Electron Microscopy of Synaptic Contacts on Dendrite Spines of the Cerebral Cortex. Nature *183*, 1592–1593.
50. Gray, J.A., Shi, Y., Usui, H., During, M.J., Sakimura, K., and Nicoll, R.A. (2011). Distinct modes of AMPA receptor suppression at developing synapses by GluN2A and GluN2B: single-cell NMDA receptor subunit deletion in vivo. Neuron *71*, 1085–1101.

51. Gray, N.W., Fourgeaud, L., Huang, B., Chen, J., Cao, H., Oswald, B.J., Hémar, A., and McNiven, M.A. (2003). Dynamin 3 is a component of the postsynapse, where it interacts with mGluR5 and Homer. Curr. Biol. *13*, 510–515.
52. Grunditz, A., Holbro, N., Tian, L., Zuo, Y., and Oertner, T.G. (2008). Spine neck plasticity controls postsynaptic calcium signals through electrical compartmentalization. J. Neurosci. *28*, 13457–13466.
53. Guirado, R., Perez-Rando, M., Sanchez-Matarredona, D., Castillo-Gómez, E., Liberia, T., Rovira-Esteban, L., Varea, E., Crespo, C., Blasco-Ibánez, J.M., and Nacher, J. (2014). The dendritic spines of interneurons are dynamic structures influenced by PSA-NCAM expression. Cereb. Cortex *24*, 3014–3024.
54. Hanse, E., Seth, H., and Riebe, I. (2013). AMPA-silent synapses in brain development and pathology. Nat. Rev. Neurosci. *14*, 839–850.
55. Hardingham, G.E., and Bading, H. (2010). Synaptic versus extrasynaptic NMDA receptor signalling: implications for neurodegenerative disorders. Nat. Rev. Neurosci. *11*, 682–696.
56. Harris, K.M., Jensen, F.E., and Tsao, B. (1992). Three-dimensional structure of dendritic spines and synapses in rat hippocampus (CA1) at postnatal day 15 and adult ages: implications for the maturation of synaptic physiology and long-term potentiation. J. Neurosci. *12*, 2685–2705.
57. Harvey, C.D., Yasuda, R., Zhong, H., and Svoboda, K. (2008). The spread of Ras activity triggered by activation of a single dendritic spine. Science *321*, 136–140.
58. Hasegawa, S., Sakuragi, S., Tominaga-Yoshino, K., and Ogura, A. (2015). Dendritic spine dynamics leading to spine elimination after repeated inductions of LTD. Sci. Rep. *5*, 7707.
59. Häusser, M., Spruston, N., Stuart, G.J., and Hausser, M. (2000). Diversity and Dynamics Signaling of Dendritic Signalling. Science (80-.). *290*, 739–744.
60. Hayashi, Y., Shi, S.H., Esteban, J. a, Piccini, a, Poncer, J.C., and Malinow, R. (2000). Driving AMPA receptors into synapses by LTP and CaMKII: requirement for GluR1 and PDZ domain interaction. Science *287*, 2262–2267.
61. Hell, J.W. (2014). CaMKII: claiming center stage in postsynaptic function and organization. Neuron *81*, 249–265.
62. Higley, M.J. (2014). Localized GABAergic inhibition of dendritic Ca2+ signalling. Nat. Rev. Neurosci. *15*, 567–572.
63. Hiroi, T., Someya, A., Thompson, W., Moss, J., and Vaughan, M. (2006). GEP100/BRAG2: activator of ADP-ribosylation factor 6 for regulation of cell adhesion and actin cytoskeleton via E-cadherin and alpha-catenin. Proc. Natl. Acad. Sci. U. S. A. *103*, 10672–10677.
64. Hoffmann, H., Gremme, T., Hatt, H., and Gottmann, K. (2000). Synaptic activity-dependent developmental regulation of NMDA receptor subunit expression in cultured neocortical neurons. J. Neurochem. *75*, 1590–1599.
65. Hollmann, M., and Heinemann, S. (1994). Cloned glutamate receptors. Annu. Rev. Neurosci. *17*, 31–108.
66. Hsia, a Y., Malenka, R.C., and Nicoll, R. a (1998). Development of excitatory circuitry in the hippocampus. J Neurophysiol *79*, 2013–2024.
67. Isaac, J.T.R., Nicoll, R.A., and Malenka, R.C. (1995). Evidence for silent synapses: Implications for the expression of LTP. Neuron *15*, 427–434.
68. Jaworski, J. (2007). ARF6 in the nervous system. Eur. J. Cell Biol. *86*, 513–524.
69. Kandel, E., and Schwartz, J. (2013). Principles of Neural Science, Fifth Edition.
70. Katz, Y., Menon, V., Nicholson, D.A., Geinisman, Y., Kath, W.L., and Spruston, N. (2009). Synapse Distribution Suggests a Two-Stage Model of Dendritic Integration in CA1 Pyramidal Neurons. Neuron *63*, 171–177.
71. Kennedy, M.B. (2000). Signal-processing machines at the postsynaptic density. Science *290*, 750–754.
72. Kennedy, M.B., Beale, H.C., Carlisle, H.J., and Washburn, L.R. (2005). Integration of biochemical signalling in spines. Nat. Rev. Neurosci. *6*, 423–434.
73. Kim, E., Naisbitt, S., Hsueh, Y.P., Rao, A., Rothschild, A., Craig, A.M., and Sheng, M. (1997). GKAP, a novel synaptic protein that interacts with the guanylate kinase-like domain of the PSD-95/SAP90 family of channel clustering molecules. J. Cell Biol. *136*, 669–678.
74. Kim, Y., Lee, S.E., Park, J., Kim, M., Lee, B., Hwang, D., and Chang, S. (2015). ADP-ribosylation factor 6 (ARF6) bidirectionally regulates dendritic spine formation depending on neuronal maturation and activity. J. Biol. Chem. *290*, 7323–7335.
75. Kirov, S.A., and Harris, K.M. (1999). Dendrites are more spiny on mature hippocampal neurons when synapses are inactivated. Nat. Neurosci. *2*, 878–883.
76. Köhr, G., Jensen, V., Koester, H.J., Mihaljevic, A.L. a, Utvik, J.K., Kvello, A., Ottersen, O.P., Seeburg,

P.H., Sprengel, R., and Hvalby, Ø. (2003). Intracellular domains of NMDA receptor subtypes are determinants for long-term potentiation induction. J. Neurosci. *23*, 10791–10799.

77. Krauss, M., Kinuta, M., Wenk, M.R., De Camilli, P., Takei, K., and Haucke, V. (2003). ARF6 stimulates clathrin/AP-2 recruitment to synaptic membranes by activating phosphatidylinositol phosphate kinase type Igamma. J. Cell Biol. *162*, 113–124.
78. Lamprecht, R., and LeDoux, J. (2004). Structural plasticity and memory. Nat. Rev. Neurosci. *5*, 45–54.
79. Leonard, A.S., Lim, I.A., Hemsworth, D.E., Horne, M.C., and Hell, J.W. (1999). Calcium/calmodulin-dependent protein kinase II is associated with the N-methyl-D-aspartate receptor. Proc. Natl. Acad. Sci. U. S. A. *96*, 3239–3244.
80. Li, M., Cui, Z., Niu, Y., Liu, B., Fan, W., Yu, D., and Deng, J. (2010). Synaptogenesis in the developing mouse visual cortex. Brain Res. Bull. *81*, 107–113.
81. Lorra, C., and Huttner, W.B. (1999). The mesh hypothesis of Golgi dynamics. Nat. Cell Biol. *1*, E113–E115.
82. Lowenthal, M.S., Markey, S.P., and Dosemeci, A. (2015). Quantitative mass spectrometry measurements reveal stoichiometry of principal postsynaptic density proteins. J. Proteome Res. *14*, 2528–2538.
83. Lu, J., Helton, T.D., Blanpied, T.A., Rácz, B., Newpher, T.M., Weinberg, R.J., and Ehlers, M.D. (2007). Postsynaptic Positioning of Endocytic Zones and AMPA Receptor Cycling by Physical Coupling of Dynamin-3 to Homer. Neuron *55*, 874–889.
84. Lüscher, C., and Malenka, R.C. (2012). NMDA receptor-dependent long-term potentiation and long-term depression (LTP/LTD). Cold Spring Harb. Perspect. Biol. *4*.
85. Lüscher, C., Xia, H., Beattie, E.C., Carroll, R.C., von Zastrow, M., Malenka, R.C., and Nicoll, R.A. (1999). Role of AMPA Receptor Cycling in Synaptic Transmission and Plasticity. Neuron *24*, 649–658.
86. Macia, E., Luton, F., Partisani, M., Cherfils, J., Chardin, P., and Franco, M. (2004). The GDP-bound form of Arf6 is located at the plasma membrane. J. Cell Sci. *117*, 2389–2398.
87. Markram, H., Lubke, J., Frotscher, M., and Sakmann, B. (1997). Regulation of synaptic efficacy by coincidence of postsynaptic APs and EPSPs. Science (80-.). *275*, 213–215.
88. Matsuzaki, M., Honkura, N., Ellis-Davies, G.C.R., and Kasai, H. (2004). Structural basis of long-term potentiation in single dendritic spines. Nature *429*, 761–766.
89. Matthews, E.A., and Dietrich, D. (2015). Buffer mobility and the regulation of neuronal calcium domains. Front. Cell. Neurosci. *9*, 48.
90. McKay, S., Griffiths, N.H., Butters, P.A., Thubron, E.B., Hardingham, G.E., and Wyllie, D.J.A. (2012). Direct pharmacological monitoring of the developmental switch in NMDA receptor subunit composition using TCN 213, a GluN2A-selective, glycine-dependent antagonist. Br. J. Pharmacol. *166*, 924–937.
91. Miyazaki, H., Yamazaki, M., Watanabe, H., Maehama, T., Yokozeki, T., and Kanaho, Y. (2005). The small GTPase ADP-ribosylation factor 6 negatively regulates dendritic spine formation. FEBS Lett. *579*, 6834–6838.
92. Monaghan, D.T., Bridges, R.J., and Cotman, C.W. (1989). Pharmacology , and Distinct Properties In System. Ann. Rev. Pharmacol. Toxicol.
93. Mondin, M., Labrousse, V., Hosy, E., Heine, M., Tessier, B., Levet, F., Poujol, C., Blanchet, C., Choquet, D., and Thoumine, O. (2011). Neurexin-Neuroligin Adhesions Capture Surface-Diffusing AMPA Receptors through PSD-95 Scaffolds. J. Neurosci. *31*, 13500–13515.
94. Montagnac, G., De Forges, H., Smythe, E., Gueudry, C., Romao, M., Salamero, J., and Chavrier, P. (2011). Decoupling of activation and effector binding underlies ARF6 priming of fast endocytic recycling. Curr. Biol. *21*, 574–579.
95. Monyer, H., Burnashev, N., Laurie, D.J., Sakmann, B., and Seeburg, P.H. (1994). Developmental and regional expression in the rat brain and functional properties of four NMDA receptors. Neuron *12*, 529–540.
96. Morleo, M., Iaconis, D., Chitayat, D., Peluso, I., Marzella, R., Renieri, A., Mari, F., and Franco, B. (2008). Disruption of the IQSEC2 transcript in a female with X;autosome translocation t(X;20)(p11.2;q11.2) and a phenotype resembling X-linked infantile spasms (ISSX) syndrome. Mol. Med. Rep. *1*, 33–39.
97. Moss, J., and Vaughan, M. (1993). ADP-ribosylation factors, 20,000 M(r) guanine nucleotide-binding protein activators of cholera toxin and components of intracellular vesicular transport systems. Cell. Signal. *5*, 367–379.
98. Murakoshi, H., Wang, H., and Yasuda, R. (2011). Local, persistent activation of Rho GTPases during plasticity of single dendritic spines. Nature *472*, 100–104.
99. Myers, K.R., and Casanova, J.E. (2008). Regulation of actin cytoskeleton dynamics by Arf-family

GTPases. Trends Cell Biol. *18*, 184–192.
100. Myers, K.R., Wang, G., Sheng, Y., Conger, K.K., Casanova, J.E., and Zhu, J.J. (2012). Arf6-GEF BRAG1 Regulates JNK-Mediated Synaptic Removal of GluA1-Containing AMPA Receptors: A New Mechanism for Nonsyndromic X-Linked Mental Disorder. J. Neurosci. *32*, 11716–11726.
101. Myung, J.K., Dunah, A.W., Yu, T.W., and Sheng, M. (2005). Differential roles of NR2A- and NR2B-containing NMDA receptors in Ras-ERK signaling and AMPA receptor trafficking. Neuron *46*, 745–760.
102. Naisbitt, S., Kim, E., Tu, J.C., Xiao, B., Sala, C., Valtschanoff, J., Weinberg, R.J., Worley, P.F., and Sheng, M. (1999). Shank, a novel family of postsynaptic density proteins that binds to the NMDA receptor/PSD-95/GKAP complex and cortactin. Neuron *23*, 569–582.
103. Naraghi, M., and Neher, E. (1997). Linearized buffered Ca2+ diffusion in microdomains and its implications for calculation of [Ca2+] at the mouth of a calcium channel. J. Neurosci. *17*, 6961–6973.
104. Newpher, T.M., and Ehlers, M.D. (2008). Glutamate Receptor Dynamics in Dendritic Microdomains. Neuron *58*, 472–497.
105. Newpher, T.M., and Ehlers, M.D. (2009). Spine microdomains for postsynaptic signaling and plasticity. Trends Cell Biol. *19*, 218–227.
106. Nithianantharajah, J., Komiyama, N.H., McKechanie, A., Johnstone, M., Blackwood, D.H., St Clair, D., Emes, R.D., van de Lagemaat, L.N., Saksida, L.M., Bussey, T.J., et al. (2013). Synaptic scaffold evolution generated components of vertebrate cognitive complexity. Nat. Neurosci. *16*, 16–24.
107. Nowak, L., Bregestovski, P., Ascher, P., Herbet, A., and Prochiantz, A. (1984). Magnesium gates glutamate-activated channels in mouse central neurones. Nature *307*, 462–465.
108. Okabe, S. (2007). Molecular anatomy of the postsynaptic density. Mol. Cell. Neurosci. *34*, 503–518.
109. Oku, Y., and Huganir, R.L. (2013). AGAP3 and Arf6 regulate trafficking of AMPA receptors and synaptic plasticity. J. Neurosci. *33*, 12586–12598.
110. Opazo, P., Labrecque, S., Tigaret, C.M., Frouin, A., Wiseman, P.W., De Koninck, P., and Choquet, D. (2010). CaMKII triggers the diffusional trapping of surface AMPARs through phosphorylation of stargazin. Neuron *67*, 239–252.
111. Palmer, I., and Wingfield, P.T. (2004). Preparation and extraction of insoluble (inclusion-body) proteins from Escherichia coli. Curr. Protoc. Protein Sci. *Chapter 6*, Unit 6.3.
112. Paoletti, P., Bellone, C., and Zhou, Q. (2013). NMDA receptor subunit diversity: impact on receptor properties, synaptic plasticity and disease. Nat. Rev. Neurosci. *14*, 383–400.
113. Park, M., Penick, E.C., Edwards, J.G., Kauer, J.A., and Ehlers, M.D. (2004). Recycling endosomes supply AMPA receptors for LTP. Science *305*, 1972–1975.
114. Patterson, M., and Yasuda, R. (2011). Signalling pathways underlying structural plasticity of dendritic spines. Br. J. Pharmacol. *163*, 1626–1638.
115. Piguel, N.H., Fievre, S., Blanc, J.-M., Carta, M., Moreau, M.M., Moutin, E., Pinheiro, V.L., Medina, C., Ezan, J., Lasvaux, L., et al. (2014). Scribble1/AP2 complex coordinates NMDA receptor endocytic recycling. Cell Rep. *9*, 712–727.
116. Purpura, D.P. (1974). Dendritic spine “dysgenesis” and mental retardation. Science *186*, 1126–1128.
117. Purves, D. (1988). Body and Brain. A Trophic Theory of Neural Connections. Harvard Univ. Press *231*, 993.
118. Rácz, B., Blanpied, T.A., Ehlers, M.D., and Weinberg, R.J. (2004). Lateral organization of endocytic machinery in dendritic spines. Nat. Neurosci. *7*, 917–918.
119. Radhakrishna, H. (1997). ADP-Ribosylation Factor 6Regulates a Novel Plasma Membrane Recycling Pathway. J. Cell Biol. *139*, 49–61.
120. Raemaekers, T., Peric, A., Baatsen, P., Sannerud, R., Declerck, I., Baert, V., Michiels, C., and Annaert, W. (2012). ARF6-mediated endosomal transport of Telencephalin affects dendritic filopodia-to-spine maturation. EMBO J. *31*, 3252–3269.
121. Randazzo, P.A., Nie, Z., Miura, K., and Hsu, V.W. (2000). Molecular aspects of the cellular activities of ADP-ribosylation factors. Sci STKE *2000*, re1.
122. Ryan, T.J., Kopanitsa, M. V, Indersmitten, T., Nithianantharajah, J., Afinowi, N.O., Pettit, C., Stanford, L.E., Sprengel, R., Saksida, L.M., Bussey, T.J., et al. (2013). Evolution of GluN2A/B cytoplasmic domains diversified vertebrate synaptic plasticity and behavior. Nat. Neurosci. *16*, 25–32.
123. Sabe, H. (2003). Requirement for Arf6 in cell adhesion, migration, and cancer cell invasion. J. Biochem. *134*, 485–489.
124. Sakagami, H., Katsumata, O., Hara, Y., Tamaki, H., Watanabe, M., Harvey, R.J., and Fukaya, M. (2013). Distinct synaptic localization patterns of brefeldin A-resistant guanine nucleotide exchange factors BRAG2 and BRAG3 in the mouse retina. J. Comp. Neurol. *521*, 860–876.
125. Sanda, M., Kamata, A., Katsumata, O., Fukunaga, K., Watanabe, M., Kondo, H., and Sakagami, H.

(2009). The postsynaptic density protein, IQ-ArfGEF/BRAG1, can interact with IRSp53 through its proline-rich sequence. Brain Res. *1251*, 7–15.

126. Santy, L.C., and Casanova, J.E. (2001). Activation of ARF6 by ARNO stimulates epithelial cell migration through downstream activation of both Rac1 and phospholipase D. J. Cell Biol. *154*, 599–610.
127. Sanz-Clemente, A., Gray, J.A., Ogilvie, K.A., Nicoll, R.A., and Roche, K.W. (2013). Activated CaMKII Couples GluN2B and Casein Kinase 2 to Control Synaptic NMDA Receptors. Cell Rep. *3*, 607–614.
128. Sarnat, H.B., and Netsky, M.G. (1985). The brain of the planarian as the ancestor of the human brain. Can. J. Neurol. Sci. *12*, 296–302.
129. Schall, T.J., Lewis, M., Koller, K.J., Lee, A., Rice, G.C., Wong, G.H.W., Gatanaga, T., Granger, G.A., Lentz, R., Raab, H., et al. (1990). Molecular cloning and expression of a receptor for human tumor necrosis factor. Cell *61*, 361–370.
130. Scholz, R., Berberich, S., Rathgeber, L., Kolleker, A., Köhr, G., and Kornau, H.C. (2010). AMPA Receptor Signaling through BRAG2 and Arf6 Critical for Long-Term Synaptic Depression. Neuron *66*, 768–780.
131. Schwechter, B., Rosenmund, C., and Tolias, K.F. (2013). RasGRF2 Rac-GEF activity couples NMDA receptor calcium flux to enhanced synaptic transmission. Proc. Natl. Acad. Sci. *110*, 14462–14467.
132. Schwenk, J., Harmel, N., Brechet, A., Zolles, G., Berkefeld, H., Müller, C.S., Bildl, W., Baehrens, D., Hüber, B., Kulik, A., et al. (2012). High-resolution proteomics unravel architecture and molecular diversity of native AMPA receptor complexes. Neuron *74*, 621–633.
133. Segev, N. (2009). Trafficking Inside Cells (New York, NY: Springer New York).
134. Sheng, M., and Hoogenraad, C.C. (2007). The postsynaptic architecture of excitatory synapses: a more quantitative view. Annu. Rev. Biochem. *76*, 823–847.
135. Shoubridge, C., Tarpey, P.S., Abidi, F., Ramsden, S.L., Rujirabanjerd, S., Murphy, J.A., Boyle, J., Shaw, M., Gardner, A., Proos, A., et al. (2010). Mutations in the guanine nucleotide exchange factor gene IQSEC2 cause nonsyndromic intellectual disability. Nat. Genet. *42*, 486–488.
136. Skroblin, P., Grossmann, S., Schäfer, G., Rosenthal, W., and Klussmann, E. (2010). Mechanisms of protein kinase A anchoring. Int. Rev. Cell Mol. Biol. *283*, 235–330.
137. Sobczyk, A., Scheuss, V., and Svoboda, K. (2005). NMDA receptor subunit-dependent [Ca2+] signaling in individual hippocampal dendritic spines. J. Neurosci. *25*, 6037–6046.
138. Steele, R.J., and Morris, R.G. (1999). Delay-dependent impairment of a matching-to-place task with chronic and intrahippocampal infusion of the NMDA-antagonist D-AP5. Hippocampus *9*, 118–136.
139. Um, K., Niu, S., Duman, J.G., Cheng, J.X., Tu, Y.-K., Schwechter, B., Liu, F., Hiles, L., Narayanan, A.S., Ash, R.T., et al. (2014). Dynamic control of excitatory synapse development by a Rac1 GEF/GAP regulatory complex. Dev. Cell *29*, 701–715.
140. Unoki, T., Matsuda, S., Kakegawa, W., Van, N.T.B., Kohda, K., Suzuki, A., Funakoshi, Y., Hasegawa, H., Yuzaki, M., and Kanaho, Y. (2012). NMDA Receptor-Mediated PIP5K Activation to Produce PI(4,5)P 2 Is Essential for AMPA Receptor Endocytosis during LTD. Neuron *73*, 135–148.
141. Valderrama, F., and Ridley, A.J. (2008). Getting invasive with GEP100 and Arf6. Nat. Cell Biol. *10*, 16–18.
142. Valtschanoff, J.G., and Weinberg, R.J. (2001). Laminar organization of the NMDA receptor complex within the postsynaptic density. J. Neurosci. *21*, 1211–1217.
143. Wu, G.Y., Zou, D.J., Rajan, I., and Cline, H. (1999). Dendritic dynamics in vivo change during neuronal maturation. J. Neurosci. *19*, 4472–4483.
144. Yashiro, K., and Philpot, B.D. (2008). Regulation of NMDA receptor subunit expression and its implications for LTD, LTP, and metaplasticity. Neuropharmacology *55*, 1081–1094.
145. Yuste, R. (2013). Electrical Compartmentalization in Dendritic Spines. Annu. Rev. Neurosci. *36*, 429–449.
146. Yuste, R., and Denk, W. (1995). Dendritic spines as basic functional units of neuronal integration. Nature *375*, 682–684.
147. Zerial, M., and McBride, H. (2001). Rab proteins as membrane organizers. Nat. Rev. Mol. Cell Biol. *2*, 107–117.
148. Zhang, Y., Cudmore, R.H., Lin, D.-T., Linden, D.J., and Huganir, R.L. (2015). Visualization of NMDA receptor–dependent AMPA receptor synaptic plasticity in vivo. Nat. Neurosci. *18*, 402–407.
149. Zheng, N., Jeyifous, O., Munro, C., Montgomery, J.M., and Green, W.N. (2015). Synaptic activity regulates AMPA receptor trafficking through different recycling pathways. Elife *4*, 1–20.
150. Zhou, X., Ding, Q., Chen, Z., Yun, H., and Wang, H. (2013). Involvement of the GluN2A and GluN2B subunits in synaptic and extrasynaptic N-methyl-D-aspartate receptor function and neuronal excitotoxicity. J. Biol. Chem. *288*, 24151–24159.
151. Zhu, J.J., Qin, Y., Zhao, M., Van Aelst, L., and Malinow, R. (2002). Ras and Rap control AMPA receptor trafficking during synaptic plasticity. Cell *110*, 443–45.

Selbstständigkeitserklärung

Ich bestätige, dass ich die vorliegende Dissertation selbstständig und ohne Benutzung anderer als der angegebenen Quellen und Hilfsmittel angefertigt habe.

Die vorliegende Arbeit ist frei von Plagiaten und wurde in gleicher oder ähnlicher Form noch bei keiner anderen Universität als Prüfungsleistung eingereicht. Alle Ausführungen, die wörtlich oder inhaltlich aus anderen Schriften entnommen sind, habe ich als solche kenntlich gemacht.

Der Lebenslauf ist in der Online-Version aus Gründen des Datenschutzes nicht enthalten.

APPENDIX

GluN2B-BRAG1 signalling axis in immature synapses of young neurons.

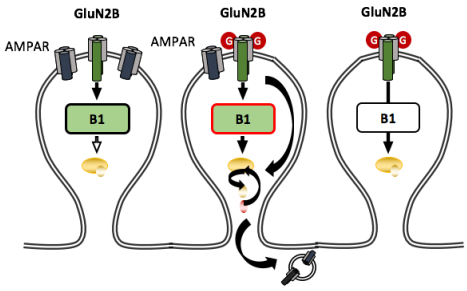

GluN2B-GluN2A subunit and BRAG1-BRAG2 signalling switch in mature synapses of old neurons.

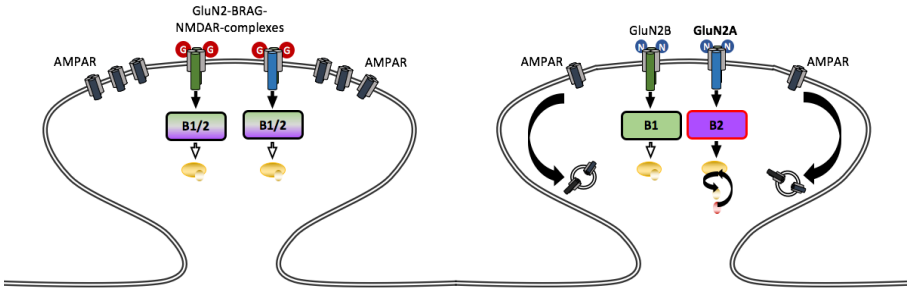

GluN2A-BRAG2-to-GluN2B-BRAG1 signalling switch after interference with mature signalling pathway.

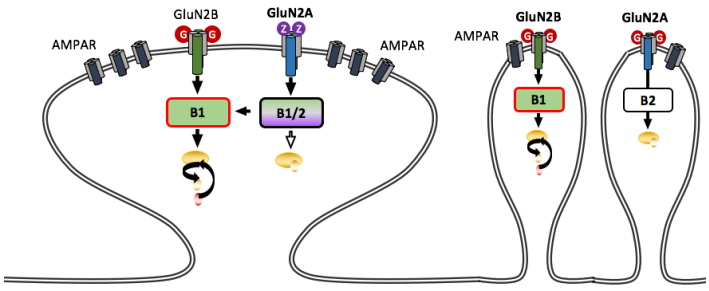

molecular BRAG activation mechanism